

Machine Learning in Least-Squares Monte Carlo Proxy Modeling of Life Insurance Companies

Anne-Sophie Krah* Zoran Nikolić† Ralf Korn*,§

September 6, 2019

Abstract

Under the Solvency II regime, life insurance companies are asked to derive their solvency capital requirements from the full loss distributions over the coming year. Since the industry is currently far from being endowed with sufficient computational capacities to fully simulate these distributions, the insurers have to rely on suitable approximation techniques such as the least-squares Monte Carlo (LSMC) method. The key idea of LSMC is to run only a few wisely selected simulations and to process their output further to obtain a risk-dependent proxy function of the loss. In this paper, we present and analyze various adaptive machine learning approaches that can take over the proxy modeling task. The studied approaches range from ordinary and generalized least-squares regression variants over GLM and GAM methods to MARS and kernel regression routines. We justify the combinability of their regression ingredients in a theoretical discourse. Further, we illustrate the approaches in slightly disguised real-world experiments and perform comprehensive out-of-sample tests.

*Department of Mathematics, TU Kaiserslautern, Erwin-Schrödinger-Straße, Gebäude 48, 67653 Kaiserslautern, Germany; anne-sophiekrah@web.de.

†Mathematical Institute, University Cologne, Weyertal 86-90, 50931 Cologne, Germany; znikolic@uni-koeln.de.

§Department Financial Mathematics, Fraunhofer ITWM, Fraunhofer-Platz 1, 67663 Kaiserslautern, Germany; korn@mathematik.uni-kl.de.

Contents

1	Introduction	1
2	Calibration & Validation in the LSMC Framework	4
2.1	Fitting & Validation Points	4
2.2	Calibration Algorithm	5
2.3	Validation Figures	7
3	Machine Learning Regression Methods	9
3.1	General Remarks	9
3.2	Ordinary Least-Squares (OLS) Regression	10
3.3	Generalized Linear Models (GLMs)	11
3.4	Generalized Additive Models (GAMs)	15
3.5	Feasible Generalized Least-Squares (FGLS) Regression	20
3.6	Multivariate Adaptive Regression Splines (MARS)	24
3.7	Kernel Regression	27
4	Numerical Experiments	30
4.1	General Remarks	30
4.2	Ordinary Least-Squares (OLS) Regression	33
4.3	Generalized Linear Models (GLMs)	36
4.4	Generalized Additive Models (GAMs)	39
4.5	Feasible Generalized Least-Squares (FGLS) Regression	43
4.6	Multivariate Adaptive Regression Splines (MARS)	46
4.7	Kernel Regression	48
5	Conclusion	50
References		56
Appendix		62

1 Introduction

LSMC Framework under Solvency II

By the Solvency II directive of the European Parliament & European Council (2009), life insurance companies are asked to derive their solvency capital requirements (SCRs) from their full loss probability distributions over the coming year if they do not want to rely on the much simpler standard formula. In order to obtain reasonably accurate full loss distributions via a nested simulations approach as described in Bauer et al. (2012), their cash-flow-projection (CFP) models would need to be simulated several hundred thousand times. But the insurers are currently far from being endowed with sufficient computational capacities to perform such expensive simulation tasks. By applying suitable approximation techniques like the least-squares Monte Carlo (LSMC) approach of Bauer & Ha (2015), the insurers are able to overcome these computational hurdles though. For example, they can implement the LSMC framework formalized by Krah et al. (2018) and applied by e.g. Bettels et al. (2014) to derive their full loss distributions. The central idea of this framework is to carry out a comparably small number of wisely chosen Monte Carlo simulations and to feed the simulation results into a supervised machine learning algorithm that translates the results into a proxy function of the insurer's loss (output) with respect to the underlying risk factors (input). To guarantee a certain approximation quality, the proxy function has to pass an additional validation procedure before it can finally be used for the full loss distribution forecast.

Machine Learning Calibration Algorithm

Apart from the calibration and validation steps, we adopt the LSMC framework from Krah et al. (2018) without any changes. Therefore, we neither repeat the simulation setting nor the procedure for the full loss distribution forecast and SCR calculation here in detail. The purpose of this exposition is to introduce different machine learning methods that can be applied in the calibration step of the LSMC framework and other high-dimensional variable selection applications, to point out their similarities and differences and to compare their out-of-sample performances in a slightly disguised real-world LSMC example. We describe the data basis used for calibration and validation in Section 2.1, the structure of the calibration algorithm in Section 2.2 and our validation approach in Section 2.3. Our focus lies on out-of-sample performance rather than computational efficiency as the latter becomes only relevant if the former gives reason for it. We analyze a very realistic data basis with 15 risk factors and validate the proxy functions based on a very comprehensive and computationally expensive nested simulations test set comprising the SCR estimate.

The idea is to combine different regression methods with an adaptive algorithm, in which the proxy functions are built up of basis functions in a stepwise fashion. In a

four risk factor LSMC example, Teuguia et al. (2014) applied a full model approach, forward selection, backward elimination and a bidirectional approach as e.g. discussed in Hocking (1976) with orthogonal polynomial basis functions. They stated that only forward selection and the bidirectional approach were feasible when the number of risk factors or polynomial degree exceeded 7 as the other models exploded then. Life insurance companies covering a wide range of contracts in their portfolio are typically exposed to even more risk factors like e.g. 15. In complex business regulation frameworks such as in Germany, they furthermore require polynomial degrees of at least 4. In these cases, even the standard forward selection and bidirectional approaches become infeasible as the sets of candidate terms from which the basis functions are chosen will explode then as well. We therefore follow the suggestion of Krah et al. (2018) to implement the so-called principle of marginality, an iteration-wise update technique of the set of candidate terms that lets the algorithm get along with comparably few carefully selected candidate terms.

Regression Methods & Model Selection Criteria

Our main contribution is to identify, explain and illustrate a collection of regression methods and model selection criteria from the jungle of regression design options that provide suitable proxy functions in the LSMC framework when applied in combination with the principle of marginality. After some general remarks in Section 3.1, we describe ordinary least-squares (OLS) regression in Section 3.2, generalized linear models (GLMs) by Nelder & Wedderburn (1972) in Section 3.3, generalized additive models (GAMs) by Hastie & Tibshirani (1986) and Hastie & Tibshirani (1990) in Section 3.4, feasible generalized least-squares (FGLS) regression in Section 3.5, multivariate adaptive regression splines (MARS) by Friedman (1991) in Section 3.6, and kernel regression by Watson (1964) and Nadaraya (1964) in Section 3.7. While some regression methods such as OLS and FGLS regression or GLMs can immediately be applied in conjunction with numerous model selection criteria such as Akaike information criterion (AIC), Bayesian information crierion (BIC), Mallow's C_P or generalized cross-validation (GCV), other regression methods such as GAMs, MARS, kernel, ridge or robust regression require thought-through modifications thereof or work only with non-parametric alternatives such as k -fold or leave-one-out cross-validation. For adaptive approaches of FGLS, ridge and robust regression in life insurance proxy modeling, see also Hartmann (2015), Krah (2015) and Nikolić et al. (2017), respectively.

In the theory sections, we present the models with their assumptions, important properties and popular estimation algorithms and demonstrate how they can be embedded in the adaptive algorithm by proposing feasible implementation designs and combinable model selection criteria. While we shed light on the theoretical basic concepts of the models to lay the groundwork for the application and interpretation of the later following numerical experiments, we forego to describe in detail technical enhancements or peculiarities of the involved algorithms and instead refer the interested reader here and there to some

further sources. Additionally we provide the practitioners with R packages containing useful implementations of the presented regression routines. We complement the theory sections by practice sections 4.1, 4.2, 4.3, 4.4, 4.5, 4.6 and 4.7, respectively, throughout which we perform the same Monte Carlo approximation task to make the performance of the various methods comparable. We measure the approximation quality of the resulting proxy functions by means of aggregated validation figures on three out-of-sample test sets.

Further Machine Learning Alternatives

Conceivable alternatives to the entire adaptive algorithm are other typical machine learning techniques such as artificial neural networks (ANNs), decision tree learning or support vector machines. In particular, the classical feed forward networks proposed by Hejazi & Jackson (2017) and applied in various ways by Kopczyk (2018), Castellani et al. (2018), Born (2018) and Schelthoff (2019) were shown to capture the complex nature of CFP models well. A major challenge here is not only to find reliable hyperparameters such as the numbers of hidden layers and nodes in the network, batch size, weight initializer probability distribution, learning rate or activation function but also the high dependence on the random seeds. Future research should therefore be dedicated to hyperparameter search algorithms and stabilization methods such as ensemble methods. As an alternative to feed forward networks, Kazimov (2018) suggested to use radial basis function networks albeit so far none of the tested approaches worked out well.

In decision tree learning, random forests and tree-based gradient boosting machines were considered by Kopczyk (2018) and Schoenenwald (2019). While random forests were outperformed by feed forward networks but did better than the least absolute shrinkage and selection operator (LASSO) by Tibshirani (1996) in the example of the former author, they generally performed worse than the adaptive approaches by Krah et al. (2018) with OLS regression in numerous examples of the latter author. The gradient boosting machines, requiring more parameter tuning and thus being more versatile and demanding, came overall very close to the adaptive approaches. The tree-based methods belong by definition to the aforementioned ensemble methods, a modeling concept transferrable to arbitrary regression techniques, mitigating random model artefacts through averaging.

Castellani et al. (2018) compared support vector regression (SVR) by Drucker et al. (1997) to ANNs and the adaptive approaches by Teugua et al. (2014) in a seven risk factor example and found the performance of SVR placed somewhere inbetween the other two approaches with the ANNs getting closest to the nested simulations benchmark. As some further non-parametric approaches, Sell (2019) tested least-squares support-vector machines (LS-SVM) by Suykens & Vandewalle (1999) and shrunk additive least-squares approximations (SALSA) by Kandasamy & Yu (2016) in comparison to ANNs and the adaptive approaches by Krah et al. (2018) with OLS regression. In his examples, SALSA was able to beat the other two approaches whereas LS-SVM was left far behind. The analyzed machine learning alternatives have in common that they require at least to

some degree a fine-tuning of some model hyperparameters. Since this is often a non-trivial but crucial task for generating suitable proxy functions, finding efficient search algorithms should become a subject of future research.

2 Calibration & Validation in the LSMC Framework

2.1 Fitting & Validation Points

Outer Scenarios & Inner Simulations

In the LSMC approach, the proxy function of the economic variable (e.g. the loss, available capital or best estimate of liabilities) is calibrated conditional on the *fitting points* which have been generated besides the *validation points* by the Monte Carlo simulations of the CFP model in the step before. The fitting and validation points describe relationships between the economic variable and the different financial and actuarial risk factors the insurance company is exposed to such as the interest rate, equity, property, credit, mortality, morbidity, lapse or expense stresses. By an *outer scenario* we refer to a specific stress level combination of these risk factors, and by an *inner simulation* to a stochastic path of an outer scenario in the CFP model under the given risk-neutral probability measure. The fitting values of the economic variable are defined as the mean values over only few inner simulations of the same outer fitting scenario whereas the validation values of the economic variable are defined as the mean values over many inner simulations of the same outer validation scenario.

Different Trade-off Requirements

According to the law of large numbers, this construction makes the fitting values very volatile and the validation values comparably stable. Typically, the very limited fitting and validation simulation budgets are of similar sizes. Hence the few inner simulations in the case of the fitting points allow a great diversification among the outer scenarios whereas the many inner simulations in the case of the validation points let the validation values be quite close to their expectations but at the cost of only little diversification among the outer scenarios. These opposite ways to deal with the trade-off between the numbers of outer scenarios and inner simulations reflect the different requirements for the fitting and validation points in the LSMC approach. While the fitting scenarios should cover the domain of the real-world scenarios well to serve as a good regression basis, the validation values should approximate the expectations of the economic variable at the validation scenarios well to provide appropriate target values for the proxy functions.

2.2 Calibration Algorithm

Five Major Components

The calibration of the proxy function is performed by an adaptive algorithm that can be decomposed into the following five major components: (1) a set of allowed basis function types for the proxy function, (2) a regression method, (3) a model selection criterion, (4) a candidate term update principle, and (5) the number of steps per iteration and the directions of the algorithm. For illustration, we adopt the flowchart of the adaptive algorithm from Krah et al. (2018) and depict it in Figure 1. While components (1) and (5) enter the flowchart implicitly through the start proxy, candidate terms and the order of the processes and decisions in the chart, components (2), (3) and (4) are explicitly indicated through the labels “Regression”, “Model Selection Criterion” and “Get Candidate Terms”.

Let us briefly recapitulate the adaptive algorithm under some standard choices of components (1), (2), (3), (4) and (5) which have already been successfully applied in the insurance industry. As the function types for the basis functions (1), let only monomials be allowed. Let the regression method (2) be ordinary least-squares (OLS) regression and the model selection criterion (3) Akaike information criterion (AIC) from Akaike (1973). Let the set of candidate terms (4) be updated by the principle of marginality to which we will return in greater detail below. Lastly, when building up the proxy function iteratively, let the algorithm make only one step per iteration in the forward direction (5) meaning that in each iteration exactly one basis function is selected which cannot be removed anymore (adaptive forward stepwise selection).

Iterative Procedure

The algorithm starts in the upper left side of Figure 1 with the specification of the start proxy basis functions. We specify only the intercept so that the first regression ($k = 0$) reduces to averaging over all fitting values. In order to harmonize the choices of OLS regression and AIC, we assume that the errors are normally distributed and homoscedastic because then the OLS estimator coincides with the maximum likelihood estimator. AIC is a relative measure for the goodness-of-fit of the proxy function and is defined as twice the negative of the maximum log-likelihood plus twice the number of degrees of freedom. The smaller the AIC score, the better is the fit and thus the trade-off between a too complex (overfitting) and too simple model (underfitting).

At the beginning of each iteration ($k = 1, \dots, K - 1$), the set of candidate terms is updated by the principle of marginality which is compatible with the choice of a monomial basis. Using such a principle saves computational costs by selecting the basis functions conditionally on the current proxy function structure. According to the principle of marginality, a monomial basis function becomes a candidate if and only if all its derivatives are already included in the proxy function. In the first iteration ($k = 1$), all linear monomials of the risk factors become candidates as their derivatives are constant values

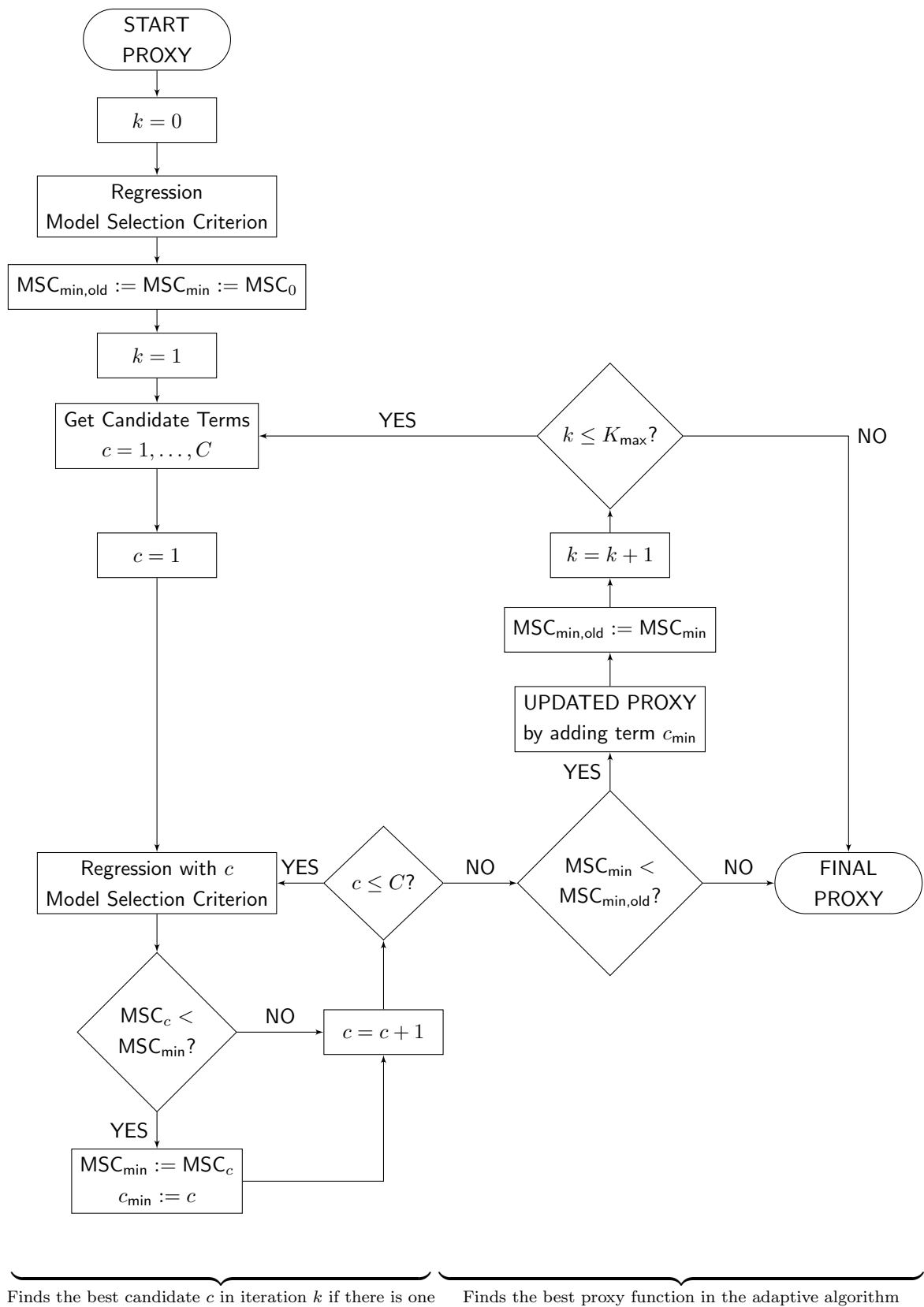


Figure 1: Flowchart of the calibration algorithm

which are represented by the intercept.

The algorithm proceeds on the lower left side of the flowchart with a loop in which all candidate terms are separately added to the proxy function structure and tested with regard to their additional explanatory power. With each candidate, the fitting values are regressed against the fitting scenarios and the AIC score is calculated. If no candidate reduces the currently smallest AIC score, the algorithm is terminated, and otherwise, the proxy function is updated by the one which reduces AIC most. Then the next iteration ($k + 1$) begins with the update of the set of candidate terms, and so on. As long as no termination occurs, this procedure is repeated until the prespecified maximum number of terms K_{\max} is reached.

2.3 Validation Figures

Validation Sets

Since it is the objective of this paper to propose suitable regression methods for the proxy function calibration in the LSMC framework, we introduce several validation figures serving as indicators for the approximation quality of the proxy functions. We measure the out-of-sample performance of each proxy function on three different validation sets by calculating five validation figures per set.

The three validation sets are a Sobol set, a nested simulations set and a capital region set. Unlike the Sobol set, the nested simulations and capital region sets do not serve as feasible validation sets in the LSMC routine as they require massive computational capacities but can be regarded as the natural benchmark for the LSMC-based method and are thus very valuable for this analysis. The Sobol set consists of e.g. between $L = 15$ and $L = 200$ Sobol validation points, of which the scenarios follow a Sobol sequence covering the fitting space uniformly. Thereby is the fitting space the cube on which the outer fitting scenarios are defined. It has to cover the space of real-world scenarios used for the full loss distribution forecast sufficiently well. For interpretive reasons, sometimes the Sobol set is extended by points with e.g. one-dimensional risk scenarios or scenarios producing a risk capital close to the SCR (= 99.5% value-at-risk) in previous risk capital calculations.

The nested simulations set comprises the e.g. $L = 820$ to $L = 6554$ validation points of which the scenarios correspond to the e.g. highest 2.5% to 5% losses from the full loss distribution forecast made by the proxy function that had been derived under the standard calibration algorithm choices described in Section 2.2. Like in the example of Ch. 5.2 in Krah et al. (2018), the order of these losses - which scenarios lead to which quantiles - following from the forth and last step of the LSMC approach is very similar to the order following from the nested simulations approach. Therefore the scenarios of the nested simulations set are simply given by the order of the losses resulting from the LSMC approach. Several of these scenarios consist of stresses falling out of the fitting space. Few

points with severe outliers due to extreme stresses far beyond the fitting space should be excluded from the set. The capital region set is a subset of the nested simulations set containing the nested simulations SCR estimate and the e.g. 64 losses above and below, which makes in total e.g. $L = 129$ validation points.

Validation Figures

The five validation figures reported in our numerical experiments comprise two normalized mean absolute errors (MAEs), one with respect to the magnitude of the economic variable itself and one with respect to the magnitude of the corresponding market value of assets. Further, they comprise the mean of the residuals, the normalized MAE of the deviation of the economic variable from the base value (see the definition of the base value below) with respect to the magnitude of that deviation and last but not least the mean of the residuals of these deviations. The smaller the normalized MAEs are, the better the proxy function approximates the economic variable. However, the validation values are afflicted with Monte Carlo errors so that the normalized MAEs serve only as meaningful indicators as long as the proxy functions do not become too precise. The means of the residuals should be possibly close to zero since they indicate systematic deviations of the proxy functions from the validation values. While the first three validation figures measure how well the proxy function reflects the economic variable in the CFP model, the latter two address the approximation effects on the SCR, compare Ch. 3.4.1 of Krah et al. (2018).

Let us write the absolute value as $|\cdot|$ and let L denote the number of validation points. Then we can express the MAE of the proxy function $\hat{f}(x^i)$ evaluated at the validation scenarios x^i versus the validation values y^i as $\frac{1}{L} \sum_{i=1}^L |y^i - \hat{f}(x^i)|$. After normalizing the MAE with respect to the mean of the absolute values of the economic variable or the market value of assets, i.e. $\frac{1}{L} \sum_{i=1}^L |d^i|$ with $d^i \in \{y^i, a^i\}$, we obtain the first two validation figures, i.e.

$$\text{mae} = \frac{\sum_{i=1}^L |y^i - \hat{f}(x^i)|}{\sum_{i=1}^L |d^i|}. \quad (1)$$

In the following, we will refer to (1) with $d^i = y^i$ as the MAE with respect to the *relative metric*, and to (1) with $d^i = a^i$ as the MAE with respect to the *asset metric*. The mean of the residuals is given by

$$\text{res} = \frac{1}{L} \sum_{i=1}^L (y^i - \hat{f}(x^i)). \quad (2)$$

Let us refer by the base value y^0 to the validation value corresponding to the base scenario x^0 in which no risk factor has an effect on the economic variable. In analogy to (1) but only with respect to the relative metric, we introduce another normalized MAE by

$$\text{mae}^0 = \frac{\sum_{i=1}^L |(y^i - y^0) - (\hat{f}(x^i) - \hat{f}(x^0))|}{\sum_{i=1}^L |y^i - y^0|}. \quad (3)$$

The mean of the corresponding residuals is given by

$$\text{res}^0 = \frac{1}{L} \sum_{i=1}^L \left((y^i - y^0) - (\hat{f}(x^i) - \hat{f}(x^0)) \right). \quad (4)$$

In addition to these five validation figures, let us define the base residual which can be used as a substitute for (4) depending on personal taste. The base residual can easily be extracted from (2) and (4) by

$$\text{res}^{\text{base}} = y^0 - \hat{f}(x^0) = \text{res} - \text{res}^0. \quad (5)$$

3 Machine Learning Regression Methods

3.1 General Remarks

As the main part of our work, we will compare various types of machine learning regression approaches for determining suitable proxy functions in the LSMC framework. The methods we present in this section range from ordinary and generalized least-squares regression variants over GLM and GAM approaches to multivariate adaptive regression splines and kernel regression approaches. The performance of the newly derived proxy functions when applied to the validation sets is one way of how to judge the different methods. Their compatibility with the principle of marginality and a suitable model selection criterion such as AIC to compare iteration-wise the candidate models inside the approaches is another way.

We make two approximations to express the expected value of the economic variable $Y(X)$ under the risk-neutral probability measure \mathbb{Q} by a proxy function with respect to the risk factors X . The approximations are necessary since the sets of basis functions (K basis functions) and fitting points (sample size N) are finite in practice. Unlike Bauer & Ha (2015) and Krah et al. (2018), who denote the conditional expectation of the economic variable relative to the outer scenario X by $\text{AC}(X)$, we use the notation $Y(X)$ to account for the fact that the economic variable does not have to be the available capital but can instead be e.g. the best estimate of liabilities or the market value of assets. Note that the expectation operator is included in the notation of $Y(X)$. In accordance with this reduced notation, we will refer to the conditional expectation of the economic variable only as the economic variable. Only when we will use the term economic variable in the context of data realizations such as of the fitting or validation values, we will not mean its expectation.

Let the D -dimensional fitting scenarios be distributed under the physical probability measure \mathbb{P}' on the fitting space which itself is a subspace of \mathbb{R}^D .

3.2 Ordinary Least-Squares (OLS) Regression

Classical Linear Regression Model

In iteration $K - 1$ of the adaptive forward stepwise algorithm, we can write the linear predictor $f(X)$ for $Y(X)$, containing the first approximation, as a linear combination of suitable linear independent basis functions $e_k(X) \in L^2(\mathbb{R}^D, \mathcal{B}, \mathbb{P}')$, $k = 0, 1, \dots, K - 1$, i.e.

$$Y(X) \stackrel{K \leq \infty}{\approx} f(X) = \sum_{k=0}^{K-1} \beta_k e_k(X). \quad (6)$$

With the fitting points (x^i, y^i) , $i = 1, \dots, N$, and uncorrelated errors ϵ^i having the same variance $\sigma^2 > 0$ (= homoscedastic errors), we obtain the classical linear regression model

$$y^i = \sum_{k=0}^{K-1} \beta_k e_k(x^i) + \epsilon^i, \quad (7)$$

where $e_0(x^i) = 1$ and β_0 is the intercept. Then the ordinary least-squares (OLS) estimator $\hat{\beta}_{\text{OLS}}$ of the coefficients is given by

$$\hat{\beta}_{\text{OLS}} = \arg \min_{\beta \in \mathbb{R}^K} \left\{ \sum_{i=1}^N \left(y^i - \sum_{k=0}^{K-1} \beta_k e_k(x^i) \right)^2 \right\}. \quad (8)$$

Since the residuals corresponding to the OLS solution are $\hat{\epsilon}^i = y^i - \sum_{k=0}^{K-1} \hat{\beta}_{\text{OLS}, k} e_k(x^i)$, the OLS estimator minimizes by definition the residual sum of squares. By substituting $\hat{\beta}_{\text{OLS}}$ for β in (6), we account for the second approximation and arrive at the proxy function $\hat{f}(X)$ for the economic variable $Y(X)$ conditional on any outer scenario X , i.e.

$$Y(X) \stackrel{K, N \leq \infty}{\approx} \hat{f}(X) = \sum_{k=0}^{K-1} \hat{\beta}_{\text{OLS}, k} e_k(X). \quad (9)$$

If we use the notation $z_{ik} = e_k(x^i)$, we can replace the minimization problem (8) by the closed-form expression of the OLS estimator in which $Z = (z_{ik})_{\substack{i=1, \dots, N \\ k=0, \dots, K-1}}$ denotes the design matrix and $\mathbf{y} = (y^1, \dots, y^N)^T$ the response vector, i.e.

$$\hat{\beta}_{\text{OLS}} = (Z^T Z)^{-1} Z^T \mathbf{y}. \quad (10)$$

The system $(Z^T Z) \hat{\beta}_{\text{OLS}} = Z^T \mathbf{y}$ equivalent to (10) is in practice often solved via a QR or singular value decomposition of Z to increase numerical stability. For a practical implementation see e.g. function $lm(\cdot)$ in R package *stats* of R Core Team (2018). The sample variance is obtained by $s_{\text{OLS}} = \frac{1}{N-K} \hat{\epsilon}^T \hat{\epsilon}$ where $\hat{\epsilon} = \mathbf{y} - Z \hat{\beta}_{\text{OLS}}$ is the residual vector. With $\mathbf{z} = (e_0(X), \dots, e_{K-1}(X))^T$, (9) becomes in matrix notation $Y(X) \stackrel{K, N \leq \infty}{\approx} \hat{f}(X) = \mathbf{z}^T \hat{\beta}_{\text{OLS}}$.

Gauss-Markov Theorem, ML Estimation & AIC

We formulate the Gauss-Markov theorem in our setting conditional on the fitting scenarios and in line with Hayashi (2000) under the assumptions of strict exogeneity $E[\epsilon | Z] = \mathbf{0}$ (A1), a spherical error variance $V[\epsilon | Z] = \sigma^2 I_N$, where I_N is the N -dimensional identity matrix (A2), and no multicollinearity, that is, linear independent basis functions (A3).

Gauss-Markov theorem. *The OLS estimator is the best linear unbiased estimator (BLUE) of the coefficients in the classical linear regression model (7) under Assumptions (A1)-(A3).*

Akaike information criterion (AIC) needs to be evaluated at the maximum likelihood (ML) estimators of the coefficients and variance of the errors. For this purpose, we have to make an assumption about the distribution of the economic variable, or equivalently the errors. In order to make AIC and OLS regression easily combinable we assume in addition to (A1), (A2) and (A3) that the errors are normally distributed conditional on the fitting scenarios (A4) because then Proposition 1.5 of Hayashi (2000) states the following.

Theorem 1. *The ML coefficient estimator coincides with the OLS coefficient estimator and the ML estimator of the error variance $\hat{\sigma}^2$ can be expressed as $\frac{N-K}{N}$ times the OLS sample variance s_{OLS} , i.e. $\hat{\sigma}^2 = \frac{1}{N}\hat{\epsilon}^T\hat{\epsilon}$, under Assumptions (A1)-(A4).*

Furthermore, the OLS estimator is the efficient estimator under these assumptions according to Greene (2002).

According to Krah et al. (2018), AIC has the form of a suitably weighted sum of the calibration error and the number of basis functions under Assumption (A4), i.e.

$$\begin{aligned} \text{AIC} &= -2l(\hat{\beta}_{OLS}, \hat{\sigma}^2) + 2(K+1) \\ &= N(\log(2\pi\hat{\sigma}^2) + 1) + 2(K+1). \end{aligned} \quad (11)$$

More generally, the calibration error corresponds to twice the negative of the log-likelihood $l(\cdot)$ of the model and the number of basis functions corresponds to the degrees of freedom of the model. The smaller the AIC score is, the better is the fitted model supposed to approximate the underlying data. AIC penalizes both a small log-likelihood and a high model complexity and helps thus select a possibly simple model with a possibly high goodness-of-fit. However, since AIC is only a relative measure of the goodness-of-fit, the final proxy function has to pass an additional out-of-sample validation procedure in the LSMC algorithm.

3.3 Generalized Linear Models (GLMs)

Random Component, Systematic Component & Link Function

Nelder & Wedderburn (1972) developed the class of generalized linear models (GLMs) as a generalization of the classical linear model in (7). A GLM consists of a random

component, a systematic component and a link function. From the perspective of a GLM and maximum likelihood (ML) estimation, one has to assume that the economic variable under the risk-neutral probability measure follows a certain distribution. We have already seen with Theorem 1 that the OLS estimator of the coefficients equals the ML estimator if the economic variable, or equivalently the errors, are normally distributed conditional on the fitting scenarios (A4).

By following Ch. 2.2 in McCullagh & Nelder (1989), we generalize the linear model in the adaptive algorithm. In a GLM, the economic variable is allowed to come from any distribution of the exponential family conditional on the outer scenario, for instance from the normal, gamma, or inverse gaussian distribution. The distribution of the economic variable in a GLM is reflected by the random component. Its canonical form with canonical parameter θ is given by the density function

$$\pi(y | \theta, \phi) = \exp\left(\frac{y\theta - b(\theta)}{a(\phi)} + c(y, \phi)\right), \quad (12)$$

where $a(\phi)$, $b(\theta)$ and $c(y, \phi)$ are specific functions. While the canonical parameter θ is related to the expected value of the distribution $E[y] = \mu = b'(\theta)$, the dispersion parameter ϕ only affects the variance $V[y] = b''(\theta)a(\phi) = V[\mu]a(\phi)$, whereby we refer to $V[\mu]$ as the variance function. Since we consider only equal prior weights, we can set $a(\phi) = \phi$ constant over all observations. For example, a normally distributed economic variable with mean μ and variance σ^2 is given by $a(\phi) = \phi$, $b(\theta) = \frac{\theta^2}{2}$ and $c(y, \phi) = -\frac{1}{2}\left(\frac{y^2}{\sigma^2} + \log(2\pi\sigma^2)\right)$ with $\theta = \mu$ and $\phi = \sigma^2$ because then (12) becomes $\pi(y | \theta, \phi) = \frac{1}{\sqrt{2\pi\sigma^2}} \exp\left(-\frac{(y-\mu)^2}{2\sigma^2}\right)$. Here, the distribution of the errors is obtained by shifting the mean to $\mu = 0$. The equivalence between the distribution assumption of the economic variable and raw errors $\epsilon = y - \mu$ persists in GLMs.

The systematic component of a GLM is exactly the linear predictor $\eta = f(X)$ as defined in the linear model in (6). However, the first equality in (6) does not generally hold anymore. Instead a monotonic link function $g(\cdot)$ relates now the economic variable to the linear predictor, in literature usually formalized by $g(\mu) = \eta$, here by

$$g(\underbrace{Y(X)}_{= \mu}) \stackrel{K \leq \infty}{\approx} \underbrace{f(X)}_{= \eta} = \sum_{k=0}^{K-1} \beta_k z_k = \mathbf{z}^T \boldsymbol{\beta} \quad (13)$$

with $\mathbf{z} = (e_0(X), \dots, e_{K-1}(X))^T$. When the link function is the identity as in the normal model this extension disappears, i.e. $\mu = \eta$.

Applying a link function to the economic variable is especially appealing when the range of the linear predictor may deviate substantially from that of the economic variable. For example, an economic variable capturing service times that follow a gamma distribution can only be positive but the linear predictor may also take on negative values. With e.g. $g(\cdot) = \log(\cdot)$ such a potential inconsistency can be eliminated. Another popular choice are the canonical link functions $\tilde{g}(\cdot)$ which express the canonical parameter $\theta = \theta(X)$

with regard to the expected value $\mu = Y(X)$ if the variance is known, i.e. $\tilde{g}(\mu) = \theta$, hence due to (13) also $\theta \stackrel{K \leq \infty}{\approx} f(X)$ with $\tilde{g}(\cdot)$. For instance, the canonical link functions are $g(\mu) = \text{id}(\mu)$ for the normal, $g(\mu) = \frac{1}{\mu}$ for the gamma, and $g(\mu) = \frac{1}{\mu^2}$ for the inverse gaussian distribution.

The log-likelihood of a single observation is the logarithm of (12), i.e. $l^i(\boldsymbol{\beta}, \phi^i) = \log \pi(y^i | \theta^i, \phi^i)$ with the dependence $\theta^i = \theta^i(\mu^i(\eta^i(\boldsymbol{\beta}, x^i)))$ due to the equality $\mu = b'(\theta)$ and (13). Thus, with constant dispersion $a(\phi^i) = \phi^i = \phi$, $i = 1, \dots, N$, the GLM estimator $\hat{\boldsymbol{\beta}}_{\text{GLM}}$ of the coefficients is given as the maximizer of $l(\boldsymbol{\beta}, \phi) = \sum_{i=1}^N \log \pi(y^i | \theta^i, \phi)$, that is as the ML estimator, i.e.

$$\hat{\boldsymbol{\beta}}_{\text{GLM}} = \arg \max_{\boldsymbol{\beta} \in \mathbb{R}^K} \left\{ \sum_{i=1}^N \left(\frac{y^i \theta^i - b(\theta^i)}{\phi} + c(y^i, \phi) \right) \right\}. \quad (14)$$

While for the Poisson or binomial distribution the dispersion is taken as 1, for the other distributions from the exponential family the dispersion ϕ is unknown. Assuming a random component of the form (12) with a constant dispersion (A5), or in other words, with equal prior weights, makes the factors $a(\phi^i)$ disappear in the first-order ML condition. Using unequal prior weights might be beneficial, however it is not clear how they should be selected in the adaptive algorithm, and they would make the estimation procedure more complicated. Since the dispersion is not required for the derivation of $\hat{\boldsymbol{\beta}}_{\text{GLM}}$ in our setting, it is omitted in the IRLS algorithm described below. Once $\hat{\boldsymbol{\beta}}_{\text{GLM}}$ is known, the dispersion is estimated with the aid of the Pearson residual chi-squared statistic.

GLM Estimation via IRLS Algorithm

Under (A5), there generally does not exist a closed-form solution for the GLM coefficient estimator (14). In Ch. 2.5, McCullagh & Nelder (1989) apply Fisher's scoring method, a standard approach in log-likelihood maximization, to obtain an approximation to the GLM estimator, i.e.

$$\hat{\boldsymbol{\beta}}^{(t+1)} = \hat{\boldsymbol{\beta}}^{(t)} + I^{-1} \frac{\partial l}{\partial \boldsymbol{\beta}}. \quad (15)$$

Here, $\hat{\boldsymbol{\beta}}^{(t)}$ is the coefficient estimator in iteration t , $\frac{\partial l}{\partial \boldsymbol{\beta}}$ the score function, and $I = E \left[-\frac{\partial^2 l}{\partial \boldsymbol{\beta} \partial \boldsymbol{\beta}^T} \right]$ the Fisher information matrix (equal to the negative of the expected value of the Hessian matrix) with the expectation being taken with respect to the random component. While $\frac{\partial l}{\partial \boldsymbol{\beta}}$ depends on the regressors and response values, I depends only on the regressors due to the expectation operator. Both have to be evaluated at $\hat{\boldsymbol{\beta}}^{(t)}$. Further, McCullagh & Nelder (1989) justify how Fisher's scoring method can be cast in the form of the iteratively reweighted least squares (IRLS) algorithm. As an alternative, they suggest the Newton-Raphson method, which coincides with Fisher's scoring method if canonical link functions are used since the actual value of the Hessian matrix equals its expected value then.

The IRLS algorithm works in our context as follows. Let the dependent variable in the iterative procedure be

$$\tilde{s}^i(\hat{\beta}^{(t)}) = \hat{\eta}_{(t)}^i + (y^i - \hat{\mu}_{(t)}^i) \left(\frac{d\eta}{d\mu}(\hat{\mu}_{(t)}^i) \right), \quad (16)$$

where $\hat{\eta}_{(t)}^i = \hat{f}(x^i)$ is the estimate for the linear predictor or the proxy function evaluated at fitting scenario x^i , compare (13), where $\hat{\mu}_{(t)}^i = g^{-1}(\hat{\eta}_{(t)}^i)$ derived from $\hat{\eta}_{(t)}^i$ is the estimate for the economic variable, and $\frac{d\eta}{d\mu}(\hat{\mu}_{(t)}^i) = g'(\hat{\mu}_{(t)}^i)$ is the first derivative of the link function with respect to the economic variable evaluated at $\hat{\mu}_{(t)}^i$. Let $\hat{\mathbf{s}}^{(t)} = (\hat{s}^1(\hat{\beta}^{(t)}), \dots, \hat{s}^N(\hat{\beta}^{(t)}))^T$ denote the vector of the dependent variable over all fitting points.

Furthermore, the (quadratic) weight in the iterative procedure is given by

$$\hat{w}^i(\hat{\beta}^{(t)}) = \left(\frac{d\eta}{d\mu}(\hat{\mu}_{(t)}^i) \right)^{-2} V[\hat{\mu}_{(t)}^i]^{-1}, \quad (17)$$

where $V[\hat{\mu}_{(t)}^i]$ is the variance function from above evaluated at $\hat{\mu}_{(t)}^i$. Then the (quadratic) weight matrix is defined by $W^{(t)} = \text{diag}(w^1(\hat{\beta}^{(t)}), \dots, w^N(\hat{\beta}^{(t)}))$.

IRLS algorithm. *Perform the following iterative approximation procedure with e.g. an initialization of $\hat{\mu}_{(0)}^i = y^i + 0.1$ and $\hat{\eta}_{(0)}^i = g(\hat{\mu}_{(0)}^i)$ as proposed by Dutang (2017) until convergence:*

$$\begin{aligned} \hat{\beta}^{(t+1)} &= \arg \min_{\beta \in \mathbb{R}^K} \left\{ \sum_{i=1}^N w^i(\hat{\beta}^{(t)})^{-1} \left(\tilde{s}^i(\hat{\beta}^{(t)}) - \sum_{k=0}^{K-1} \beta_k z_{ik} \right)^2 \right\} \\ &= (Z^T W^{(t)} Z)^{-1} Z^T W^{(t)} \hat{\mathbf{s}}^{(t)}. \end{aligned} \quad (18)$$

After convergence, we have $\hat{\beta}_{\text{GLM}} = \hat{\beta}^{(t+1)}$.

For example, Green (1984) proposes to solve system $(Z^T W^{(t)} Z) \hat{\beta}^{(t+1)} = Z^T W^{(t)} \hat{\mathbf{s}}^{(t)}$ equivalent to (18) via a QR decomposition to increase numerical stability. For a practical implementation of GLMs using the IRLS algorithm, see e.g. function `glm()` in R package `stats` of R Core Team (2018).

By inserting (16), (17) and the GLM estimator into (18) and by using (13), we arrive at the property

$$\hat{\beta}_{\text{GLM}} = \arg \min_{\beta \in \mathbb{R}^K} \left\{ \sum_{i=1}^N V[\hat{\mu}_{\text{GLM}}^i] (y^i - \hat{\mu}_{\text{GLM}}^i)^2 \right\}, \quad (19)$$

that is, the GLM estimator minimizes the squared sum of raw residuals scaled by the estimated individual variances of the economic variable. The Pearson residuals are defined as the raw residuals divided by the estimated individual standard deviations, i.e.

$$\tilde{\epsilon}^i = \frac{y^i - \hat{\mu}_{\text{GLM}}^i}{\sqrt{V[\hat{\mu}_{\text{GLM}}^i]}}. \quad (20)$$

For example, in the normal model from above with mean μ and variance σ^2 , we have $b(\theta) = \frac{\theta^2}{2}$ and thus constant estimated individual variances across all observations $V[\mu] = b''(\theta) = 1$ so that no actual weighting takes place.

AIC & Dispersion Estimation

Since AIC depends on the ML estimators, it is combinable with GLMs in the adaptive algorithm. Here, it has the form

$$\text{AIC} = -2l\left(\widehat{\beta}_{\text{GLM}}, \widehat{\phi}\right) + 2(K + p), \quad (21)$$

where K is the number of coefficients and p indicates the number of the additional model parameters associated with the distribution of the random component. For instance, in the normal model, we have $p = 1$ due to the error variance/dispersion. A typical estimate of the dispersion in GLMs is the Pearson residual chi-squared statistic divided by $N - K$ as described by Zuur et al. (2009) and implemented e.g. in function $glm(\cdot)$ belonging to R package *stats*, i.e.

$$\widehat{\phi} = \frac{1}{N - K} \sum_{i=1}^N (\widehat{\epsilon}^i)^2, \quad (22)$$

with $\widehat{\epsilon}^i$ given by (20). Even though this is not the ML estimator, it is a good estimate because, if the model is specified correctly, the Pearson residual chi-squared statistic divided by the dispersion is asymptotically χ^2_{N-K} distributed and the expected value of a chi-squared distribution with $N - K$ degrees of freedom is $N - K$.

3.4 Generalized Additive Models (GAMs)

Richly Parameterized GLM with Smooth Functions

The class of generalized additive models (GAMs) was invented by Hastie & Tibshirani (1986) and Hastie & Tibshirani (1990) to unite the properties of GLMs and additive models. Based on Wood (2006), we introduce one of the most obvious applications of GAMs in the adaptive algorithm of the LSMC framework. It is conceivable that other varieties of GAMs allowing e.g. only linear basis functions of single risk factors are the more natural approach from a theoretical point of view. While GAMs inherit from GLMs the random component (12) and the link function (13), they inherit from the additive models of Friedman & Stuetzle (1981) the linear predictor with the smooth functions. In the adaptive algorithm, we apply GAMs of the form

$$g(\underbrace{Y(X)}_{= \mu}) \stackrel{K < \infty}{\approx} \underbrace{f(X)}_{= \eta} = \beta_0 + \sum_{k=1}^{K-1} h_k(z_k), \quad (23)$$

where $z_k = e_k(X)$, β_0 is the intercept and $h_k(\cdot)$, $k = 1, \dots, K - 1$, are the smooth functions to be estimated. In addition to the smooth functions, GAMs could also include

simple linear terms of the basis functions as they appear in the linear predictor of GLMs. A smooth function $h_k(\cdot)$ can be written as a basis expansion

$$h_k(z_k) = \sum_{j=1}^J \beta_{kj} b_{kj}(z_k), \quad (24)$$

with coefficients β_{kj} and known basis functions $b_{kj}(z_k)$, $j = 1, \dots, J$, which should not be confused with their arguments, namely the first-order basis functions $z_k = e_k(X)$, $k = 0, \dots, K - 1$. Slightly adjusted Figure 2 from Wood (2006) depicts an exemplary approximation of y by a GAM with a basis expansion in one dimension z_k without an intercept. The solid colorful curves represent the pure basis functions $b_{kj}(z_k)$, $j = 1, \dots, J$, the dashed colorful curves show them after scaling with the coefficients $\beta_{kj} b_{kj}(z_k)$, $j = 1, \dots, J$, and the black curve is their sum (24). Typical examples for basis functions are

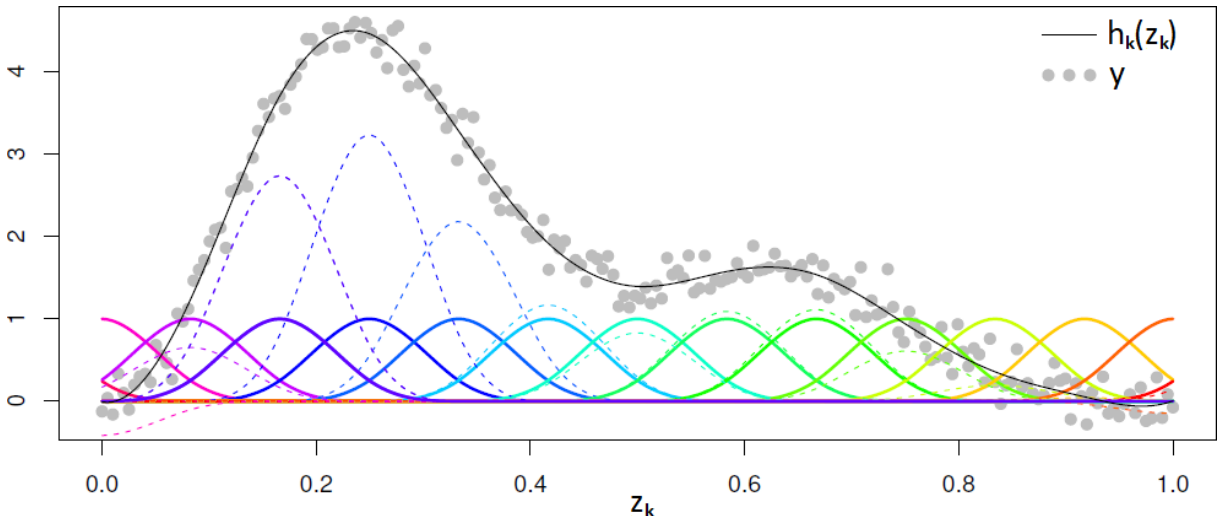


Figure 2: GAM with a basis expansion in one dimension

thin plate regression splines, duchon splines, penalized cubic regression splines or Eilers and Marx style P-splines. See e.g. function $gam(\cdot)$ in R package *mgcv* of Wood (2018) for a practical implementation of GAMs admitting these types of basis functions and using the PIRLS algorithm, which we present below.

In vector notation, we can write $\boldsymbol{\beta} = (\beta_0, \boldsymbol{\beta}_1^T, \dots, \boldsymbol{\beta}_{K-1}^T)^T$ with $\boldsymbol{\beta}_k = (\beta_{k1}, \dots, \beta_{kJ})^T$ and $\mathbf{a} = \left(1, \mathbf{b}_1(z_1)^T, \dots, \mathbf{b}_{K-1}(z_{K-1})^T\right)^T$ with $\mathbf{b}_k(z_k) = (b_{k1}(z_k), \dots, b_{kJ}(z_k))^T$, hence (23) becomes

$$\underbrace{g(Y(X))}_{= \mu} \stackrel{K < \infty}{\approx} \underbrace{f(X)}_{= \eta} = \mathbf{a}^T \boldsymbol{\beta}. \quad (25)$$

This parameterization is a richer version of (13) so that a GAM having a random component from the exponential family (12) can be viewed as a richly parameterized GLM. In order to make the smooth functions $h_k(\cdot)$, $k = 1, \dots, K - 1$, identifiable, identifiability constraints $\sum_{i=1}^N h_k(z_{ik}) = 0$ with $z_{ik} = e_k(x^i)$ can be imposed. According to Wood

(2006) this can be achieved by modification of the basis functions $b_{kj}(\cdot)$ with one of them being lost.

Let the deviance corresponding to observation y^i be $D^i(\boldsymbol{\beta}) = 2(l_{\text{sat}}^i - l^i(\boldsymbol{\beta}, \phi))\phi$ where $D^i(\boldsymbol{\beta})$ is independent of dispersion ϕ , where $l_{\text{sat}}^i = \max_{\boldsymbol{\beta}^i} l^i(\boldsymbol{\beta}^i, \phi)$ is the saturated log-likelihood and $l^i(\boldsymbol{\beta}, \phi)$ the log-likelihood. Then the model deviance can be written as $D(\boldsymbol{\beta}) = \sum_{i=1}^N D^i(\boldsymbol{\beta})$. It is a generalization of the residual sum of squares for ML estimation. For instance, in the normal model the unit deviance is $(y^i - \mu^i)^2$. For given smoothing parameters $\lambda_k > 0$, $k = 1, \dots, K-1$, the GAM estimator $\hat{\boldsymbol{\beta}}_{\text{GAM}}$ of the coefficients is defined as the minimizer of the penalized deviance

$$\begin{aligned}\hat{\boldsymbol{\beta}}_{\text{GAM}} &= \arg \min_{\boldsymbol{\beta} \in \mathbb{R}^{(K-1)J+1}} \left\{ D(\boldsymbol{\beta}) + \sum_{k=1}^{K-1} \lambda_k \int h_k''(z_k)^2 dz_k \right\}, \text{ where} \\ \int h_k''(z_k)^2 dz_k &= \boldsymbol{\beta}_k^T \left(\int \mathbf{b}_k''(z_k) \mathbf{b}_k''(z_k)^T dz_k \right) \boldsymbol{\beta}_k = \boldsymbol{\beta}_k^T \mathcal{S}_k \boldsymbol{\beta}_k\end{aligned}\quad (26)$$

are the smoothing penalties and the smoothing parameters λ_k control the trade-off between a too wiggly model (overfitting) and a too smooth model (underfitting). The larger the λ_k values are, the more pronounced is the wigginess of the basis functions reflected by their second derivatives in the minimization problem (26), and the higher is thus the penalty associated with the coefficients and the smoother is the estimated model. Similar to how we have defined the GAM estimator as the minimizer of the penalized deviance, we could have defined the GLM estimator (14) as the minimizer of the unpenalized deviance.

GAM Estimation via PIRLS Algorithm

Buja et al. (1989) proposed to estimate GAMs by a backfitting procedure which can be shown to be the Gauss-Seidel iterative method for solving a set of normal equations associated with the additive model. Their backfitting procedure works for any scatterplot smoother so that the random component does no longer have to come from the exponential family, in fact, non-parametric models such as running-mean, running-line or kernel smoothers are possible as well. However, their suggestions to select the degree of smoothness through e.g. graphical analyses or cross-validation are for practitioners still difficult to implement. Therefore, GAMs have recently been increasingly defined in the form of (23) with basis expansions (24) of which the degree of smoothness is controlled by the smoothing penalties (26). A major advantage of this definition is its compatibility with information criteria and other model selection criteria such as generalized cross-validation. Besides, the resulting penalty matrix favors numerical stability in the PIRLS algorithm.

Since the saturated log-likelihood is a constant for a fixed distribution and set of fitting points, we can turn the minimization problem (26) into the maximization task of the penalized log-likelihood, i.e.

$$\hat{\boldsymbol{\beta}}_{\text{GAM}} = \arg \max_{\boldsymbol{\beta} \in \mathbb{R}^{(K-1)J+1}} \left\{ l(\boldsymbol{\beta}, \phi) - \frac{1}{2} \sum_{k=1}^{K-1} \lambda_k \boldsymbol{\beta}_k^T \mathcal{S}_k \boldsymbol{\beta}_k \right\}. \quad (27)$$

Wood (2000) points out that Fisher's scoring method can be cast in a penalized version of the iteratively reweighted least squares (PIRLS) algorithm when being used to approximate the GAM coefficient estimator (27). This derivation is very similar to the one of the IRLS algorithm in the GLM context with the constant dispersion ϕ disappearing in the first-order condition. We formulate the PIRLS algorithm based on Marx & Eilers (1998) who indicate the iterative solution explicitly.

Let $\hat{\beta}^{(t)}$ now be the GAM coefficient approximation in iteration t . Then the vector of the dependent variable $\hat{s}^{(t)} = (\hat{s}^1(\hat{\beta}^{(t)}), \dots, \hat{s}^N(\hat{\beta}^{(t)}))^T$ and the weight matrix given by $W^{(t)} = \text{diag}(w^1(\hat{\beta}^{(t)}), \dots, w^N(\hat{\beta}^{(t)}))$ have the same form as in the IRLS algorithm, see (16) and (17). Additionally, let $S = \text{blockdiag}(0, \lambda_1 \mathcal{S}_1, \dots, \lambda_{K-1} \mathcal{S}_{K-1})$ with $S_{11} = 0$ belonging to the intercept be the penalty matrix.

PIRLS algorithm. *Perform the following iterative approximation procedure with e.g. an initialization of $\hat{\mu}_{(0)}^i = y^i + 0.1$ and $\hat{\eta}_{(0)}^i = g(\hat{\mu}_{(0)}^i)$ in analogy to the IRLS algorithm until convergence:*

$$\begin{aligned}\hat{\beta}^{(t+1)} &= \arg \min_{\beta \in \mathbb{R}^{(K-1)J+1}} \left\{ \sum_{i=1}^N w^i(\hat{\beta}^{(t)})^{-1} \left(\hat{s}^i(\hat{\beta}^{(t)}) - \beta_0 - \sum_{k=1}^{K-1} \sum_{j=1}^J \beta_{kj} b_{kj}(z_{ik}) \right)^2 + \sum_{k=1}^{K-1} \lambda_k \beta_k^T S_k \beta_k \right\} \\ &= (Z^T W^{(t)} Z + S)^{-1} Z^T W^{(t)} \hat{s}^{(t)}.\end{aligned}\quad (28)$$

After convergence, we have $\hat{\beta}_{\text{GAM}} = \hat{\beta}^{(t+1)}$.

Smoothing Parameter Selection, AIC & GCV

The smoothing parameters λ_k can be selected such that they minimize a suitable model selection criterion, for the sake of consistency preferably the one used in the adaptive algorithm for basis function selection. The GAM estimator (27) does not exactly maximize the log-likelihood, therefore AIC has another form for GAMs than for GLMs. The degrees of freedom need to be adjusted with respect to the smoothing effects of the penalties on the coefficients. The reasoning behind this adjustment is that high smoothing parameters restrict the coefficients more than low smoothing parameters and need therefore be associated with less effective degrees of freedom.

Hastie & Tibshirani (1990) propose a widely used version of AIC for GAMs, which uses effective degrees of freedom df in place of the number of coefficients $(K-1)J+1$. This is

$$\text{AIC} = -2l(\hat{\beta}_{\text{GAM}}, \hat{\phi}) + 2(\text{df} + p), \quad (29)$$

where

$$\text{df} = \text{tr}((I + S)^{-1} I). \quad (30)$$

The expression $I = Z^T W Z$ for the Fisher information matrix with the weight matrix W evaluated at the GAM estimator is obtained as a by-product when casting Fisher's scoring method in the form of the PIRLS algorithm. Without the penalty matrix S , we have

$\text{df} = \text{tr}(I^{-1}I) = (K-1)J+1$. If we follow Wood (2006) by denoting the unpenalized GAM estimator by $\widehat{\beta}_{\text{GAM}}^0$ and the so-called shrinkage matrix by $F = (Z^T W Z + S)^{-1} Z^T W Z$ with $\widehat{\beta}_{\text{GAM}} = F \widehat{\beta}_{\text{GAM}}^0$, we arrive at the equality $\text{df} = \text{tr}(F)$ revealing the shrinkage effects on the effective degrees of freedom. After convergence of the PIRLS algorithm, the dependent variable is constant, i.e. $\widehat{s} = \widehat{s}^{(t)}$, and the hat matrix H satisfies $(\widehat{\eta}^1, \dots, \widehat{\eta}^N)^T = Z \widehat{\beta}_{\text{GAM}} = H \widehat{s}$ so that $H = Z (Z^T W Z + S)^{-1} Z^T W$. Due to the cyclic property of the trace, the effective degrees of freedom can thus also be written as $\text{df} = \text{tr}(H)$. For GAMs, an estimate of the dispersion $\widehat{\phi}$ is obtained similarly to GLMs by (22). The parameter p is defined as in (21). For a refinement of (29) accounting for the uncertainty of the smoothing parameters and tending to select models less prone to overfitting, see Wood et al. (2016).

Another popular and effective smoothing parameter selection criterion invented by Craven & Wahba (1979) is generalized cross-validation (GCV), i.e.

$$\text{GCV} = \frac{ND(\widehat{\beta}_{\text{GAM}})}{(N - \text{df})^2}, \quad (31)$$

with the model deviance $D(\widehat{\beta}_{\text{GAM}})$ evaluated at the GAM estimator and the effective degrees of freedom defined just like for AIC.

Adaptive Forward Stagewise Selection & Performance

In situations where the economic variable depends on many risk factors and where large sample sizes are required to derive reliable proxy functions, the adaptive forward stepwise algorithm depicted in Figure 1 can become computationally infeasible with GAMs as opposed to e.g. GLMs. In iteration k , a GAM has $(K-1)J+1$ coefficients which need to be estimated while a GLM has only K coefficients. This difference in the estimation effort is increased further due to the iterative nature of the IRLS and PIRLS algorithms. Moreover, GAMs involve the task of optimal smoothing parameter selection. Thereby entails each smoothing parameter constellation of which the goodness-of-fit is assessed in terms of AIC or GCV not only a full coefficient estimation stream but also a quite costly evaluation of the degrees of freedom so that the estimation effort for GAMs is scaled once more tremendously.

Wood (2000) has found a way to make smoothing parameter selection more efficient. Furthermore, Wood et al. (2015) and Wood et al. (2017) have developed practical GAM fitting methods for large data sets. These methods also involve e.g. iterative update schemes which require only subblocks of the design matrix to be recomputed and parallelization. The suitable application of these methods in the adaptive algorithm is beyond the scope of this analysis though since our focus does not lie on computational performance. Besides parallelizing the candidate loop on the lower left side of Figure 1, we achieve the necessary performance gains in GAMs by replacing the stepwise algorithm by a stagewise algorithm. This means that in each iteration, a predefined number L or

proportion of candidate terms is selected simultaneously until a termination criterion is fulfilled. Thereby we select in one stage those basis functions which reduce the model selection criterion of our choice most when added separately to the current proxy function structure. When there are not at least as many basis functions as targeted, the algorithm shall be terminated after the ones which lead to a reduction in the model selection criterion have been selected.

3.5 Feasible Generalized Least-Squares (FGLS) Regression

Generalized Regression Model

While in the classical linear regression model the errors are assumed to be uncorrelated and have the same unknown variance $\sigma^2 > 0$, in the generalized regression model, they are assumed to have the covariance matrix $\Sigma = \sigma^2\Omega$ where Ω is positive definite and known and $\sigma^2 > 0$ is unknown. We transform the generalized regression model according to Hayashi (2000) to obtain a model (*) which satisfies Assumptions (A1), (A2) and (A3) of the classical linear regression model. As Ω is by construction symmetric and positive definite, there exists an invertible matrix H such that $\Omega^{-1} = H^T H$. The matrix H is not unique but this is not important since any choice of H works. The generalized response vector \mathbf{y}^* , design matrix Z^* and error vector $\boldsymbol{\epsilon}^*$ are then given by

$$\mathbf{y}^* = H\mathbf{y}, \quad Z^* = HZ, \quad \boldsymbol{\epsilon}^* = \mathbf{y}^* - Z^*\boldsymbol{\beta} = H(\mathbf{y} - Z\boldsymbol{\beta}) = H\boldsymbol{\epsilon}. \quad (32)$$

Strict exogeneity (A1) is satisfied by the transformed regression model (*) as $E[\boldsymbol{\epsilon}^* | Z^*] = HE[\boldsymbol{\epsilon} | Z] = \mathbf{0}$, the error variance is spherical (A2) because of $\Sigma^* = V[\boldsymbol{\epsilon}^* | Z^*] = HV[\boldsymbol{\epsilon} | Z]H^T = H[\sigma^2\Omega]H^T = H[\sigma^2(H^T H)^{-1}]H^T = \sigma^2 I_N$ with the N -dimensional identity matrix I_N and the no-multicollinearity assumption (A3) holds as Ω is positive definite.

In analogy to the OLS estimator, the generalized least-squares (GLS) estimator $\hat{\boldsymbol{\beta}}_{\text{GLS}}$ of the coefficients is given as the minimizer of the generalized residual sum of squares, i.e.

$$\hat{\boldsymbol{\beta}}_{\text{GLS}} = \arg \min_{\boldsymbol{\beta} \in \mathbb{R}^K} \left\{ \sum_{i=1}^N (\epsilon^{*,i})^2 \right\}. \quad (33)$$

The closed-form expression of the GLS estimator is

$$\hat{\boldsymbol{\beta}}_{\text{GLS}} = (Z^{*T}Z^*)^{-1}Z^{*T}\mathbf{y}^* = (Z^T\Omega^{-1}Z)^{-1}Z^T\Omega^{-1}\mathbf{y}, \quad (34)$$

and the proxy function becomes

$$\hat{f}(X) = \mathbf{z}^T \hat{\boldsymbol{\beta}}_{\text{GLS}}, \quad (35)$$

where $\mathbf{z} = (e_0(X), \dots, e_{K-1}(X))^T$. The scalar σ^2 can be estimated in analogy to OLS regression by $s_{\text{GLS}} = \frac{1}{N-K} \hat{\boldsymbol{\epsilon}}^{*T} \hat{\boldsymbol{\epsilon}}^*$ where $\hat{\boldsymbol{\epsilon}}^* = \mathbf{y}^* - Z^* \hat{\boldsymbol{\beta}}_{\text{GLS}}$ is the residual vector.

Gauss-Markov-Aitken Theorem & ML Estimation

We formulate the Gauss-Markov-Aitken theorem conditional on the fitting scenarios in line with Huang (1970) and Hayashi (2000) under the assumptions of strict exogeneity (A1), no multicollinearity (A3) and a covariance matrix $\Sigma = \sigma^2\Omega$ of which Ω is positive definite and known (A6).

Gauss-Markov-Aitken theorem. *The GLS estimator is the BLUE of the coefficients in the generalized regression model (7) under Assumptions (A1), (A3) and (A6).*

In order to make AIC and GLS regression combinable, we assume additionally to (A1), (A3) and (A6) that the economic variable, or equivalently the errors, are jointly normally distributed conditional on the fitting scenarios (A7). The transformation (*) transfers to the ML function of the generalized regression model so that we can state the following theorem in analogy to Theorem 1, see e.g. Hartmann (2015).

Theorem 2. *The ML coefficient estimator coincides with the GLS coefficient estimator and the ML estimator of the scalar $\widehat{\sigma}^2$ can be expressed as $\frac{N}{N-K}$ times s_{GLS} , i.e. $\widehat{\sigma}^2 = \frac{1}{N}\widehat{\epsilon}^{*T}\widehat{\epsilon}^*$, under Assumptions (A1), (A3), (A6) and (A7).*

Moreover, the GLS estimator is the efficient estimator under these assumptions according to Greene (2002).

FGLS Estimation via ML Algorithm

In the LSMC framework, Ω is unknown. If a consistent estimator $\widehat{\Omega}$ exists, we can apply feasible generalized least-squares (FGLS) regression, of which the estimator

$$\widehat{\beta}_{\text{FGLS}} = \left(Z^T \widehat{\Omega}^{-1} Z \right)^{-1} Z^T \widehat{\Omega}^{-1} \mathbf{y} \quad (36)$$

has asymptotically the same properties as the GLS estimator (34). Greene (2002) remarks furthermore that the asymptotic efficiency of the FGLS estimator does not carry over to finite samples. In small sample studies with no severe heteroscedasticity, the OLS estimator has been shown to be sometimes more efficient than the FGLS estimator. However, if heteroscedasticity is more severe, the FGLS estimator has been shown to outperform the OLS estimator. With $\mathbf{z} = (e_0(X), \dots, e_{K-1}(X))^T$ the FGLS proxy function is then given as

$$\widehat{f}(X) = \mathbf{z}^T \widehat{\beta}_{\text{FGLS}}. \quad (37)$$

Without loss of generality, we set $\sigma^2 = 1$ so that $\Sigma = \Omega$ and refer to Σ in the following. Hereby, any specification of $\sigma^2 > 0$ is possible as long as Ω is rescaled accordingly so that $\Sigma = \sigma^2\Omega$ is satisfied since the GLS and FGLS coefficient estimators are invariant to a scaling of Ω and $\widehat{\Omega}$, respectively. Furthermore, we assume in addition to (A1), (A3) and (A7) that the elements of the covariance matrix Σ are twice differentiable functions of parameters $\boldsymbol{\alpha} = (\alpha_0, \dots, \alpha_{M-1})^T$ with $K + M \leq N$ so that we can write $\Sigma = \Sigma(\boldsymbol{\alpha})$

(A8). Theorem 1 of Magnus (1978) characterizes the ML estimators $\hat{\beta}_{\text{ML}}$ and $\hat{\alpha}_{\text{ML}}$ under these assumptions. We will relate the FGLS coefficient estimator to the ML coefficient estimator later in this section.

Theorem 3. *The generalized regression model (7) under Assumptions (A1), (A3), (A7) and (A8) has the following first-order ML conditions:*

$$\hat{\beta}_{\text{ML}} = \left(Z^T \hat{\Sigma}^{-1} Z \right)^{-1} Z^T \hat{\Sigma}^{-1} \mathbf{y}, \quad (38)$$

$$\frac{\partial l}{\partial \alpha_m} = \frac{1}{2} \text{tr} \left(\frac{\partial \Sigma^{-1}}{\partial \alpha_m} \Sigma \right)_{\alpha=\hat{\alpha}_{\text{ML}}} - \frac{1}{2} \hat{\epsilon}^T \left(\frac{\partial \Sigma^{-1}}{\partial \alpha_m} \right)_{\alpha=\hat{\alpha}_{\text{ML}}} \hat{\epsilon} = 0, \quad (39)$$

where $m = 0, \dots, M-1$, $\hat{\Sigma} = \Sigma(\hat{\alpha}_{\text{ML}})$ and $\hat{\epsilon} = \mathbf{y} - Z \hat{\beta}_{\text{ML}}$.

Since the system in (38) and (39) typically does not have a closed-form solution, we suggest to solve it iteratively, e.g. according to Magnus (1978). We start the procedure with $\beta^{(0)}$ instead of with an arbitrary admissible vector $\alpha^{(0)}$ though. The vector $\hat{\alpha}^{(t+1)}$ can be estimated iteratively conditional on $\hat{\epsilon}^{(t+1)}$, that is, $\beta^{(t)}$ e.g. by using PORT optimization routines as described in Gay (1990) and implemented in function *nlinmb*(\cdot) belonging to R package *stats* of R Core Team (2018). In this iterative routine, $\hat{\alpha}^{(t+1)}$ can be initialized e.g. by random numbers from the standard normal distribution.

ML algorithm. *Perform the following iterative approximation procedure with e.g. an initialization of $\hat{\beta}^{(0)} = \hat{\beta}_{\text{OLS}}$ until convergence:*

1. Calculate the residual vector $\hat{\epsilon}^{(t+1)} = \mathbf{y} - Z \hat{\beta}^{(t)}$.
2. Substitute $\hat{\epsilon}^{(t+1)}$ into the M equations in M unknowns α_m given by (39) and solve them. If an explicit solution exists, set $\hat{\alpha}^{(t+1)} = \alpha(\hat{\epsilon}^{(t+1)})$. Otherwise, select the maximum likelihood solution $\hat{\alpha}^{(t+1)}$ iteratively, e.g. by using PORT optimization routines.
3. Calculate

$$\begin{aligned} \hat{\Sigma}^{(t+1)} &= \Sigma(\hat{\alpha}^{(t+1)}), \\ \hat{\beta}^{(t+1)} &= \left(Z^T \left(\hat{\Sigma}^{(t+1)} \right)^{-1} Z \right)^{-1} Z^T \left(\hat{\Sigma}^{(t+1)} \right)^{-1} \mathbf{y}. \end{aligned} \quad (40)$$

Continue with the next iteration.

After convergence, we have $\hat{\beta}_{\text{ML}} = \hat{\beta}^{(t+1)}$ and $\hat{\alpha}_{\text{ML}} = \hat{\alpha}^{(t+1)}$.

Theorem 5 of Magnus (1978) states some regularity conditions guaranteeing the consistency of the ML estimators. Then $\hat{\Sigma} = \Sigma(\hat{\alpha}_{\text{ML}})$ is a consistent estimator so that the ML coefficient estimator (38) provides the FGLS coefficient estimator (36).

Theorem 4. *The FGLS coefficient estimator can be derived as the ML coefficient estimator by the ML algorithm under Assumptions (A1), (A3), (A7) and (A8) and some further regularity conditions stated in Theorem 5 of Magnus (1978).*

Heteroscedasticity & Breusch-Pagan Test

Besides Assumption (A8) about the structure of the covariance matrix, we assume that the errors are uncorrelated with further on different variances (= heteroscedastic errors), i.e. $\Sigma = \text{diag}(\sigma_1^2, \dots, \sigma_N^2)$. We model each variance σ_i^2 , $i = 1, \dots, N$, by a twice differentiable function in dependence of parameters $\boldsymbol{\alpha} = (\alpha_0, \dots, \alpha_{M-1})^T$ and a suitable set of linear independent basis functions $e_m(X) \in L^2(\mathbb{R}^D, \mathcal{B}, \mathbb{P}')$, $m = 0, 1, \dots, M-1$, with $\mathbf{v}^i = (e_0(x^i), \dots, e_{M-1}(x^i))^T$, i.e.

$$\sigma_i^2 = \sigma^2 V[\boldsymbol{\alpha}, \mathbf{v}^i], \quad (41)$$

where $V[\boldsymbol{\alpha}, \mathbf{v}^i]$ is referred to as the variance function in analogy to $V[\mu]$ for GLMs and GAMs. Without loss of generality, we set again $\sigma^2 = 1$.

Hartmann (2015) has already applied FGLS regression with different variance models in the LSMC framework. In her numerical examples, variance models with multiplicative heteroscedasticity led to the best performance of the proxy function in the validation. Therefore, we restrict our analysis on these kinds of structures, compare e.g. Harvey (1976), i.e.

$$V[\boldsymbol{\alpha}, \mathbf{v}^i] = \exp(\mathbf{v}^{iT} \boldsymbol{\alpha}). \quad (42)$$

We should only apply FGLS regression as a substitute of OLS regression if heteroscedasticity prevails. If the variance function has the structure

$$V[\boldsymbol{\alpha}, \mathbf{v}^i] = h(\mathbf{v}^{iT} \boldsymbol{\alpha}), \quad (43)$$

where the function $h(\cdot)$ is twice differentiable and the first element of \mathbf{v}^i is $v_0^i = 1$, the Breusch-Pagan test of Breusch & Pagan (1979) can be used to diagnose heteroscedasticity under the assumption of normally distributed errors. We use it in the numerical computations to check if heteroscedasticity still prevails during the iterative procedure.

Variance Model Selection & AIC

Like the proxy function, the variance function (42) has to be calibrated to apply FGLS regression, which means that the variance function has to be composed of suitable basis functions. Again, such a composition can be found with the aid of a model selection criterion. We stick to AIC but have to take care of the fact that the covariance matrix has now M unknown parameters instead of only one as in the OLS case (the same variance for all observations). Under Assumption (A7), AIC is given as

$$\begin{aligned} \text{AIC} &= -2l(\widehat{\boldsymbol{\beta}}_{\text{FGLS}}, \widehat{\Sigma}) + 2(K + M) \\ &= N \log(2\pi) + \log(\det \widehat{\Sigma}) + (\mathbf{y} - Z\widehat{\boldsymbol{\beta}}_{\text{FGLS}})^T \widehat{\Sigma}^{-1} (\mathbf{y} - Z\widehat{\boldsymbol{\beta}}_{\text{FGLS}}) + 2(K + M). \end{aligned} \quad (44)$$

When using a variance model with multiplicative heteroscedasticity, AIC becomes

$$\text{AIC} = N \log(2\pi) + \left(\sum_{i=1}^N \mathbf{v}^{iT} \right) \widehat{\boldsymbol{\alpha}} + \sum_{i=1}^N \exp(-\mathbf{v}^{iT} \widehat{\boldsymbol{\alpha}}) (\widehat{\epsilon}^i)^2 + 2(K + M). \quad (45)$$

As an alternative or complement, the basis functions of the variance model can be selected with respect to their correlations with the final OLS residuals or based on graphical residual analysis.

A difficulty of variance model selection poses its potential interdependency with proxy function selection because the basis functions minimizing the model selection criterion when being added to the proxy function might depend on the selected basis functions of the variance model and vice versa. There are multiple ways to tackle the interdependency difficulty, compare Hartmann (2015), of which we implement two variants with rather short run times and promising out-of-sample validation performances. Our type I variant starts with the derivation of the proxy function by the standard adaptive OLS regression approach and then selects the variance model adaptively from the set of proxy basis functions of which the exponents sum up to at most two. The type II variant builds on the type I algorithm by taking the resulting variance model as given in its adaptive proxy basis function selection procedure with FGLS regression in each iteration.

3.6 Multivariate Adaptive Regression Splines (MARS)

OLS Regression/GLM with Hinge Functions

The multivariate adaptive regression splines (MARS) were introduced by Friedman (1991). We describe the standard MARS algorithm in the LSMC routine by Ch. 9.4 of Hastie et al. (2017). The building blocks of MARS proxy functions are reflected pairs of piecewise linear functions with knots t as depicted in Figure 3, i.e.

$$\begin{aligned} (X_d - t)_+ &= \max(X_d - t, 0), \\ (t - X_d)_+ &= \max(t - X_d, 0), \end{aligned} \quad (46)$$

where the X_d , $d = 1, \dots, D$, represent the risk factors which form together the outer scenario $X = (X_1, \dots, X_D)^T$.

For each risk factor, reflected pairs with knots at each fitting scenario stress x_d^i , $i = 1, \dots, N$, are defined. All pairs are united in the following collection serving as the initial candidate term set of the MARS algorithm, i.e.

$$C_1 = \{(X_d - t)_+, (t - X_d)_+\}_{t \in \{x_d^1, x_d^2, \dots, x_d^N\} \mid d=1, \dots, D}. \quad (47)$$

We call the elements of such a collection hinge functions and write them as functions $h(X)$ over the entire input space \mathbb{R}^D . The initial set C_1 contains in total $2DN$ basis functions.

The classical MARS model is a form of the classical linear regression model (7), where the basis functions $e_k(x^i)$ are hinge functions. Therefore, the theory of OLS regression applies in this context. However, the theory about AIC cannot be transferred without any adjustments since the notion of the degrees of freedom has to be reconsidered due to the knots in the hinge functions acting as additional degrees of freedom. Since GLMs

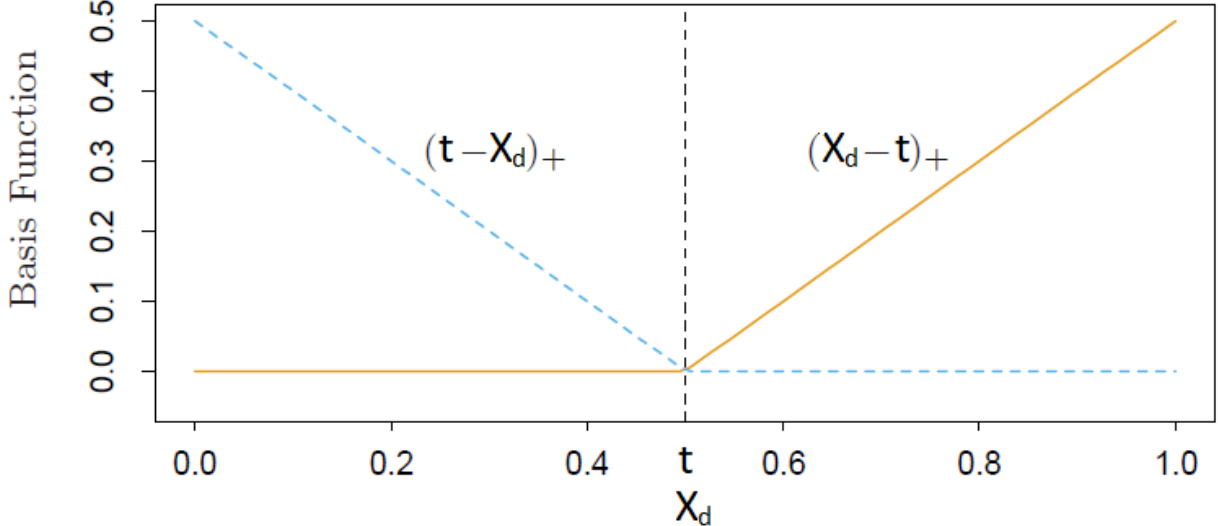


Figure 3: Reflected pair of piecewise linear functions with a knot at t

(13) are generalizations of the classical linear regression model, they can also be applied in conjunction with MARS models which we refer to in the following as generalized MARS models. In these cases, the theory of GLMs applies but again with the exception of the AIC part.

An especially fast MARS algorithm was developed by Friedman (1993) and is implemented e.g. in function *earth*(\cdot) of R package *earth* provided by Milborrow (2018).

Adaptive Forward Stepwise Selection & Forward Pass

The forward pass of the MARS algorithm can be viewed as a variation of the adaptive forward stepwise algorithm depicted in Figure 1. The start proxy function consists only of the intercept, i.e. $h_0(X) = 1$. In the classical MARS model, the regression method of choice is the standard OLS regression approach with the estimator (8), where in each iteration a reflected pair of hinge functions is selected instead of $e_k(x^i)$. Similarly, the regression method of choice in the generalized MARS model is the IRLS algorithm (18). Let us denote the MARS coefficient estimator by $\hat{\beta}_{\text{MARS}}$. As the model selection criterion serves the residual sum of squares, or equivalently, the negative of R squared.

After each iteration, the set of candidate terms is extended by the products of the last two selected hinge functions with all hinge functions in C_1 depending on risk factors the two selected hinge functions do not depend on. Let the reflected pair selected in the first iteration ($k = 1$) be

$$\begin{aligned} h_1(X) &= (X_{d_1} - t_1)_+, \\ h_2(X) &= (t_1 - X_{d_1})_+. \end{aligned} \tag{48}$$

Further, let $C_{1,-} = C_1 \setminus \{h_1(X), h_2(X)\}$. Then, the set of candidate terms is updated at

the beginning of the second iteration ($k = 2$) such that

$$\begin{aligned} C_2 = C_{1,-} \cup & \left\{ (X_d - t)_+ h_1(X), (t - X_d)_+ h_1(X) \right\}_{t \in \{x_d^1, x_d^2, \dots, x_d^N\} \mid d=1, \dots, D, d \neq d_1} \\ & \cup \left\{ (X_d - t)_+ h_2(X), (t - X_d)_+ h_2(X) \right\}_{t \in \{x_d^1, x_d^2, \dots, x_d^N\} \mid d=1, \dots, D, d \neq d_1}. \end{aligned} \quad (49)$$

The second set C_2 contains thus $2(DN - 1) + 4(D - 1)N$ basis functions. Often, the order of interaction is limited to improve the interpretability of the proxy functions. Besides the maximum allowed number of terms, a minimum threshold for the decrease in the residual sum of squares can be employed as a termination criterion in the forward pass. Typically, the proxy functions generated in the forward pass overfit the data since model complexity is only penalized conservatively by stipulating a maximum number of basis functions and a minimum threshold.

Backward Pass & GCV

Due to the overfitting tendency of the proxy function generated in the forward pass, a backward pass is executed afterwards. Apart from the direction and slight differences, the backward pass works like the forward pass. In each iteration, the hinge function of which the removal causes the smallest increase in the residual sum of squares is removed and the backward model selection criterion for the resulting proxy function evaluated. By this backward procedure, we generate the “best” proxy functions of each size in terms of the residual sum of squares. Out of all these best proxy functions, we finally select the one which minimizes the backward model selection criterion. As a result, the final proxy function will not only contain reflected pairs of hinge functions but also single hinge functions of which the complements have been removed. Optionally, the backward pass can be omitted or alternatives to the pure backward adaptive algorithm such as combinations with forward steps can be implemented.

Let the number of basis functions in the MARS model be K , the number of knots T and the smoothing parameter c . The standard choice for the backward model selection criterion is GCV, compare its definition (31) for GAMs, i.e.

$$GCV = \frac{ND(\hat{\beta}_{MARS})}{(N - df)^2}, \quad (50)$$

with the effective degrees of freedom $df = K + cT$. For cases in which no interaction terms are allowed, Friedman & Silverman (1989) give a mathematical argument for using $c = 2$. For the other cases, Friedman (1991) concludes from a wide variety of simulation studies that a parameter of $c = 3$ is fairly effective. Across all these studies, $2 \leq c \leq 4$ was found to give the best value of c . Alternatively, but with significantly higher computational costs, c could be estimated by resampling techniques such as bootstrapping by Efron (1983) or cross-validation by Stone (1974). Since comparably few basis functions are selected in the forward passes of our numerical MARS experiments, we set $c = 0$.

3.7 Kernel Regression

One-Dimensional LC & LL Regression

Independently from each other, Nadaraya (1964) and Watson (1964) both proposed to estimate a conditional expectation of a variable relative to another variable by a non-parametric regression approach using a kernel as a weighting function. In the following, we describe at first local constant (LC) regression and local linear regression (LL) in one dimension by Ch. 6 of Hastie et al. (2017). In the next sections, we refer to Ch. 2 of Li & Racine (2007) for LC and LL regression in more dimensions and suitable model selection criteria.

We start with LC and LL regression in one dimension to carve out the idea of kernel regression, which generalizes very naturally to more dimensions. For now, let the target scenario be $x_0 \in \mathbb{R}$ and let the univariate kernel with given bandwidth $\lambda > 0$ be

$$K_\lambda(x_0, x^i) = D\left(\frac{|x^i - x_0|}{\lambda}\right), \quad (51)$$

where $D(\cdot)$ denotes the specified kernel function. While e.g. the Epanechnikov (see the yellow shaded areas of Figure 4 from Hastie et al. (2017)), tri-cube and uniform kernels are commonly used kernel functions with bounded support, the gaussian kernel is one with infinite support. Moreover, the kernels can be defined with different orders, often the second order kernels are used, see e.g. Li & Racine (2007). The LC kernel estimator or Nadaraya-Watson kernel smoother is given as the kernel-weighted average at each x_0 , i.e.

$$\hat{f}_{\text{LC}}(x_0) = \hat{\beta}_{\text{LC}}(x_0) = \frac{\sum_{i=1}^N K_\lambda(x_0, x^i) y^i}{\sum_{i=1}^N K_\lambda(x_0, x^i)}. \quad (52)$$

It is a continuous function since the weights die off smoothly with increasing distance from x_0 . As this locally constant function varies over the domain of the target scenarios x_0 , it needs to be estimated separately at all of them. Due to the asymmetry of the kernels at the boundaries of the domain, the LC kernel estimator (52) can be severely biased in that region, see the left panel of Figure 4.

We can overcome this problem by fitting locally linear functions instead of locally constant functions, see the right panel of Figure 4. At each target x_0 , the LL kernel estimator is defined as the minimizer of the kernel-weighted residual sum of squares, i.e.

$$\hat{\beta}_{\text{LL}}(x_0) = \arg \min_{\boldsymbol{\beta}(x_0) \in \mathbb{R}^2} \left\{ \sum_{i=1}^N K_\lambda(x_0, x^i) (y^i - \beta_0(x_0) - \beta_1(x_0) x^i)^2 \right\}, \quad (53)$$

with $\boldsymbol{\beta}(x_0) = (\beta_0(x_0), \beta_1(x_0))^T$. If we omit the linear term in (53) by setting $\beta_1 = 0$, the intercept $\hat{\beta}_{\text{LL},0}(x_0)$ of the LL kernel estimator becomes the LC kernel estimator (52). The proxy function at x_0 is given by

$$\hat{f}_{\text{LL}}(x_0) = \hat{\beta}_{\text{LL},0}(x_0) + \hat{\beta}_{\text{LL},1}(x_0) x_0. \quad (54)$$

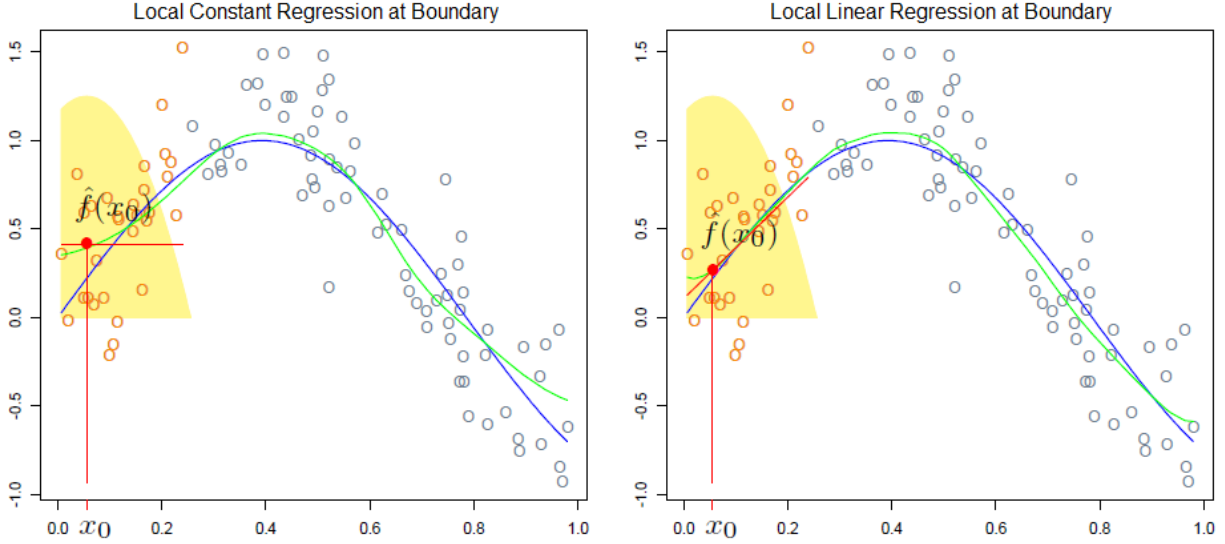


Figure 4: LC and LL kernel regression using the Epanechnikov kernel with $\lambda = 0.2$ in one dimension

In analogy to LC regression, the minimization problem (53) must be solved separately for all target scenarios so that the coefficients of the proxy function vary across their domain. Each proxy function is only evaluated at the target scenario it has been derived for. Since (53) is a weighted least-squares (WLS) problem with weights $K_\lambda(x_0, x^i)$, its solution is the WLS estimator

$$\hat{\beta}_{\text{LL}}(x_0) = (Z^T W(x_0) Z)^{-1} Z^T W(x_0) \mathbf{y}, \quad (55)$$

where \mathbf{y} is the response vector, $W(x_0) = \text{diag}(K_\lambda(x_0, x^1), \dots, K_\lambda(x_0, x^N))$ the weight matrix and Z the design matrix which contains row-wise the vectors $(1, x^i)^T$. We call H the hat matrix if $\hat{\mathbf{y}} = H\mathbf{y}$ such that $\hat{\mathbf{y}} = (\hat{f}_{\text{LL}}(x^1), \dots, \hat{f}_{\text{LL}}(x^N))^T$ contains the proxy function values at their target scenarios.

When we use proxy functions in LL regression that are composed of polynomial basis functions with exponents greater than one, we could also speak of local polynomial regression.

Multidimensional LC & LL Regression

We generalize LC regression to \mathbb{R}^K by expressing the kernel with respect to the basis function vector $\mathbf{z} = (e_0(X), \dots, e_{K-1}(X))^T$ following from the adaptive forward stepwise selection with OLS regression and small K_{\max} . At each target scenario vector $\mathbf{z}_0 \in \mathbb{R}^K$ with elements z_{0k} , basis function vector $\mathbf{z}^i \in \mathbb{R}^K$ with elements z_{ik} evaluated at fitting scenario x^i and given bandwidth vector $\boldsymbol{\lambda} = (\lambda_0, \dots, \lambda_{K-1})^T$, the multivariate kernel is defined as the product of univariate kernels, i.e.

$$K_{\boldsymbol{\lambda}}(\mathbf{z}_0, \mathbf{z}^i) = \prod_{k=0}^{K-1} D\left(\frac{|z_{ik} - z_{0k}|}{\lambda_k}\right). \quad (56)$$

The LC kernel estimator or Nadaraya-Watson kernel smoother in \mathbb{R}^K is defined at each \mathbf{z}_0 as

$$\hat{f}_{\text{LC}}(\mathbf{z}_0) = \hat{\beta}_{\text{LC}}(\mathbf{z}_0) = \frac{\sum_{i=1}^N K_{\lambda}(\mathbf{z}_0, \mathbf{z}^i) y^i}{\sum_{i=1}^N K_{\lambda}(\mathbf{z}_0, \mathbf{z}^i)}. \quad (57)$$

Since we let $e_0(X)$ represent the intercept so that $z_{i0} = z_{00} = 1$, the corresponding univariate kernel $D\left(\frac{|z_{i0}-z_{00}|}{\lambda_0}\right) = D(0)$ is constant over all fitting points, cancels thus out in (57) and can be omitted in (56).

The LL kernel estimator in \mathbb{R}^K is given as the multidimensional analogue of (53) at each \mathbf{z}_0 , i.e.

$$\hat{\beta}_{\text{LL}}(\mathbf{z}_0) = \arg \min_{\boldsymbol{\beta}(\mathbf{z}_0) \in \mathbb{R}^K} \left\{ \sum_{i=1}^N K_{\lambda}(\mathbf{z}_0, \mathbf{z}^i) (y^i - \mathbf{z}^{i,T} \boldsymbol{\beta}(\mathbf{z}_0))^2 \right\}, \quad (58)$$

with $\boldsymbol{\beta}(\mathbf{z}_0) = (\beta_0(\mathbf{z}_0), \dots, \beta_{K-1}(\mathbf{z}_0))^T$ and the proxy function at \mathbf{z}_0 is given by

$$\hat{f}_{\text{LL}}(\mathbf{z}_0) = \mathbf{z}_0^T \hat{\boldsymbol{\beta}}_{\text{LL}}(\mathbf{z}_0). \quad (59)$$

The LL kernel estimator can again be computed by WLS regression, i.e.

$$\hat{\boldsymbol{\beta}}_{\text{LL}}(\mathbf{z}_0) = (Z^T W(\mathbf{z}_0) Z)^{-1} Z^T W(\mathbf{z}_0) \mathbf{y}, \quad (60)$$

where $W(\mathbf{z}_0) = \text{diag}(K_{\lambda}(\mathbf{z}_0, \mathbf{z}^1), \dots, K_{\lambda}(\mathbf{z}_0, \mathbf{z}^N))$ is the weight matrix and Z the design matrix containing row-wise the vectors $\mathbf{z}^{i,T}$. The hat matrix H satisfies $\hat{\mathbf{y}} = H\mathbf{y}$ with $\hat{\mathbf{y}} = (\hat{f}_{\text{LL}}(\mathbf{z}^1), \dots, \hat{f}_{\text{LL}}(\mathbf{z}^N))^T$ containing the proxy function values at their target scenario vectors.

Bandwidth Selection, AIC & LOO-CV

The bandwidths λ_k in kernel regression can be selected similarly to the smoothing parameters in GAMs by minimization of a suitable model selection criterion. In fact, kernel smoothers can be interpreted as local non-parametric GLMs with identity link functions. More precisely, at each target scenario the kernel smoother can be viewed as a GLM (13) where the parametric weights $V[\hat{\mu}_{\text{GLM}}^i]$ in (19) are the non-parametric kernel weights $K_{\lambda}(\mathbf{z}_0, \mathbf{z}^i)$ in (58). Since GLMs are special cases of GAMs and the bandwidths in kernel regression can be understood as smoothing parameters, kernel smoothers and GAMs are sometimes lumped together in one category. If the numbers N of the fitting points and K of the basis functions are large, from a computational perspective it might be beneficial to perform bandwidth selection based on a reduced set of fitting points.

Hurvich et al. (1998) propose to select the bandwidths $\lambda_1, \dots, \lambda_{K-1}$ based on an improved version of AIC which works in the context of non-parametric proxy functions that can be written as linear combinations of the observations. It has the form

$$\text{AIC} = \log(\hat{\sigma}^2) + \frac{1 + \text{tr}(H)/N}{1 - (\text{tr}(H) + 2)/N}, \quad (61)$$

where $\hat{\sigma}^2 = \frac{1}{N} (\mathbf{y} - \hat{\mathbf{y}})^T (\mathbf{y} - \hat{\mathbf{y}})$ and H is the hat matrix.

As an alternative, non-parametric leave-one-out cross-validation (LOO-CV) is suggested by Li & Racine (2004) for bandwidth selection. Let us refer to

$$\widehat{\boldsymbol{\beta}}_{\text{LL},-j}(\mathbf{z}_0) = \arg \min_{\boldsymbol{\beta}(\mathbf{z}_0) \in \mathbb{R}^K} \left\{ \sum_{i \neq j, i=1}^N K_{\lambda}(\mathbf{z}_0, \mathbf{z}^i) (y^i - \mathbf{z}^{i,T} \boldsymbol{\beta}(\mathbf{z}_0))^2 \right\} \quad (62)$$

as the leave-one-out LL kernel estimator and to $\widehat{f}_{\text{LL},-j}(\mathbf{z}_0) = \mathbf{z}_0^T \widehat{\boldsymbol{\beta}}_{\text{LL},-j}(\mathbf{z}_0)$ as the leave-one-out proxy function at \mathbf{z}_0 . The objective of LOO-CV is to choose the bandwidths $\lambda_1, \dots, \lambda_{K-1}$ which minimize

$$\text{CV} = \frac{1}{N} \sum_{i=1}^N (y^i - \widehat{f}_{\text{LL},-i}(\mathbf{z}_0))^2. \quad (63)$$

Adaptive Forward Stepwise OLS Selection

A practical implementation of kernel regression can be found e.g. in the combination of functions *npreg()* and *npregbw()* from R package *np* of Racine & Hayfield (2018).

In the other sections, basis function selection depends on the respective regression methods. Since the crucial process of bandwidth selection in kernel regression takes a very long time in the implementation of our choice, it would be infeasible to proceed here in the same way. Therefore, we derive the basis functions for LC and LL regression by adaptive forward stepwise selection based on OLS regression, by risk factor wise linear selection or a combination thereof. Thereby, we keep the maximum allowed number of terms K_{\max} rather small as we aim to model the subtleties by kernel regression.

4 Numerical Experiments

4.1 General Remarks

Data Basis

In our slightly disguised real-world example, the life insurance company has a portfolio with a large proportion of traditional annuity business. In order to challenge the regression techniques, the traditional annuity business features by construction very high interest rate guarantees so that the insurer suffers huge losses in low interest rate environments. We let the insurance company be exposed to $D = 15$ relevant financial and actuarial risk factors. For the derivation of the fitting points, we run its CFP model conditional on $N = 25,000$ fitting scenarios with each of these outer scenarios entailing two antithetic inner simulations. The Sobol validation set is generated based on $L = 51$ validation scenarios with 1,000 inner simulations, where the 51 scenarios comprise 26 Sobol scenarios, 16 one-dimensional risk scenarios and 9 scenarios that turned out to be capital region scenarios in the previous year risk capital calculations. The nested simulations set which is due to its high computational costs not available in the regular LSMC approach reflects the

highest 5% real-world losses and is based on $L = 1,638$ outer scenarios with respectively 4,000 inner simulations. From the 1,638 real-world scenarios, 14 exhibit extreme stresses far beyond the bounds of the fitting space and are therefore excluded from the analysis. The capital region set consists of the $L = 129$ nested simulations points which correspond to the nested simulations SCR estimate ($= 99.5\%$ highest loss) and the 64 losses above and below ($= 99.3\%$ to 99.7% highest losses).

Validation Figures

We will output validation figure (1) with respect to the relative and asset metric, and figures (2), (3) and (4). While figures (3) and (4) are evaluated with respect to a base value resulting from 1,000 inner simulations on the Sobol set, i.e. $v.mae^0$, $v.res^0$, they are computed with respect to a base value resulting from 16,000 inner simulations on the nested simulations set, i.e. $ns.mae^0$, $ns.res^0$, and capital region set, i.e. $cr.mae^0$, $cr.res^0$. The latter base value is supposed to be the more reliable validation value since it is the one associated with a lower standard error. Therefore it is worth noting here that figure $v.res^0$ can easily be transformed such that it is also evaluated with respect to the latter base value by subtracting from it the difference of 14 which the two different base values incur. We will not explicitly state the base residual (5) as it is just (2) minus (4).

Economic Variables

We derive the OLS proxy functions for two economic variables, namely for the best estimate of liabilities (BEL) and the available capital (AC) over a one-year risk horizon, i.e. $Y(X) \in \{BEL(X), AC(X)\}$. Their approximation quality is assessed by validation figures (1) with respect to the relative and asset metric and (2). Essentially, AC is obtained as the market value of assets minus BEL, which means that AC reflects the negative behavior of BEL. Therefore, we will only derive BEL proxy functions with the other regression methods. The profit resulting from a certain risk constellation captured by an outer scenario X can be computed as $AC(X)$ minus the base AC. Validation figures (3) and (4) address the approximation quality of this difference. Taking the negative of the profit yields the loss and evaluating the loss at all real-world scenarios the real-world loss distribution from which the SCR is derived as the 99.5% value-at-risk. The out-of-sample performances of two different OLS proxy functions of BEL on the Sobol, nested simulations and capital region sets serve as the benchmark for the other regression methods.

Numerical Stability

Let us discuss the subject of numerical stability of QR decompositions in the OLS regression design under a monomial basis. If the weighting in the weighted least-squares problems associated with GLMs, heteroscedastic FGLS regression and kernel regression is

good-natured, similar arguments apply as they can also be solved via QR decompositions according to Green (1984) where the weighting is just a scaling. However, the weighting itself raises additional numerical questions that need to be taken into consideration when making the regression design choices. In GLMs, these choices are the random component (12) and link function (13), in FGLS regression it is the functional form of the heteroscedastic variance model (41) and in kernel regression it is the kernel function (56). The following arguments do not apply to GAMs and MARS models as these are constructed out of spline functions, see (24) and (46), respectively. In GAMs, the penalty matrix increases numerical stability.

McLean (2014) justifies that from the perspective of numerical stability performing a QR decomposition on a monomial design matrix Z is asymptotically equivalent to using a Legendre design matrix Z' and transforming the resulting coefficient estimator into the monomial one. Under the assumption of an orthonormal basis, Weiß & Nikolić (2018) have derived an explicit upper bound for the condition number of non-diagonal matrix $\frac{1}{N}(Z')^T(Z')$ for $N < \infty$, where the factor $\frac{1}{N}$ is used for technical reasons. This upper bound increases in (1) the number of basis functions, (2) the Hardy-Krause variation of the basis, (3) the convergence constant of the low-discrepancy sequence, and (4) the outer scenario dimension. Our previously defined type of restriction setting controls aspect (1) through the specification of K_{\max} and aspect (2) through the limitation of exponents $d_1 d_2 d_3$. Aspects (3) and (4) are beyond the scope of the calibration and validation steps of the LSMC framework and therefore left aside here.

Interpolation & Extrapolation

In the LSMC framework, let us refer by interpolation to prediction inside the fitting space and by extrapolation to prediction outside the fitting space. Runge (1901) found that high-degree polynomial interpolation at equidistant points can oscillate toward the ends of the interval with the approximation error getting worse the higher the degree is. In a least-squares problem, Runge's phenomenon was shown by Dahlquist & Björck (1974) not to apply to polynomials of degree d fitted based on N equidistant points if the inequality $d < 2\sqrt{N}$ holds. With $N = 25,000$ fitting points the inequality becomes $d < 316$ so that we clearly do not have to impose any further restrictions in OLS, FGLS and kernel regression as well as in GLMs to keep this phenomenon under control. Splines as they occur in GAMs and MARS models do not suffer from this oscillation issue by construction.

Since Runge's phenomenon concerns the ends of the interval and the real-world scenarios for the insurer's full loss distribution forecast in the forth step of the LSMC framework partly go beyond the fitting space, its scope comprises the extrapolation area as well. High-degree polynomial extrapolation can worsen the approximation error and play a crucial role if many real-world scenarios go far beyond the fitting space.

Principle of Parsimony

Another problem that can occur in an adaptive algorithm is overfitting. Burnham & Anderson (2002) state that overfitted models often have needlessly large sampling variances which means that their precision of the predictions is poorer than that of more parsimonious models which are also free of bias. In cases where AIC leads to overfitting, implementing restriction settings of the form $K_{\max} - d_1 d_2 d_3$ becomes relevant for adhering to the principle of parsimony.

4.2 Ordinary Least-Squares (OLS) Regression

Settings

We build the OLS proxy functions (9) of $Y(X) \in \{\text{BEL}(X), \text{AC}(X)\}$ with respect to an outer scenario X out of monomial basis functions that can be written as $e_k(X) = \prod_{l=1}^{15} X_l^{r_k^l}$ with $r_k^l \in \mathbb{N}_0$ so that each basis function can be represented by a 15-tuple (r_k^1, \dots, r_k^{15}) . The final proxy function depends on the restrictions applied in the adaptive algorithm. The purpose of setting restrictions is to guarantee numerical stability, to keep the extrapolation behavior under control and the proxy functions parsimonious. In order to illustrate the impact of restrictions, we run the adaptive algorithm for BEL under two different restriction settings with the second one being so relaxed that it will not take effect in our example. Additionally, we run the adaptive algorithm under the first restriction setting for AC to give an example of how the behavior of BEL can transfer to AC. As the first ingredient of our restriction setting acts the maximum allowed number of terms K_{\max} . Furthermore, we limit the exponents in the monomial basis. Firstly we apply a uniform threshold to all exponents, i.e. $r_k^l \leq d_1$. Secondly we restrict the degree, i.e. $\sum_{l=1}^{15} r_k^l \leq d_2$. Thirdly we restrict the exponents in interaction basis functions, i.e. if there are some $l_1 \neq l_2$ with $r_k^{l_1}, r_k^{l_2} > 0$, we require $r_k^{l_1}, r_k^{l_2} \leq d_3$. Let us denote this type of restriction setting by $K_{\max} - d_1 d_2 d_3$.

As the first and second restriction settings, we choose 150-443 and 300-886, respectively, motivated by Teugui et al. (2014) who found in their LSMC example in Ch. 4 with four risk factors and 50,000 fitting scenarios entailing two inner simulations that the validation error computed based on 14 validation scenarios started to stabilize at degree 4 when using monomial or Legendre basis functions in different adaptive basis function selection procedures. Furthermore, they pointed out that the LSMC approach becomes infeasible for degrees higher than 12.

We apply R function $lm(\cdot)$ implemented in R package *stats* of R Core Team (2018).

Results

Table 1 contains the final BEL proxy function derived under the first restriction setting 150-443 with the basis function representations and coefficients. Thereby reflect the rows

the iterations of the adaptive algorithm and depict thus the sequence in which the basis functions are selected. Moreover, the iteration-wise AIC scores and out-of-sample MAEs (1) with respect to the relative metric in % on the Sobol, nested simulations and capital region sets are reported, i.e. v.mae, ns.mae and cr.mae. Table 2 contains the AC counterpart of the BEL proxy function derived under 150-443 and Table 3 the final BEL proxy function derived under the more relaxed restriction setting 300-886. Tables 4 and 5 indicate respectively for the BEL and AC proxy functions derived under 150-443 the AIC scores and all five previously defined validation figures evaluated on the Sobol, nested simulations and capital region sets after each tenth iteration. Similarly, Table 6 reports these figures for the BEL proxy function derived under 300-886. Here the last row corresponds to the final iteration.

Lastly, we manipulate the validation values on all three validation sets twice insofar as we subtract respectively add pointwise 1.96 times the standard errors from respectively to them (inspired by 95% confidence interval of gaussian distribution). We then evaluate the validation figures for the final BEL proxy functions under both restriction settings on these manipulated sets of validation value estimates and depict them in Table 7 in order to assess the impact of the Monte Carlo error associated with the validation values.

Improvement by Relaxation

Tables 1 and 2 state that the adaptive algorithm terminates under 150-443 for both BEL and AC when the maximum allowed number of terms is reached. This gives reason to relax the restriction setting to e.g. 300-886 which eventually lets the algorithm terminate due to no further reduction in the AIC score without hitting restrictions 886, compare Table 3 for BEL. In fact, only restrictions 224-464 are hit. Except for the already very small figures cr.mae, cr.mae^a and cr.res all validation figures are further improved by the additional basis functions, see Tables 4 and 6. The largest improvement takes place between iterations 180 and 190. The result that at maximum degrees 464 are selected is consistent with the result of Teugui et al. (2014) who conclude in their numerical examples of Ch. 4 that under a monomial, Legendre or Laguerre basis the optimum degree is probably 4 or 5. Furthermore, Bauer & Ha (2015) derive a similar result in their one risk factor LSMC example of Ch. 6 when using 50,000 fitting scenarios and Legendre, Hermite, Chebychev basis functions or eigenfunctions.

According to our Monte Carlo error impact assessment in Table 7, the slight deterioration at the end of the algorithm is not sufficient to indicate a slight overfitting tendency of AIC. Under the standard choices of the five major components, compare Section 2.2, the adaptive algorithm manages thus to provide a numerically stable and parsimonious proxy function even without a restriction setting. Here, allowing a priori unlimited degrees of freedom is thus beneficial to capturing the complex interactions in the CFP model.

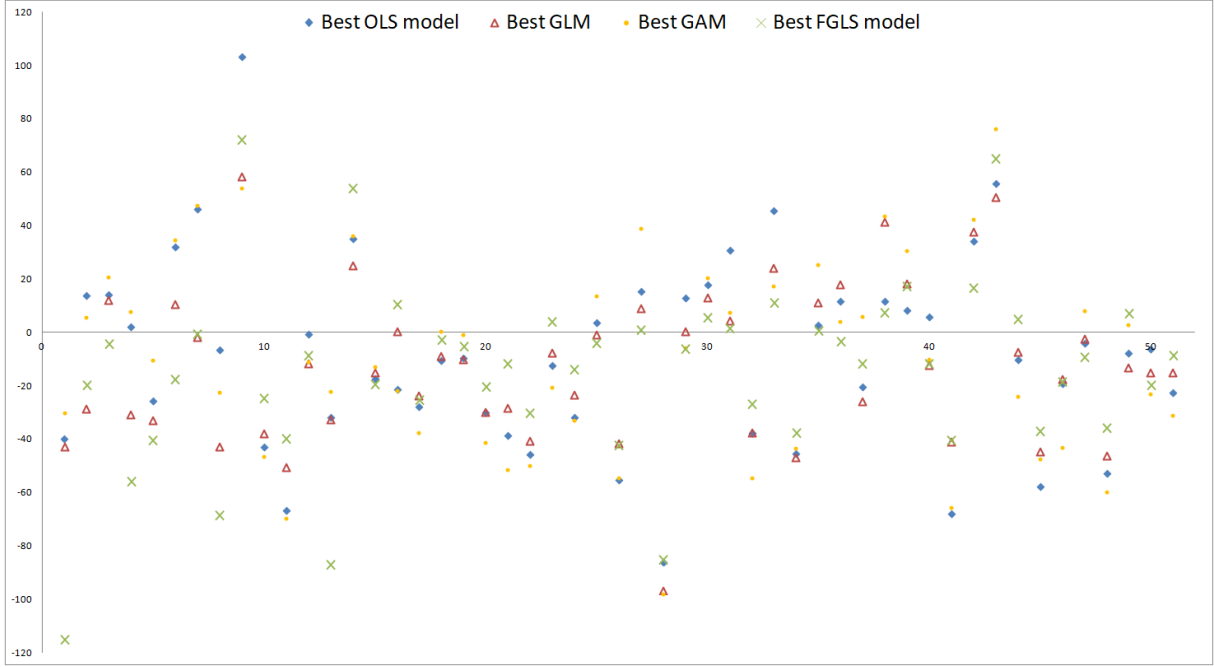


Figure 5: Residual Plots on Sobol Set

Reduction of Bias

Overall, the systematic deviations indicated by the means of residuals (2) and (4) are reduced significantly on the three validation sets by the relaxation but not completely eliminated. For the 300-886 OLS residuals on the three sets, see the blue residuals in Figures (5), (6) and (7), respectively. While the reduction of the bias comes along with the general improvement stated above, the remainder of the bias indicates that sample size is not sufficiently large or that the functional form still has some flaws. Note that if the functional form is correctly specified, Proposition 3.2 of Bauer & Ha (2015) states that if sample size is not sufficiently large, the AC proxy function will on average be positively biased in the tail reflecting the high losses and the BEL proxy function will thus be negatively biased there. Since Propositions 1 and 2 of Gordy & Juneja (2010) state that this result holds for the nested simulations estimators as well, the validation values of the nested simulations and capital region sets need to be more accurate in order to serve for bias detection in this case. For an illustration of such as bias, see Figures 5 and 6 of Bauer & Ha (2015). The bias in our one sample example is in the opposite systematic direction.

Unlike figures (1) and (2), figures (3) and (4) do not forgive a bad fit of the base value if the validation values are well approximated by a proxy function. Contrariwise, if a proxy function shows the same systematic deviation from the validation values and the base value, (3) and (4) will be close to zero whereas (1) and (2) will be not. The comparisons $|v.res| < |v.res^0|$, $|cr.res| < |cr.res^0|$ but $|ns.res| > |ns.res^0|$, holding under both restrictions settings, indicate that on the Sobol and capital region sets primarily the base value is not approximated well whereas on the nested simulations set not only the

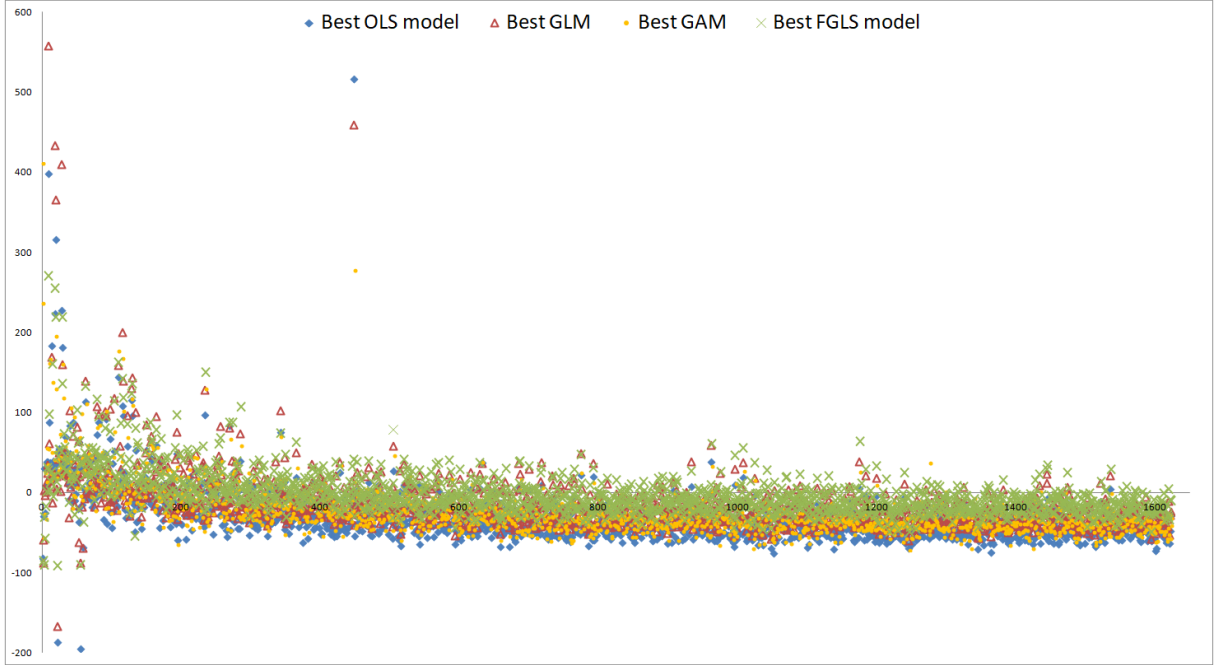


Figure 6: Residual Plots on Nested Simulations Set

base value but also the validation values are missed. The MAEs capture this result, too, i.e. $v.mae, cr.mae < ns.mae$ but $ns.mae^0 < v.mae^0, cr.mae^0$.

Relationship between BEL & AC

The MAEs with respect to the relative metric for BEL are much smaller than for AC since the two economic variables are subject to similar absolute fluctuations with e.g. in the base case BEL being approximately 20 times the size of AC. The similar absolute fluctuations are reflected by the iteration-wise very similar MAEs with respect to the asset metric of BEL and AC, compare $v.mae^a, ns.mae^a$ and $cr.mae^a$ given in % in Tables 4 and 5. Furthermore, they manifest themselves in the iteration-wise opposing means of residuals $v.res, v.res^0, ns.res$ and $cr.res$ as well as in the similar-sized MAEs $v.mae^0, ns.mae^0$ and $cr.mae^0$.

4.3 Generalized Linear Models (GLMs)

Settings

We derive the GLMs (13) of BEL under restriction settings 150-443 and 300-886 which we also employed for the derivation of the OLS proxy functions. Thereby, we run each restriction setting with the canonical choices of random components for continuous (non-negative) response variables, that is, the gaussian, gamma and inverse gaussian distributions, compare McCullagh & Nelder (1989). In cases where the economic variable can also attain negative values (e.g. AC), a suitable shift of the response values in a preceding step would be required. We combine each of the three random component choices with the

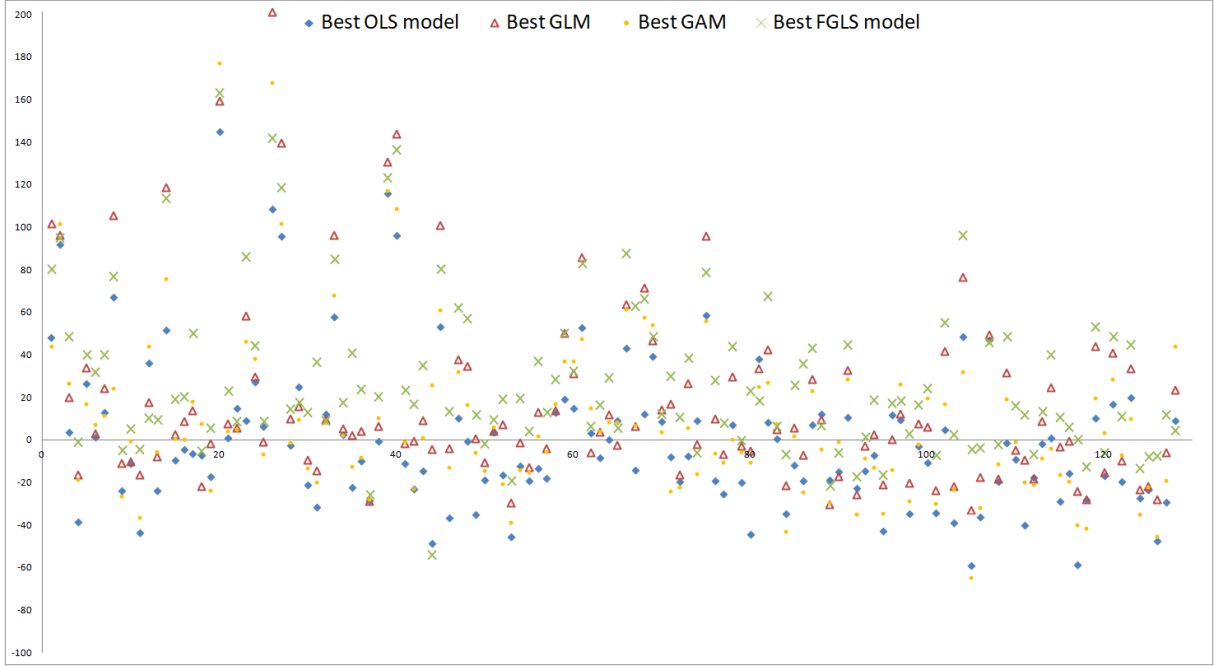


Figure 7: Residual Plots on Capital Region Set

commonly used identity, inverse and log link functions, i.e. $g(\mu) \in \left\{ \text{id}(\mu), \frac{1}{\mu}, \log(\mu) \right\}$, compare Hastie & Pregibon (1992). In combination with the inverse gaussian random component, we consider additionally link function $\frac{1}{\mu^2}$. Further choices are conceivable but go beyond this first shot.

We take R function $glm(\cdot)$ implemented in R package *stats* of R Core Team (2018).

Results

While Tables 8, 9 and 10 display the AIC scores and five previously defined validation figures after each tenth iteration for the just mentioned combinations under 150-443, Tables 11, 12 and 13 do so under 300-886 and include furthermore the final iterations. Table 14 gives an overview of the AIC scores and validation figures corresponding to all considered final GLMs and highlights in green and red respectively the best and worst values observed per figure.

Improvement by Relaxation

The OLS regression is the special case of a GLM with gaussian random component and identity link function which is why the first sections of Tables 8 and 11 coincide respectively with Tables 4 and 6. The adaptive algorithm terminates under 150-443 not only for this combination but also for all other ones when the maximum allowed number of terms is reached. Under 300-886 termination occurs due to no further reduction in the AIC score without hitting the restrictions - the different GLMs stop between 208-454 and 250-574.

For all GLMs except for the one with gamma random component and identity link, the AIC scores and eight most significant validation figures for measuring the approximation quality, namely leftmost figure v.mae to rightmost figure ns.res in the tables, are improved through the relaxation as can be seen in Table 14. For gamma random component with identity link, the deteriorations are negligible. Overall, figures ns.mae⁰ and cr.mae⁰ are deteriorated by at maximum 0.5% points and figures ns.res⁰ and cr.res⁰ by at maximum 4 units. Figures cr.mae and cr.mae^a are especially small under 150-443 so that slight deteriorations by at maximum 0.05% points under 300-886 towards the levels of v.mae and v.mae^a or ns.mae and ns.mae^a are not surprising. Similar arguments apply to the acceptability of the maximum deterioration of cr.res by 13 to 17 units for inverse gaussian with $\frac{1}{\mu^2}$ link. We conclude that the more relaxed restriction setting 300-886 performs better than 150-443 for all GLMs in our numerical example. This result appears plausible in comparison with the OLS result from the previous section and hence also compared to the OLS results of Teugui et al. (2014) and Bauer & Ha (2015).

AIC cannot be said to show an overfitting tendency according to Tables 11, 12 and 13 and also Table 7 since the validation figures do not deteriorate in the late iterations more than they underly Monte Carlo fluctuations, compare the OLS interpretation. Using GLMs instead of OLS regression in the standard adaptive algorithm, compare Section 2.2, lets the algorithm thus maintain its property to yield numerically stable and parsimonious proxy functions even without restriction settings.

Reduction of Bias

According to Table 14, inverse gaussian with $\frac{1}{\mu^2}$ link shows the most significant decrease in v.mae by -0.088% points when moving from 150-443 to 300-886. Under 300-886 this combination even outperforms all other ones (highlighted in green) whereas under 150-443 it is vice versa (highlighted in red). Hence, the performance of a random component link combination under 150-443 does not generalize to 300-886. On the Sobol and nested simulations sets, the MAEs (1) are not only considerably lower for inverse gaussian with $\frac{1}{\mu^2}$ link than for all others but also the closest together even when the capital region set is included. This speaks for a great deal of consistency.

In fact, the systematic overestimation of 81% of the points on the nested simulations set by inverse gaussian with $\frac{1}{\mu^2}$ link is certainly smaller than e.g. that of 89% by gaussian with identity link but still very pronounced. On the capital region set, the overestimation rates for these two combinations are 41% and 56%, respectively, meaning that here the bias is negligible. Surprisingly, for most GLMs the bias is here smaller than for inverse gaussian with $\frac{1}{\mu^2}$ link but since this result does not generalize to the nested simulations set, we regard it as a chance event and do not question the rather mediocre performance of inverse gaussian with $\frac{1}{\mu^2}$ link here further. Interpreting the mean of residuals (2) provides similar insights.

In particular, for inverse gaussian $\frac{1}{\mu^2}$ link GLM the reduction of the bias comes along

with the general improvement by the relaxation. The small remainder of the bias indicates not only that this GLM is a promising choice here but also that identifying suitable regression methods and functional forms is crucial to further improving the accuracy of the proxy function. For the residuals on the three sets, see the red residuals in Figures (5), (6) and (7), respectively.

Major & Minor Role of Link Function & Random Component

Apart from the just considered case, for all three random components, the relaxation to 300-886 yields the largest out-of-sample performance gains in terms of v.mae with identity link (between -0.047% and -0.058% points), closely followed by log link (between -0.033% and -0.047% points), and the least gains with inverse link (between -0.017% and -0.020% points). While with identity link the largest improvements before finalization take place for gaussian, gamma and inverse gaussian random components between iterations 180 to 190, 170 to 180, and 150 to 160, respectively, with log link they occur much sooner between iterations 120 to 130, 110 to 120, and 110 to 120, respectively, see Tables 11, 12 and 13. As a result of this behavior, under 150-443 log link performs better than identity link for gaussian and inverse gaussian whereas under 300-886 it is vice versa. Inverse link always performs worse than identity and log links, in particular under 300-886.

Applying the same link with different random components does not bring much variation under 300-886 with gamma and inverse gaussian being slightly better than gaussian for all considered links though. A possible explanation is that the distribution of BEL is slightly skewed conditional on the outer scenarios. Thereby results the skewness in the inner simulations from an asymmetric profit sharing mechanism in the CFP model: While the policyholders are entitled to participate at the profits of an insurance company, see e.g. Mourik (2003), the company has to bear its losses fully by itself. Since gaussian performs only slightly worse than the skewed distributions, it should still be considered for practical reasons because it has a closed-form solution and a great deal of statistical theory has been developed for it, compare e.g. Dobson (2002). By conclusion, the choice of the link is more important than that of the random component so that trying alternative link functions might be beneficial.

4.4 Generalized Additive Models (GAMs)

Settings

For the derivation of the GAMs (25) of BEL, we apply only restriction settings $K_{\max}=443$ with $K_{\max} \leq 150$ in the adaptive algorithm since we use smooth functions (24) constructed out of splines that may already have exponents greater than 1 to which the monomial first-order basis functions are raised. As the model selection criterion we take GCV (31) used by our chosen implementation by default. We vary different ingredients of GAMs while

holding others fixed to carve out possible effects of these ingredients on the approximation quality of GAMs in adaptive algorithms and our application.

We rely on R function $gam(\cdot)$ implemented in R package *mgcv* of Wood (2018).

Results

Table 15 contains the validation figures for GAMs with varying number of spline functions per smooth function, i.e. $J \in \{4, 5, 8, 10\}$, after each tenth and the finally selected smooth function. In the case of adaptive forward stepwise selection the iteration numbers coincide with the numbers of selected smooth functions. In contrast, table sections with adaptive forward stagewise selection results do not display the iteration numbers in the smooth function column k . In Table 16, we display the effective degrees of freedom, p-values and significance codes of each smooth function of the $J = 4$ and $J = 10$ GAMs from the previous table at stages $k \in \{50, 100, 150\}$. The p-values and significance codes are based on a test statistic of Marra & Wood (2012) having its foundations in the frequentist properties of Bayesian confidence intervals analyzed in Nychka (1988). Tables 17 and 18 report the validation figures respectively for GAMs with numbers $J = 5$ and $J = 10$, where the types of the spline functions are varied. Thin plate regression splines, penalized cubic regression splines, duchon splines and Eilers and Marx style P-splines are considered. Thereafter, Tables 19 and 20 display the validation figures respectively for GAMs with numbers $J = 4$ and $J = 8$ and different random component link function combinations. As in GLMs, we apply the gaussian, gamma and inverse gaussian distributions with identity, log, inverse and $\frac{1}{\mu^2}$ (only inverse gaussian) link functions.

Table 21 compares by means of two exemplary GAMs the effects of adaptive forward stagewise selection of length $L = 5$ and adaptive forward stepwise selection. Last but not least, Table 22 contains a mixture of GAMs challenging the results which we will have deduced from the other GAM tables. Table 23 gives an overview of the validation figures corresponding to all derived final GAMs and highlights in green and red respectively the best and worst values observed per figure.

Efficiency & Performance Gains by Tailoring the Spline Function Number

Table 15 indicates that the MAEs (1) and (3) of the exemplary GAMs built up of thin plate regression splines with gaussian random component and identity link tend to increase with the number J of spline functions per dimension until $k = 100$. Running more iterations reverses this behavior until $k = 150$. Hence, as long as comparably few smooth functions have been selected in the adaptive algorithm fewer spline functions tend to yield better out-of-sample performances of the GAMs whereas many smooth functions tend to perform better with more spline functions. A possible explanation of this observation is that an omitted-variable bias due to too few smooth functions is aggravated here by an overfitting due to too many spline functions. For more details on an omitted-variable bias, see e.g.

Pindyck & Rubinfeld (1998), and for the needlessly large sampling variances and thus low estimation precision of overfitted models, see e.g. Burnham & Anderson (2002). Differently, the absolute values of the means of residuals (2) and (4) tend to become smaller with increasing J regardless of k .

According to Table 16, the components of the effective degrees of freedom (30) associated with each smooth function tend to decrease for $J = 4$ and $J = 10$ slightly in k . This is plausible as the explanatory power of each additionally selected smooth term is expected to decline by trend in the adaptive algorithm. Conditional on $\text{df} > 1$, that is for proportions of at least 40% of all smooth terms, the averages of the effective degrees of freedom belonging to $k \in \{50, 100, 150\}$ amount for $J = 4$ and $J = 10$ to $\{2.494, 2.399, 2.254\}$ and $\{5.366, 4.530, 4.424\}$, respectively. The values are by construction smaller than $J - 1$ since one degree of freedom per smooth function is lost to the identifiability constraints. Hence, for at least 40% of the smooth functions, on average $J = 6$ is a reasonable choice to capture the CFP model properly while maintaining computational efficiency, compare Wood (2017). The other side of the coin here is that up to 60% of the smooth functions are supposed to be replacable by simple linear terms without losing accuracy so that here tremendous efficiency gains can be realized by making the GAMs more parsimonious. Furthermore, setting J individually for each smooth function can help improve computational efficiency (if J should be set below average) and out-of-sample performance (if J should be set above average). However, such a tailored approach entails the challenge that the optimal J per smooth function is not stable across all k , compare row-wise the degrees of freedom in the table for $J = 4$ and $J = 10$.

Dependence of Best Spline Function Type

According to Tables 17 and 18, the adaptive algorithm terminates only due to no further decrease in GCV when the GAMs are composed of duchon splines discussed in Duchon (1977). Whether GCV has an overfitting tendency here cannot be deduced from this example since only restriction settings with $K_{\max} \leq 150$ are tested. The thin plate regression splines of Wood (2003) and penalized cubic regression splines of Wood (2017) perform similarly and significantly better than the duchon splines for both $J = 5$ and $J = 10$. For $J = 5$ the Eilers and Marx style P-splines proposed by Eilers & Marx (1996) perform by far best when $K_{\max} = 100$ smooth functions are allowed. However, for $J = 10$ they are outperformed by both the thin plate regression splines and penalized cubic regression splines when between $K_{\max} = 125$ and 150 smooth functions are allowed. This result illustrates well that the best choice of the spline function type varies with J and K_{\max} , meaning that it should be selected together with these parameters.

Minor Role of Link Function & Random Component

For GLMs, we have seen that varying the random component barely alters the validation results whereas varying the link function can make a noticeable impact. While this result mostly applies to the earlier compositions of GAMs as well, it certainly does not to the later ones. See for instance early composition $k = 40$ in Table 19. Here identity link GAMs with gamma and inverse gaussian random components perform more similar to each other than identity and log link GAMs with gamma random component or identity and log link GAMs with inverse gaussian random component do. Log link GAMs with gamma and inverse gaussian random components show such a behavior as well. However identity link GAM with the less flexible gaussian random component (no skewness) does not show at all a behavior similar to that of identity link GAMs with gamma or inverse gaussian random components. Now see later compositions $k \in \{70, 80\}$ to verify that all available GAMs in the table produce very similar validation results.

For another example see Table 20. For early composition $k = 50$, identity link GAMs with gaussian and gamma random components behave very similar to each other just like log link GAMs with gaussian and gamma random components do. For later compositions $k \in \{100, 110\}$, again all available GAMs produce very similar validation results. A possible explanation of this result is that the impact of the link function and random component decreases with the number of smooth functions as the latter take the modeling over. By conclusion, the choices of the random component and link function do not play a major role when the GAM is built up of many smooth functions.

Consistency of Results

Table 21 shows based on two exemplary GAMs constructed out of $J = 8$ thin plate regression splines per dimension varying in the random component and link function that the adaptive forward stagewise selection of length $L = 5$ and adaptive forward stepwise selection lead to very similar GAMs and validation results. As a result, stagewise selection should be preferred due to its considerable run time advantage. As we will see in the following, the run time can be further reduced without any drawbacks by dynamically selecting even more than 5 smooth functions per iteration.

The purpose of Table 22 is to challenge the hypotheses deduced above. Like Table 15, this table contains the results of GAMs with varying spline function number $J \in \{5, 8, 10\}$ and fixed spline function type. Instead of thin plate regression splines, now Eilers and Marx style P-splines are considered. Since adaptive forward stepwise and stagewise selection do not yield significant differences in the examples of Table 21, we do not expect that permutations thereof affect the results much here as well. This allows us to randomly assign three different adaptive forward selection approaches to the three exemplary proxy function derivation procedures. As one of these approaches, we choose a dynamic stagewise selection approach in which L is determined in each iteration as the

proportion 0.25 of the size of the candidate term set. Again we see that as long as only $k \in \{90, 100\}$ smooth functions have been selected, $J = 5$ performs better than $J = 8$ and $J = 8$ better than $J = 10$. However, $k = 150$ smooth functions are not sufficient this time for $J = 10$ to catch up with the performance of $J = 5$. The observed performance order is consistent with the hypotheses of a high stability of the GAMs with respect to the adaptive selection procedure and random component link function combination.

Potential of Improved Interaction Modeling

Table 23 presents as the most suitable GAM the one with highest allowed maximum number of smooth functions $K_{\max} = 150$ and highest number of spline functions $J = 10$ per dimension. The slight deterioration after $k = 130$ reported by Table 15 indicates that at least one of the parameters is already comparably high. According to Table 16, there are a few smooth terms which might benefit from being composed of more than ten spline functions and increasing K_{\max} might be helpful to capturing the interactions in the CFP model more appropriately, particularly in the light of the fact that the best GLM, having 250 basis functions, outperforms the best GAM on both the Sobol and nested simulations set, compare Table 14, with the best GAM showing a comparably low bias across the three validation sets though, see the orange residuals in Figures (5), (6) and (7), respectively. Variations in the random component link function combination and adaptive selection procedure are not expected to change the performance much. By conclusion, we recommend the fast gaussian identity link GAMs (several expressions in the PIRLS algorithm simplify) with tailored spline function numbers per smooth function and simple linear terms under stagewise selection approaches of suitable lengths $L \geq 5$ and more relaxed restriction settings where $K_{\max} > 150$.

4.5 Feasible Generalized Least-Squares (FGLS) Regression

Settings

Like the OLS proxy functions and GLMs, we derive the FGLS proxy functions (37) under restriction settings 150-443 and 300-886. For the performance assessment of FGLS regression, we apply type I and II algorithms with variance models of different complexity, where type I results are obtained as a by-product of type II algorithm since the latter algorithm builds upon the former one. We control the complexity through the maximum allowed numbers of variance model terms $M_{\max} \in \{2; 6; 10; 14; 18; 22\}$.

We combine R functions $nlmnb(\cdot)$ and $lm(\cdot)$ implemented in R package *stats* of R Core Team (2018).

Results

Tables 24 and 25 display respectively the adaptively selected FGLS variance models of BEL corresponding to maximum allowed numbers of terms M_{\max} based on final 150-443 and 300-886 OLS proxy functions given in Tables 1 and 3. For reasons of numerical stability and simplicity, only basis functions with exponents summing up to at max two are considered as candidates. Additionally, the AIC scores and MAEs with respect to the relative metric are reported in the tables. By construction, these results are also the type I algorithm outcomes. Tables 26 and 27 summarize respectively under 150-443 and 300-886 all iteration-wise out-of-sample test results. The results of type II algorithm after each tenth and the final iteration of adaptive FGLS proxy function selection are respectively displayed by Tables 28 and 29. Table 30 gives an overview of the AIC scores and validation figures corresponding to all final FGLS proxy functions and highlights as in the previous overview tables in green and red respectively the best and worst values observed per figure.

Consistency Gains by Variance Modeling

By looking at Tables 24 and 25 we see similar out-of-sample performance patterns during adaptive variance model selection based on the basis function sets of 150-443 and 300-886 OLS proxy functions. In both cases, the p-values of Breusch-Pagan test indicate that heteroscedasticity is not eliminated but reduced when the variance models are extended, i.e. when M_{\max} is increased. In fact, in a more good-natured LSMC example Hartmann (2015) shows that a type I alike algorithm manages to fully eliminate heteroscedasticity. While the MAEs (1) barely change on the Sobol set, they decrease significantly on the nested simulations set and increase noticeably on the capital region set. Under 300-886 the effects are considerably smaller than under 150-443 since the capital region performance of 300-886 OLS proxy function is less extraordinarily good than that of 150-443 OLS proxy function. The three MAEs approach each other under both restriction settings. Hence the reductions in heteroscedasticity lead to consistency gains across the three validation sets.

Tables 26 and 27 complete the just discussed picture. The remaining validation figures on the Sobol set improve through type I FGLS regression slightly compared to OLS regression. Like ns.mae, figure ns.res and the base residual improve a lot with increasing M_{\max} under 150-443 and a little less under 300-886 but ns.mae⁰ and ns.res⁰ do not alter much as the aforementioned two figures cancel each other out here. On the capital region set, the figures deteriorate or remain comparably high in absolute values. The type I FGLS figures converge fast so that increasing M_{\max} successively from 10 to 22 barely affects the out-of-sample performance anymore. As a result of heteroscedasticity modeling, the proxy functions are shifted such that overall approximation quality increases. Unfortunately, this does not guarantee an improvement in the relevant region for SCR estimation as our

example illustrates well.

Monotonicity in Complexity

Let us address the type II FGLS results under 150-443 in Table 28 now. For $M_{\max} = 2$, figures (3) and (4) are improved on all three validation sets significantly compared to OLS regression with the type I figures lying inbetween. The other validation figures are similar for OLS, type I and II FGLS regression, which traces the performance gains in (3) and (4) back to a better fit of the base value. For $M_{\max} = 6$ to 22, the type II figures show the same effects as the type I ones but more pronouncedly, see the previous two paragraphs. These effects are by trend the more distinct the more complex the variance model becomes. The type II figures stabilize less than the type I ones because of the additional variability coming along with adaptive FGLS proxy function selection. Hartmann (2015) shows in terms of Sobol figures in her LSMC example that increasing the complexity while omitting only one regressor from the simpler variance model can deteriorate the out-of-sample performance dramatically. Intuitively, it is plausible that the FGLS validation figures are the farther from the OLS figures away the more elaborately heteroscedasticity is modeled.

Now let us relate the type II FGLS results under 300-886 in Table 29 to the other FGLS results. Under 300-886 for $M_{\max} = 2$, figures (3) and (4) are already at a comparably good level with both OLS and type I FGLS regression so that they do not alter much or even deteriorate with type II FGLS regression. Like under 150-443 for $M_{\max} = 6$ to 22, the type II figures show the effects of the type I ones more pronouncedly. Under both restriction settings, ns.mae and ns.res decrease thereby significantly. While this barely causes ns.res⁰ to change under 150-443, it lets ns.res⁰ increase in absolute values under 300-886. The slight improvements on the Sobol set and the deteriorations on the capital region set carry over to 300-886. When M_{\max} is increased up to 22, the type II FGLS validation figures under 300-886 do not stop fluctuating. The variability entailed by adaptive FGLS proxy function selection intensifies thus through the relaxation of the restriction setting in this numerical example. According to Breusch-Pagan test, heteroscedasticity is neither eliminated by the type II algorithm here nor by a type II alike approach of Hartmann (2015) in her more good-natured example.

Improvement by Relaxation

Among all FGLS proxy functions listed in Table 30, we consider type II with $M_{\max} = 14$ in variance model selection under 300-886 as the best performing one. Apart from nested simulations validation under type I algorithm, 300-886 performs better than 150-443. Since on the other hand type II algorithm performs better than type I algorithm under the respective restriction settings, 300-886 and type II algorithm are the most promising choices here. Differently $M_{\max} = 14$ does not constitute a stable choice due to the high

variability coming along with 300-886 and type II algorithm.

While all type I FGLS proxy functions are by definition composed of the same basis functions as the OLS proxy function, the compositions of type II FGLS proxy functions vary with M_{\max} because of their renewed adaptive selection. Consequently, under 300-886 all type I FGLS proxy functions hit the same restrictions 224-464 as the OLS proxy function does, whereas the restrictions hit by type II FGLS proxy functions vary between 224-454 and 258-564. This variation is consistent with the OLS and GLM results from the previous sections and hence the OLS results of Teugua et al. (2014) and Bauer & Ha (2015).

AIC does not have an overfitting tendency according to Tables 26, 27, 28 and 29 as the validation figures do not deteriorate in the late iterations more than they underly Monte Carlo fluctuations, compare the OLS and GLM interpretations. Using FGLS instead of OLS regression in the standard adaptive algorithm, compare Section 2.2, lets the algorithm thus yield numerically stable and parsimonious proxy functions without restriction settings as well.

Reduction of Bias

The type II $M_{\max} = 14$ FGLS proxy function under 300-886 reaches with 258 terms the highest observed number across all numerical experiments and not only outperforms all derived GLMs and GAMs in terms of combined Sobol and nested simulations validation, it also shows by far the smallest bias on these two validation sets and approximates the base value comparably well. This observation speaks for a high interaction complexity of the CFP model. The reduction of the bias comes again along with the general improvement by the relaxation. Given the fact that the capital region set presents the most extreme and challenging validation set in our analysis, the still mediocre performance here can be regarded as acceptable for now. Nevertheless, especially the bias on this set motivates the search for even more suitable regression methods and functional forms. For the residuals of the 300-886 FGLS proxy function on the three sets, see the green residuals in Figures (5), (6) and (7), respectively.

4.6 Multivariate Adaptive Regression Splines (MARS)

Settings

We undertake a two-step approach to identify suitable generalized MARS models out of numerous possibilities. In the first step, we vary several MARS ingredients over a wide range and obtain in this way a large number of different MARS models. To be more specific, we vary the maximum allowed number of terms $K_{\max} \in \{50, 113, 175, 237, 300\}$ and the minimum threshold for the decrease in the residual sum of squares $t_{\min} \in \{0, 1.25, 2.5, 3.75, 5\} \cdot 10^{-5}$ in the forward pass, the order of interaction $o \in \{3, 4, 5, 6\}$, the pruning method $p \in \{'n', 'b', 'f', 's'\}$ with ' n ' = 'none', ' b ' = 'backward', ' f ' = 'forward'

and 's' = 'seqrep' in the backward pass, as well as the random component link function combination of the GLM extension. In addition to the 10 random component link function combinations applied in the numerical experiments of the GLMs, compare e.g. Table 14, we use poisson random component with identity, log and squareroot link functions. We work with the default fast MARS parameter `fast.k = 20` of our chosen implementation.

We use R function `earth()` implemented in R package `earth` of Milborrow (2018).

Results

In total, these settings yield $4 \cdot 5 \cdot 5 \cdot 4 \cdot 13 = 5,200$ MARS models with a lot of duplicates in our first step. We validate the 5,200 MARS models on the Sobol, nested simulations and capital region sets through evaluation of the five validation figures. Then we collect the five best performing MARS models in terms of each validation figure per set which gives us in total $5 \cdot 5 = 25$ best performing models per first step validation set. Since the MAEs (1) with respect to the relative and asset metric entail the same best performing models, only $5 \cdot 4 = 20$ of the collected models per first step set are potentially different. Based on the ingredients of each of these 20 MARS models per first step set, we define $5 \cdot 5 = 25$ new sets of ingredients varying only with respect to K_{\max} and t_{\min} and derive the corresponding new but similar MARS models in the second step. As a result, we obtain in total $20 \cdot 25 = 500$ new MARS models per first step set. Again, we assess their out-of-sample performances through evaluation of the five validation figures on the three validation sets. Out of the 500 new MARS models per first step set, we collect then the best performing ones in terms of each validation figure per second step set. Now this gives us in total $5 \cdot 3 = 15$ best MARS models per first step set, or taking into account that the MAEs (1) with respect to the relative and asset metric entail once more the same best performing models, $4 \cdot 3 = 12$ potentially different best models per first step set. In total, this makes $12 \cdot 3 = 4 \cdot 9 = 36$ best MARS models, which can be found in Table 31 sorted by first and second step validation sets.

Poor Interaction Modeling & Extrapolation

In Table 31, the out-of-sample performances of all MARS models derived in our two-step approach are sorted using the first step validation set as the primary and the second step validation set as the secondary sort key. Let us address the first step second step validation set combinations by the headlines in Table 31. By construction, the combinations Sobol set², Nested simulations set² and Capital region set² yield respectively the MARS models with the best validation figures (1), (2), (3) and (4) on the Sobol, nested simulations and capital region sets. See that in the table all corresponding diagonal elements are highlighted in green. But the best MAEs (1) and (3) are not even close to what OLS regression, GLMs, GAMs and FGLS regression achieve. Finding small residuals (2) and (4) regardless of the other validation figures is not sufficient. The performances on the

nested simulations and capital region sets, comprising several scenarios beyond the fitting space, are especially poor. All these results indicate that MARS models do not seem very suitable for our application. Despite the possibility to select up to 300 basis functions, the MARS algorithm selects only at maximum 148 basis functions, which suggests that without any alterations, the algorithm is not able to capture the behavior of the CFP model properly, in particular extrapolation behavior is comparably poor.

The MARS model with the set of ingredients $K_{\max} = 50$, $t_{\min} = 0$, $o = 4$, $p = 'b'$, inverse gaussian random component and identity link function is selected as the best one six times out of 36, or once for each Sobol and nested simulations first step validation set combination. Furthermore, this model performs best in terms of $v.\text{res}^0$, $ns.\text{mae}^0$ and $ns.\text{mae}^a$. Since there is no other MARS model with a similar high occurrence and performance, we consider it the best performing and most stable one found in our two-step approach. For illustration of a MARS model, see this one in Table 32. The fact that this best MARS model performs worse than other ones in terms of several validation figures stresses the infeasibility of MARS models in this application.

Limitations

Table 31 suggests that, up to a certain upper limit, the higher the maximum allowed number of terms K_{\max} the higher tends the performance on the Sobol set to be. However, this result does not generalize to the nested simulations and capital region sets. Since at maximum 148 basis functions are selected here even if up to 300 basis functions are allowed, extending the range of K_{\max} in the first step of this numerical experiment would not affect the output in this regard. The threshold t_{\min} is an instrument controlling the number of basis functions selected in the forward pass up to K_{\max} which cannot be extended below zero, meaning that its variability has already been exhausted here as well. For the interaction order o similar considerations as for K_{\max} apply. The pruning method p used in the backward pass does not play a large role compared to the other ingredients as it only helps reduce the set of selected basis functions. In terms of Sobol validation, inverse gaussian random component with identity link performs best, whereas in terms of nested simulations and capital region validation, inverse gaussian random component with any link or log link with gaussian or poisson random component perform best. We conclude that if there was a suitable MARS model for our application, our two-step approach would have found it.

4.7 Kernel Regression

Settings

We make a series of adjustments affecting either the structure or the derivation process of the multidimensional LC and LL proxy functions (57) and (59) to get as broad a picture of the potential of kernel regression in our application as possible. Our adjustments concern

the kernel function and its order, the bandwidth selection criterion, the proportion of fitting points used for bandwidth selection, and the sets of basis functions of which the local proxy functions are composed of. Thereby we combine in various ways the gaussian, Epanechnikov and uniform kernels, orders $o \in \{2, 4, 6, 8\}$, bandwidth selection criteria LOO-CV and AIC, and between 2,500 (proportion $bw = 0.1$) and 25,000 (proportion $bw = 1$) fitting points for bandwidth selection.

We work with R functions $npregbw(\cdot)$ and $npreg(\cdot)$ implemented in R package *np* of Racine & Hayfield (2018).

Results

Furthermore, we alternate the four basis function sets contained in Tables 33 and 34. The first two basis function sets with $K_{\max} \in \{16, 27\}$ are derived by adaptive forward stepwise selection based on OLS regression, the third one with $K_{\max} = 15$ by risk factor wise linear selection and the last one with $K_{\max} = 22$ by a combination thereof. All combinations including their out-of-sample performances can be found in Table 35. Again, the best and worst values observed per validation figure are highlighted in green and red, respectively.

Poor Interaction Modeling & Extrapolation

We draw the following conclusions based on the validation results in Table 35. The comparisons of LC and LL regression applied with gaussian kernel and 16 basis functions or Epanechnikov kernel and 15 basis functions suggest that LL regression performs better than LC regression. However, even the best Sobol, nested simulations and capital region results of LL regression are still outperformed by OLS regression, GLMs, GAMs and FGLS regression. Possible explanations for this observation are that kernel regression is not able to model the interactions of the risk factors equally well with its few basis functions and that local regression approaches perform rather poorly close to and especially beyond the boundary of the fitting space because of the thinned out to missing data basis in this region. While the first explanation applies to all three validation sets, the latter one applies only to the nested simulations and capital region sets on which the validation figures are indeed worse than on the Sobol set. While LC regression produces interpretable results with the sets of 22 and 27 basis functions, the more complex LL regression does not in most cases.

Limitations

On the Sobol and capital region sets, both LC and LL regression show similar behaviors when relying on gaussian kernel and 16 basis functions compared to Epanechnikov kernel and 15 basis functions. But on the nested simulations set, gaussian kernel and 16 basis functions are the superior choices. Using a uniform kernel with LC regression deteriorates the out-of-sample performance. The results of LC regression indicate furthermore that

an extension of the basis function sets from 15 to 27 only slightly affects the validation performance. With gaussian kernel switching from 16 to 27 basis functions barely has an impact and with Epanechnikov kernel only the nested simulations and capital region validation performance improve when using 27 as opposed to 15, 16 or 22 basis functions. While increasing the order of the gaussian or Epanechnikov kernel deteriorates the validation figures dramatically, for the uniform kernel the effects can go in both directions. AIC performs worse than LOO-CV when used for bandwidth selection of the gaussian kernel in LC regression. For LC regression, increasing the proportion of fitting points entering bandwidth selection improves all validation figures until a specific threshold is reached. But thereafter the nested simulations and capital region figures are deteriorated. For LL regression no such deterioration is observed.

Overall we do not see much potential in kernel regression for our practical example compared to most of the previously analyzed regression methods. Nonetheless in order to achieve comparably good kernel regression results, we consider LL regression more promising than LC regression due to the superior but still poor modeling close to and beyond the boundary of the fitting space. We would apply it with gaussian, Epanechnikov or other similar kernel functions. A high proportion of fitting points for bandwidth selection is recommended and it might be worth trying alternative comparably small basis function sets reflecting e.g. the risk factor interactions better than in our examples.

5 Conclusion

General Remarks

For high-dimensional variable selection applications such as the calibration step in the LSMC framework, we have presented various machine learning regression approaches ranging from ordinary and generalized least-squares regression variants over GLM and GAM approaches to multivariate adaptive regression splines and kernel regression approaches. At first we have justified the combinability of the ingredients of the regression routines such as the estimators and proposed model selection criteria in a theoretical discourse. Afterwards we have applied numerous configurations of these machine learning routines to the same slightly disguised real-world example in the LSMC framework. With the aid of different validation figures, we have analyzed the results, compared the out-of-sample performances and advised to use certain routine designs.

In this conclusion, we recap the assumptions, properties and estimation algorithms of the analyzed routines in conjunction with their results in the numerical experiments. Furthermore, we give an outlook for possible future research streams.

OLS Regression

The OLS regression algorithm in Section 3.2 requires the assumptions of strict exogeneity, homoscedastic errors and linear independent basis functions for the coefficient estimator to be the best linear unbiased estimator by Gauss-Markov theorem. The OLS estimator minimizes the residual sum of squares by definition and has a closed-form expression. For AIC to be evaluable at the OLS estimator, the errors also have to be normally distributed according to Theorem 1.

We applied the OLS regression algorithm in Section 4.2 under suitable restriction settings and found that relaxing the setting from 150-443 to 300-886 (= no actual restriction) improved out-of-sample performance considerably. Thereby the bias indicated by the means of residuals on the three validation sets was reduced, see Tables 4 and 6, but not eliminated so that we stated that the functional form of the proxy function still had some flaws, see Figure 6. We concluded that overall the adaptive algorithm managed to provide a numerically stable and parsimonious proxy function even without imposing a restriction setting and that the a priori unlimited degrees of freedom served capturing the complex CFP model better. Furthermore we pointed out that BEL and AC were subject to similar absolute fluctuations.

GLMs

The GLM algorithm in Section 3.3 is a generalization of the OLS regression algorithm insofar as the errors are now allowed to come from an arbitrary distribution of the exponential family and the economic variable is related to the linear predictor by a monotonic link function. The GLM estimator maximizes the log-likelihood and can be derived by an IRLS algorithm. Without more ado, the GLM estimator can be fed into AIC.

Like in the OLS regression algorithm, we observed in all applied GLM algorithms in Section 4.3 that relaxing the setting from 150-443 to 300-886 (= no actual restriction) helped improve out-of-sample performance and reduce the bias. From the small remainder of the bias we deduced that identifying suitable regression methods and functional forms is crucial to further improving the accuracy of the proxy function. We concluded that the adaptive algorithm maintained its property to yield numerically stable and parsimonious proxy functions without requiring restriction settings in the GLM context. The performance of a random component link combination under 150-443 did not generalize to 300-886. Moreover, we saw in the variation of the results that the choice of the link was more important than that of the random component so that regarding additional link functions might be beneficial. While continuous skewed random components led to slightly advantageous out-of-sample performances, the use of the gaussian random component had practical advantages. Compared to the OLS regression routine, there were GLM routine designs with better out-of-sample performances. While performing best on both the Sobol and nested simulations set, 300-886 inverse gaussian $\frac{1}{\mu^2}$ link GLM showed

only a mediocre performance on the capital region set. For an overview of these results, see Table 14.

GAMs

The GAM algorithm in Section 3.4 acts as a generalization of the GLM algorithm and brings in the additive models with the smooth functions as the new component. The GAM estimator maximizes the penalized log-likelihood and can be derived by a PIRLS algorithm. The penalization takes place with respect to smoothing parameters controlling the trade-off between a too wiggly and too smooth model. For AIC to be evaluable at the GAM estimator, the degrees of freedom are generalized such that they account for the smoothing. As an alternative to AIC, generalized cross-validation GCV is introduced. The smoothing parameters are selected such that they minimize the chosen model selection criterion. For reasons of computational efficiency, adaptive forward stagewise selection is suggested.

We ran the different GAM algorithms in Section 4.4 only under restriction setting 150-443. Whether GCV had an overfitting tendency in the adaptive algorithm could therefore not be assessed. We saw that as long as comparably few smooth functions had been selected fewer spline functions performed better whereas many smooth functions did better with more spline functions, compare Table 15. We gave a possible explanation of these effects by arguing that an omitted-variable bias due to too few smooth functions might have been aggravated here by an overfitting due to too many spline functions. In order to realize the efficiency and performance gains incentivized by Table 16 by making the GAMs more parsimonious, we proposed to set the spline function numbers individually for each smooth function and to use linear terms where sufficient. Another result was that the spline function type should be selected conditional on the spline function number(s) and number of smooth functions, see Tables 17 and 18. As soon as the GAM had been composed of many smooth functions, the choices of both the link and random component turned out to be less crucial which made us recommended the fast gaussian identity GAMs in the exemplary application, compare Tables 19 and 20. Since adaptive forward stagewise selection of length $L = 5$ and adaptive forward stepwise selection led to very similar GAMs according to Table 21, we suggested to use the former selection approach due to its run time advantage. From the fact that the best found GLM had 250 terms and outperformed the best found GAM reported in Table 23, we deduced that using more than 150 smooth functions might improve the results.

FGLS Regression

The FGLS regression algorithm in Section 3.5 is another generalization of the OLS regression algorithm insofar as the errors are here allowed to have any positive definite covariance matrix. For the GLS estimator to be the best linear unbiased estimator by

Gauss-Markov-Aitken theorem, the assumptions of strict exogeneity, linear independent basis functions and a known covariance matrix are required. The GLS estimator minimizes the generalized residual sum of squares. When the covariance matrix is unknown but can be estimated consistently, the FGLS estimator serves as a substitute for the GLS estimator that has asymptotically the same properties. If furthermore the errors are jointly normally distributed, the FGLS estimator can be derived by a maximum likelihood algorithm and fed into AIC according to Theorem 3. Suitable implementations are multiplicative heteroscedasticity, adaptive variance model selection procedures and Breusch-Pagan test for heterogeneity diagnosis.

Among the applied FGLS algorithms in Section 4.5, the type I algorithms led to consistency gains across the three validation sets. According to Breusch-Pagan test, they induced at least a reduction in heteroscedasticity in the generalized least-squares problem, which tended to be the more pronounced the more complex the variance models became but converged fast, compare Tables 24 and 25. Despite the overall improvement in out-of-sample performance and the base approximation, they led to a deterioration in the relevant region for SCR estimation. The type II algorithms showed the effects of the type I algorithms in an amplified and more volatile way. While the type II routines under 300-886 (= no actual restriction) constituted systematically the best choices except for on the extreme and challenging capital region set where their performance was still acceptable, there was no systematically best choice of variance model complexity due to the high variability accompanied by the type II routines under 300-886. The best found FGLS routine reached with 258 terms the highest observed number across all numerical experiments and outperformed all considered GLM and GAM routines in terms of combined Sobol and nested simulations validation. Furthermore, it reduced the bias on these two validation sets by far the most. This result spoke once more for a high interaction complexity of the CFP model. We concluded that the adaptive algorithm maintained its property to yield numerically stable and parsimonious proxy functions without requiring restriction settings in the FGLS context. Nonetheless, the bias of the best FGLS routine on the capital region set motivated the search for even more suitable regression methods and functional forms, see Figure 7. For an overview of these results, see Table 30.

MARS

The classical and generalized MARS algorithms in Section 3.6 are special cases of respectively the OLS regression algorithm and GLM algorithm, in which the basis functions are hinge functions and variable selection is carried out subsequently in a forward and backward pass. While in the forward pass the proxy functions are built up with respect to the residual sum of squares as model selection criterion, in the backward pass they are cut back with respect to GCV where the degrees of freedom are modified to account for the knots in the hinge functions.

By applying a great variety of MARS algorithms in Section 4.6 in a two-step approach,

we ensured that no comparably well suited MARS model would have been missed in our analysis. All tested MARS algorithms selected at maximum 148 basis functions and showed rather poor out-of-sample performances as well as a weak extrapolation behavior compared to the previously discussed routines, see Table 31. The conclusion was that MARS routines were not able to model the complex interactions in the CFP model appropriately.

Kernel Regression

The kernel regression algorithm in Section 3.7 is a non-parametric local regression approach using a kernel as a weighting function. While at each target point the LC kernel estimator is given as the kernel-weighted average, the LL kernel estimator minimizes there the kernel-weighted residual sum of squares. For AIC to be evaluable at a kernel estimator, a non-parametric version accounting for the bandwidths is presented. As an alternative to AIC, non-parametric leave-one-out cross-validation LOO-CV is introduced. The bandwidths are selected such that they minimize the chosen model selection criterion. For reasons of computational efficiency, the adaptive basis function selection procedures need to be performed prior to the kernel regression approach.

Like we did with MARS, we applied numerous variants of kernel regression algorithms in Section 4.7. We found that the LL regression algorithms performed better than the LC ones but still worse than the previously discussed routines, see Table 35. We traced the rather poor out-of-sample performances back to an insufficient interaction modeling by too few basis functions and a poor behavior of local regression approaches close to and beyond the boundary of the fitting space.

Outlook

In our slightly disguised real-world example and given LSMC setting, the adaptive OLS regression, GLM, GAM and FGLS regression algorithms turned out to be suitable machine learning methods for proxy modeling of life insurance companies with potential for both performance and computational efficiency gains by fine-tuning model hyperparameters and implementation designs. For recommendations of specific hyperparameter settings and designs, see the aforementioned suggestions. Differently, the MARS and kernel regression algorithms were not found to be convincing in our application. In order to study the robustness of our results, the approaches can be repeated in multiple other LSMC examples.

After all, none of our tested approaches was able to completely eliminate the bias observed in the validation figures and to yield consistent results across the three validation sets though. Investigations on whether these observations are systematic for the approaches, a result of the Monte Carlo error or a combination thereof help further narrow down the circle of recommended regression techniques. In order to assess the variance

and bias of the proxy estimates conditional on an outer scenario, seed stability analyses in which the sets of fitting points are varied and convergence analyses in which sample size is increased need to be carried out. While such analyses would be computationally very costly, they would provide valuable insights into how to further improve approximation quality, that is, whether additional fitting points are necessary to reflect the underlying CFP model more accurately, whether more suitable functional forms and estimation assumptions are required for a more appropriate proxy modeling, or whether both aspects are relevant. Furthermore, one could deduce from such an analysis the sample sizes needed by the different regression algorithms to meet certain validation criteria. Since the generation of large sample sizes is currently computationally expensive for the industry, algorithms getting along with comparably few fitting points should be striven for.

Picking a suitable calibration algorithm is most important from the viewpoint of capturing the CFP model and hence the SCR appropriately. Therefore, if the bias observed in the validation figures indicates indeed issues with the functional forms of our approaches, doing further research on techniques not entailing such a bias or at least a smaller one is vital. On the one hand, one can fine-tune the approaches of this exposition and try different configurations thereof, and on the other hand, one can analyze further machine learning alternatives such as the ones mentioned in the introduction and already used in other LSMC applications. Ideally, various approaches like adaptive OLS regression, GLM, GAM and FGLS regression algorithms, artificial neural networks, tree-based methods and support vector machines would be fine-tuned and compared based on the same realistic and comprehensive data basis. Since the major challenges of machine learning calibration algorithms are hyperparameter selection and in some cases their dependence on randomness, future research should be dedicated to efficient hyperparameter search algorithms and stabilization methods such as ensemble methods.

Acknowledgements. The first author would like to thank Christian Weiß for his valuable comments which greatly helped improve the paper. Furthermore, she is grateful to Magdalena Roth, Tamino Meyhöfer and her colleagues who have been supportive by providing her with academic time and computational resources.

References

- Akaike, H. (1973), Information theory and an extension of the maximum likelihood principle, 2nd International Symposium on Information Theory, Budapest, Hungary, pp. 267–281.
- Bauer, D. & Ha, H. (2015), A least-squares Monte Carlo approach to the calculation of capital requirements, The World Risk and Insurance Economics Congress, Munich, Germany.
- Bauer, D., Reuss, A. & Singer, D. (2012), ‘On the calculation of the solvency capital requirement based on nested simulations’, *The Journal of the International Actuarial Association* **42**(2), 453–499.
- Bettels, C., Fabrega, J. & Weiß, C. (2014), ‘Anwendung von Least Squares Monte Carlo (LSMC) im Solvency-II-Kontext – Teil 1’, *Der Aktuar* **2**, 85–91.
- Born, R. (2018), Künstliche Neuronale Netze im Risikomanagement, Master’s thesis, Universität zu Köln, Germany.
- Breusch, T. S. & Pagan, A. R. (1979), ‘A simple test for heteroscedasticity and random coefficient variation’, *Econometrica* **47**(5), 1287–1294.
- Buja, A., Hastie, T. & Tibshirani, R. (1989), ‘Linear smoothers and additive models’, *The Annals of Statistics* **17**(2), 453–510.
- Burnham, K. P. & Anderson, D. R. (2002), *Model Selection and Multimodel Inference: A Practical Information-Theoretic Approach*, 2 edn, Springer-Verlag, New York, USA.
- Castellani, G., Fiore, U., Marino, Z., Passalacqua, L., Perla, F., Scognamiglio, S. & Zanetti, P. (2018), ‘An investigation of machine learning approaches in the solvency ii valuation framework’. Available at SSRN.
URL: <https://ssrn.com/abstract=3303296>
- Craven, P. & Wahba, G. (1979), ‘Smoothing noisy data with spline functions’, *Numerische Mathematik* **31**, 377–403.
- Dahlquist, G. & Björck, A. (1974), *Numerical Methods*, Prentice-Hall, Englewood Cliffs, USA.
- Dobson, A. J. (2002), *An Introduction to Statistical Modelling*, 2 edn, Chapman & Hall/CRC, Boca Raton, London, New York, Washington D.C.
- Drucker, H., Burges, C. J., Kaufman, L., Smola, A. & Vapnik, V. (1997), Support vector regression machines, in ‘Advances in Neural Information Processing Systems 9’, MIT Press, Denver, USA, pp. 155–161.

- Duchon, J. (1977), Splines minimizing rotation-invariant semi-norms in solobev spaces, *in* W. Schempp & K. Zeller, eds, ‘Constructive Theory of Functions of Several Variables’, Springer, Berlin, Germany, pp. 85–100.
- Dutang, C. (2017), ‘Some explanations about the IWLS algorithm to fit generalized linear models’, hal-01577698, HAL, France.
- Efron, B. (1983), ‘Estimating the error rate of a prediction rule: Improvement on cross-validation’, *Journal of the American Statistical Association* **78**(382), 316–331.
- Eilers, P. H. & Marx, B. D. (1996), ‘Flexible smoothing with b-splines and penalties’, *Statistical Science* **11**(2), 89–121.
- European Parliament & European Council (2009), ‘Directive 2009/138/EC on the taking-up and pursuit of the business of insurance and reinsurance (Solvency II)’, Directive. Articles 112–127.
- Friedman, J. H. (1991), ‘Multivariate adaptive regression splines (with discussion)’, *The Annals of Statistics* **19**(1), 1–141.
- Friedman, J. H. (1993), ‘Fast MARS’, Technical Report 110. Stanford University Department of Statistics.
- Friedman, J. H. & Silverman, B. W. (1989), ‘Flexible parsimonious smoothing and additive modeling’, *Technometrics* **31**(1), 3–21.
- Friedman, J. H. & Stuetzle, W. (1981), ‘Projection pursuit regression’, *Journal of the American Statistical Association* **76**, 817–823.
- Gay, D. M. (1990), ‘Usage summary for selected optimization routines’, Computing Science Technical Report 153. AT&T Bell Laboratories, Murray Hill.
- Gordy, M. B. & Juneja, S. (2010), ‘Nested simulations in portfolio risk measurement’, *Management Science* **56**, 1833–1848.
- Green, P. J. (1984), ‘Iteratively reweighted least squares for maximum likelihood estimation, and some robust and resistant alternatives’, *Journal of the Royal Statistical Society, Series B* **46**(2), 149–192.
- Greene, W. H. (2002), *Econometric Analysis*, 5 edn, Prentice Hall, Upper Saddle River, USA.
- Hartmann, S. (2015), Verallgemeinerte lineare Modelle im Kontext des Least Squares Monte Carlo Verfahrens, Master’s thesis, Katholische Universität Eichstätt-Ingolstadt, Germany.

- Harvey, A. C. (1976), ‘Estimating regression models with multiplicative heteroscedasticity’, *Econometrica* **44**(3), 461–465.
- Hastie, T. & Pregibon, D. (1992), *Chapter 6 ‘Generalized Linear Models’ in Statistical Models in S*, Wadsworth & Brooks/Cole, Boca Raton, London, New York, Washington D.C.
- Hastie, T. & Tibshirani, R. (1986), ‘Generalized additive models’, *Statistical Science* **1**(3), 297–318.
- Hastie, T. & Tibshirani, R. (1990), *Generalized Additive Models*, Chapman & Hall, London, UK.
- Hastie, T., Tibshirani, R. & Friedman, J. H. (2017), *The Elements of Statistical Learning*, 2 edn, Springer Series in Statistics, New York, USA.
- Hayashi, F. (2000), *Econometrics*, Princeton University Press, Princeton, USA.
- Hejazi, S. A. & Jackson, K. R. (2017), ‘Efficient valuation of scr via a neural network approach’, *Journal of Computational and Applied Mathematics* **313**, 427–439.
- Hocking, R. R. (1976), ‘The analysis and selection of variables in linear regression’, *Biometrics* **32**(1), 1–49.
- Huang, D. S. (1970), *Regression and Econometric Methods*, John Wiley & Sons, New York, USA.
- Hurvich, C. M., Simonoff, J. S. & Tsai, C.-L. (1998), ‘Smoothing parameter selection in nonparametric regression using an improved Akaike information criterion’, *Journal of the Royal Statistical Society, Series B* **60**(2), 271–293.
- Kandasamy, K. & Yu, Y. (2016), Additive approximations in high dimensional nonparametric regression via the SALSA, in ‘Proceedings of the 33rd International Conference on Machine Learning’, Vol. 48, JMLR: W&CP, New York, USA, pp. 69—78.
- Kazimov, N. (2018), Least Squares Monte Carlo modeling based on radial basis functions, Master’s thesis, Universität Ulm, Germany.
- Kopczyk, D. (2018), ‘Proxy modeling in life insurance companies with the use of machine learning algorithms’. Working Paper.
URL: <https://ssrn.com/abstract=3396481>
- Krah, A.-S. (2015), Suitable information criteria and regression methods for the polynomial fitting process in the lsmc model, Master’s thesis, Julius-Maximilians-Universität Würzburg, Germany.

- Krah, A.-S., Nikolić, Z. & Korn, R. (2018), ‘A least-squares Monte Carlo framework in proxy modeling of life insurance companies’, *Risks* **6**(2), 62.
- Li, Q. & Racine, J. (2004), ‘Cross-validated local linear nonparametric regression’, *Statistica Sinica* **14**, 485–512.
- Li, Q. & Racine, J. (2007), *Nonparametric Econometrics: Theory and Practice*, Princeton University Press, Princeton, USA.
- Magnus, J. R. (1978), ‘Maximum likelihood estimation of the GLS model with unknown parameters in the disturbance covariance matrix’, *Journal of Econometrics* **7**(3), 281–312.
- Marra, G. & Wood, S. N. (2012), ‘Coverage properties of confidence intervals for generalized additive model components’, *Scandinavian Journal of Statistics* **39**(1), 53–74.
- Marx, B. D. & Eilers, P. H. (1998), ‘Direct generalized additive modeling with penalized likelihood’, *Computational Statistics & Data Analysis* **28**, 193–209.
- McCullagh, P. & Nelder, J. A. (1989), *Generalized Linear Models*, 2 edn, Chapman & Hall, London, New York.
- McLean, D. (2014), ‘Orthogonality in proxy generator’, Presentation, Moody’s Analytics, Insurance-ERS. Legendre Polynomial / QR Decomposition Equivalence in Multiple Polynomial Regression.
- Milborrow, S. (2018), *earth: Multivariate Adaptive Regression Splines*. Derived from mda:mars by Trevor Hastie and Rob Tibshirani. Uses Alan Miller’s Fortran utilities with Thomas Lumley’s leaps wrapper. R package version 4.6.3.
URL: <https://cran.r-project.org/web/packages/earth>
- Mourik, T. (2003), ‘Market risk of insurance companies’, Discussion Paper IAA Insurer Solvency Assessment Working Party.
- Nadaraya, E. A. (1964), ‘On estimating regression’, *Theory of Probability and Its Applications* **9**(1), 141–142.
- Nelder, J. A. & Wedderburn, R. W. M. (1972), ‘Generalized linear models’, *Journal of the Royal Statistical Society, Series A* **135**(3), 370–384.
- Nikolić, Z., Jonen, C. & Zhu, C. (2017), ‘Robust regression technique in lsme proxy modeling’, *Der Aktuar* **1**, 8–16.
- Nychka, D. (1988), ‘Bayesian confidence intervals for smoothing splines’, *Journal of the American Statistical Association* **83**, 1134–1143.

Pindyck, R. S. & Rubinfeld, D. L. (1998), *Econometric Models and Economic Forecasts*, Irwin/McGraw-Hill, University of Michigan, USA.

R Core Team (2018), *stats: R statistical functions*, R Foundation for Statistical Computing, Vienna, Austria. R package version 3.2.0.

URL: <http://www.R-project.org>

Racine, J. S. & Hayfield, T. (2018), *np: Nonparametric Kernel Smoothing Methods for Mixed Data Types*. R package version 0.60-8.

URL: <https://cran.r-project.org/web/packages/np>

Runge, C. (1901), ‘Über empirische Funktionen und die Interpolation zwischen äquidistanten Ordinaten’, *Zeitschrift für Mathematik und Physik* **46**, 224—243.

Schelthoff, T. (2019), Machine learning methods as alternatives to the least squares Monte Carlo model for calculating the solvency capital requirement of life and health insurance companies, Master’s thesis, Universität zu Köln, Germany.

Schoenenwald, J. J. (2019), Modelli proxy per la determinazione dei requisiti di capitale secondo Solvency II, Master’s thesis, Universitá degli Studi di Trieste, Italy.

Sell, R. (2019), Nicht-Parametrische Regression im Risikomanagement, Bachelor’s thesis, Universität zu Köln, Germany.

Stone, M. (1974), ‘Cross-validatory choice and assessment of statistical predictions’, *Journal of the Royal Statistical Society, Series B* **36**(2), 111–147.

Suykens, J. A. & Vandewalle, J. (1999), ‘Least squares support vector machine classifiers’, *Neural Processing Letters* **9**(3), 293–300.

Teuguia, O. N., Ren, J. & Planchet, F. (2014), ‘Internal model in life insurance: application of least squares monte carlo in risk assessment’, Technical Report. Laboratoire de Sciences Actuarielle et Financière.

Tibshirani, R. (1996), ‘Regression shrinkage and selection via the lasso’, *Journal of the Royal Statistical Society, Series B* **58**(1), 267–288.

Watson, G. S. (1964), ‘Smooth regression analysis’, *Sankhyā: The Indian Journal of Statistics, Series A* **26**(4), 359—372.

Weiß, C. & Nikolić, Z. (2018), ‘An aspect of optimal regression design for lsme’. Working Paper.

URL: <https://arxiv.org/pdf/1811.08509.pdf>

Wood, S. N. (2000), ‘Modelling and smoothing parameter estimation with multiple quadratic penalties’, *Journal of the Royal Statistical Society, Series B* **62**(2), 413–428.

- Wood, S. N. (2003), ‘Thin plate regression splines’, *Journal of the Royal Statistical Society, Series B* **65**(1), 95–114.
- Wood, S. N. (2006), ‘Generalized additive models’, Lecture Notes, School of Mathematics, University of Bristol, U.K.
- Wood, S. N. (2017), *Generalized Additive Models: An Introduction with R*, 2 edn, CRC Press, Boca Raton, USA.
- Wood, S. N. (2018), *mgcv: Mixed GAM Computation Vehicle with Automatic Smoothness Estimation*. R package version 1.8-24.
URL: <https://cran.r-project.org/web/packages/mgcv>
- Wood, S. N., Goude, Y. & Shaw, S. (2015), ‘Generalized additive models for large data sets’, *Journal of the Royal Statistical Society, Series C* **64**(1), 139–155.
- Wood, S. N., Li, Z., Shaddick, G. & Augustin, N. H. (2017), ‘Generalized additive models for gigadata: Modeling the u.k. black smoke network daily data’, *Journal of the American Statistical Association* **112**(519), 1199–1210.
- Wood, S. N., Pya, N. & Säfken, B. (2016), ‘Smoothing parameter and model selection for general smooth models’, *Journal of the American Statistical Association* **111**(516), 1548–1575.
- Zuur, A. F., Ieno, E. N., Walker, N. J., Saveliev, A. A. & Smith, G. M. (2009), *Mixed Effects Models and Extensions in Ecology with R*, Springer Science+Business Media, New York, USA, chapter GLM and GAM for Count Data, pp. 209–243.

Appendix

<i>k</i>	v.mae	v.mae ^a	v.res	v.mae ⁰	v.res ⁰	ns.mae	ns.mae ^a	ns.res	ns.mae ⁰	ns.res ⁰	cr.mae	cr.mae ^a	cr.res	cr.mae ⁰	cr.res ⁰
0	4.557	4.357	-238	100.000	38	3.231	3.121	0	100.000	261	4.027	3.942	106	100.000	367
10	0.839	0.802	0	21.468	104	0.389	0.376	23	21.659	113	0.650	0.636	89	27.112	179
20	0.565	0.540	-10	16.780	82	0.597	0.577	-75	8.274	2	0.454	0.445	-40	10.083	38
30	0.518	0.496	1	17.501	100	0.418	0.404	-47	7.970	37	0.264	0.259	1	13.378	85
40	0.475	0.454	-10	16.888	98	0.509	0.492	-66	6.234	27	0.291	0.285	-26	10.497	68
50	0.368	0.352	-15	13.268	78	0.391	0.378	-50	6.060	29	0.221	0.217	-9	10.674	69
60	0.306	0.293	-17	10.760	62	0.301	0.290	-36	5.863	29	0.183	0.179	5	10.651	69
70	0.291	0.278	-18	10.451	60	0.281	0.272	-33	6.060	30	0.175	0.171	8	10.958	72
80	0.263	0.251	-23	9.389	54	0.309	0.298	-41	4.837	22	0.157	0.154	-4	8.945	59
90	0.267	0.256	-24	9.196	54	0.313	0.303	-42	4.689	22	0.158	0.155	-7	8.587	57
100	0.250	0.239	-18	9.152	53	0.276	0.266	-35	4.637	22	0.136	0.133	0	8.606	57
110	0.237	0.226	-18	8.494	48	0.264	0.255	-34	4.144	18	0.129	0.126	-2	7.634	50
120	0.241	0.230	-16	8.896	50	0.267	0.258	-34	4.153	18	0.124	0.122	-2	7.679	51
130	0.250	0.239	-18	9.839	57	0.281	0.272	-37	4.810	24	0.122	0.120	-1	8.900	59
140	0.246	0.235	-15	9.855	57	0.263	0.254	-33	4.809	24	0.120	0.117	1	8.822	58
150	0.247	0.237	-14	9.924	57	0.271	0.262	-35	4.612	22	0.122	0.120	-1	8.537	56

Table 4: Out-of-sample validation figures of the OLS proxy function of BEL under 150-443 after each tenth iteration.

<i>k</i>	v.mae	v.mae ^a	v.res	v.mae ⁰	v.res ⁰	ns.mae	ns.mae ^a	ns.res	ns.mae ⁰	ns.res ⁰	cr.mae	cr.mae ^a	cr.res	cr.mae ⁰	cr.res ⁰
0	60.620	3.178	-296	100.000	-207	97.518	2.936	-453	100.000	-369	257.762	4.251	-653	100.000	-568
10	15.987	0.838	-1	29.161	-110	10.264	0.309	-6	32.492	-119	31.461	0.519	-67	31.704	-180
20	10.292	0.540	10	21.029	-82	19.163	0.577	75	12.240	-21	26.995	0.445	39	13.324	-57
30	9.444	0.495	-1	21.971	-100	13.409	0.404	47	15.583	-56	15.766	0.260	-1	18.759	-105
40	8.656	0.454	10	21.197	-98	16.359	0.492	67	12.740	-46	17.271	0.285	26	15.434	-87
50	6.718	0.352	15	16.655	-78	12.565	0.378	50	12.938	-47	13.182	0.217	9	15.666	-88
60	5.581	0.293	17	13.506	-62	9.671	0.291	36	12.985	-48	10.904	0.180	-5	15.640	-88
70	5.313	0.279	19	13.026	-59	9.095	0.274	34	13.289	-49	10.357	0.171	-8	15.975	-90
80	4.688	0.246	21	11.326	-51	9.069	0.273	36	11.131	-41	8.997	0.148	0	13.590	-77
90	4.870	0.255	24	11.525	-53	10.043	0.302	42	10.995	-41	9.414	0.155	7	13.285	-75
100	4.546	0.238	18	11.471	-53	8.847	0.266	35	11.041	-41	8.081	0.133	0	13.308	-76
110	4.313	0.226	18	10.650	-48	8.463	0.255	34	9.999	-37	7.689	0.127	2	12.181	-69
120	4.430	0.232	16	11.350	-51	8.304	0.250	33	10.596	-39	7.187	0.119	-1	12.763	-73
130	4.555	0.239	18	12.345	-57	9.024	0.272	37	11.491	-42	7.285	0.120	1	13.663	-78
140	4.532	0.238	15	12.470	-57	8.722	0.263	35	11.282	-42	7.227	0.119	0	13.448	-76
150	4.512	0.237	14	12.459	-57	8.712	0.262	35	11.136	-41	7.265	0.120	1	13.242	-75

Table 5: Out-of-sample validation figures of the OLS proxy function of AC under 150-443 after each tenth iteration.

<i>k</i>	v.mae	v.mae ^a	v.res	v.mae ⁰	v.res ⁰	ns.mae	ns.mae ^a	ns.res	ns.mae ⁰	ns.res ⁰	cr.mae	cr.mae ^a	cr.res	cr.mae ⁰	cr.res ⁰
0	4.557	4.357	-238	100.000	38	3.231	3.121	0	100.000	261	4.027	3.942	106	100.000	367
10	0.839	0.802	0	21.468	104	0.389	0.376	23	21.659	113	0.650	0.636	89	27.112	179
20	0.565	0.540	-10	16.780	82	0.597	0.577	-75	8.274	2	0.454	0.445	-40	10.083	38
30	0.518	0.496	1	17.501	100	0.418	0.404	-47	7.970	37	0.264	0.259	1	13.378	85
40	0.475	0.454	-10	16.888	98	0.509	0.492	-66	6.234	27	0.291	0.285	-26	10.497	68
50	0.368	0.352	-15	13.268	78	0.391	0.378	-50	6.060	29	0.221	0.217	-9	10.674	69
60	0.306	0.293	-17	10.760	62	0.301	0.290	-36	5.863	29	0.183	0.179	5	10.651	69
70	0.291	0.278	-18	10.451	60	0.281	0.272	-33	6.060	30	0.175	0.171	8	10.958	72
80	0.263	0.251	-23	9.389	54	0.309	0.298	-41	4.837	22	0.157	0.154	-4	8.945	59
90	0.267	0.256	-24	9.196	54	0.313	0.303	-42	4.689	22	0.158	0.155	-7	8.587	57
100	0.250	0.239	-18	9.152	53	0.276	0.266	-35	4.637	22	0.136	0.133	0	8.606	57
110	0.237	0.229	-18	9.132	52	0.269	0.260	-35	4.577	22	0.132	0.129	-1	8.358	55
120	0.242	0.231	-16	9.519	54	0.273	0.263	-35	4.569	21	0.129	0.126	-1	8.380	55
130	0.251	0.240	-18	10.506	61	0.287	0.277	-37	5.421	27	0.127	0.125	0	9.724	64
140	0.246	0.235	-15	10.530	61	0.269	0.260	-34	5.329	27	0.123	0.120	2	9.526	63
150	0.242	0.232	-14	10.556	61	0.274	0.265	-35	5.119	26	0.123	0.120	0	9.261	61
160	0.243	0.232	-15	10.483	60	0.278	0.268	-36	5.018	25	0.127	0.124	0	9.144	60
170	0.238	0.228	-13	10.140	58	0.265	0.256	-33	4.968	24	0.130	0.127	2	8.884	59
180	0.241	0.230	-12	10.128	57	0.300	0.290	-37	4.552	18	0.149	0.146	2	8.716	58
190	0.201	0.192	-13	6.458	32	0.275	0.266	-33	4.124	-2	0.173	0.169	-4	4.721	27
200	0.186	0.178	-9	6.111	29	0.262	0.254	-29	4.460	-4	0.181	0.177	3	4.920	27
210	0.184	0.176	-9	6.210	30	0.258	0.249	-28	4.337	-3	0.170	0.167	3	4.846	28
220	0.185	0.177	-8	6.433	32	0.258	0.250	-28	4.286	-3	0.165	0.161	3	4.850	28
224	0.194	0.186	-9	6.659	34	0.268	0.259	-30	4.200	-2	0.168	0.165	1	5.007	29

Table 6: Out-of-sample validation figures of the OLS proxy function of BEL under 300-886 after each tenth and the final iteration.

<i>k</i>	v.mae	v.mae ^a	v.res	v.mae ⁰	v.res ⁰	ns.mae	ns.mae ^a	ns.res	ns.mae ⁰	ns.res ⁰	cr.mae	cr.mae ^a	cr.res	cr.mae ⁰	cr.res ⁰
150-443 figures based on validation values minus 1.96 times standard errors															
150	0.286	0.273	-30	9.878	57	0.330	0.319	-46	3.915	16	0.151	0.148	-13	7.473	49
150-443 figures based on validation values															
150	0.247	0.237	-14	9.924	57	0.271	0.262	-35	4.612	22	0.122	0.120	-1	8.537	56
150-443 figures based on validation values plus 1.96 times standard errors															
150	0.231	0.221	1	9.977	57	0.219	0.212	-24	5.473	28	0.130	0.127	11	9.591	64
300-886 figures based on validation values minus 1.96 times standard errors															
224	0.236	0.225	-24	6.757	34	0.325	0.314	-41	4.610	-8	0.191	0.187	-11	4.307	22
300-886 figures based on validation values															
224	0.194	0.186	-9	6.659	34	0.268	0.259	-30	4.200	-2	0.168	0.165	1	5.007	29
300-886 figures based on validation values plus 1.96 times standard errors															
224	0.184	0.177	7	6.625	35	0.218	0.211	-19	3.982	4	0.173	0.169	13	5.813	37

Table 7: Out-of-sample validation figures of the derived OLS proxy functions of BEL under 150-443 and 300-886 after the final iteration based on three different sets of validation value estimates. Thereby emerges the first set of validation value estimates from pointwise subtraction of 1.96 times the standard errors from the original set of validation values. The second set is the original set. The third set is the addition counterpart of the first set.

<i>k</i>	AIC	v.mae	v.mae ^a	v.res	v.mae ⁰	v.res ⁰	ns.mae	ns.mae ^a	ns.res	ns.mae ⁰	ns.res ⁰	cr.mae	cr.mae ^a	cr.res	cr.mae ⁰	cr.res ⁰
Gaussian with identity link																
0	437, 251	4.557	4.357	-238	100.000	38	3.231	3.121	0	100.000	261	4.027	3.942	106	100.000	367
10	345, 045	0.839	0.802	0	21.468	104	0.389	0.376	23	21.659	113	0.650	0.636	89	27.112	179
20	333, 447	0.565	0.540	-10	16.780	82	0.597	0.577	-75	8.274	2	0.454	0.445	-40	10.083	38
30	330, 361	0.518	0.496	1	17.501	100	0.418	0.404	-47	7.970	37	0.264	0.259	1	13.378	85
40	328, 832	0.475	0.454	-10	16.888	98	0.509	0.492	-66	6.234	27	0.291	0.285	-26	10.497	68
50	327, 432	0.368	0.352	-15	13.268	78	0.391	0.378	-50	6.060	29	0.221	0.217	-9	10.674	69
60	326, 787	0.306	0.293	-17	10.760	62	0.301	0.290	-36	5.863	29	0.183	0.179	5	10.651	69
70	326, 453	0.291	0.278	-18	10.451	60	0.281	0.272	-33	6.060	30	0.175	0.171	8	10.958	72
80	326, 245	0.263	0.251	-23	9.389	54	0.309	0.298	-41	4.837	22	0.157	0.154	-4	8.945	59
90	326, 116	0.267	0.256	-24	9.196	54	0.313	0.303	-42	4.689	22	0.158	0.155	-7	8.587	57
100	326, 038	0.250	0.239	-18	9.152	53	0.276	0.266	-35	4.637	22	0.136	0.133	0	8.606	57
110	325, 968	0.237	0.226	-18	8.494	48	0.264	0.255	-34	4.144	18	0.129	0.126	-2	7.634	50
120	325, 928	0.241	0.230	-16	8.896	50	0.267	0.258	-34	4.153	18	0.124	0.122	-2	7.679	51
130	325, 896	0.250	0.239	-18	9.839	57	0.281	0.272	-37	4.810	24	0.122	0.120	-1	8.900	59
140	325, 873	0.246	0.235	-15	9.855	57	0.263	0.254	-33	4.809	24	0.120	0.117	1	8.822	58
150	325, 850	0.247	0.237	-14	9.924	57	0.271	0.262	-35	4.612	22	0.122	0.120	-1	8.537	56
Gaussian with inverse link																
0	437, 251	4.557	4.357	-238	100.000	38	3.231	3.121	0	100.000	261	4.027	3.942	106	100.000	367
10	343, 426	1.036	0.990	1	33.705	192	0.650	0.628	-63	21.481	114	0.391	0.382	44	33.482	221
20	334, 985	0.689	0.659	-6	21.313	118	0.515	0.498	-62	10.319	49	0.324	0.317	-4	16.493	107
30	331, 426	0.512	0.490	-16	18.836	109	0.393	0.380	-45	12.277	65	0.248	0.243	15	18.960	125
40	328, 875	0.433	0.414	-5	14.354	82	0.317	0.306	-26	9.312	47	0.294	0.288	26	15.188	99
50	327, 877	0.383	0.366	-8	12.959	76	0.285	0.276	-24	8.961	46	0.271	0.265	25	14.592	95
60	327, 274	0.337	0.323	-16	12.572	73	0.328	0.316	-37	7.636	38	0.219	0.215	10	13.087	85
70	326, 875	0.290	0.277	-14	11.248	64	0.271	0.261	-32	6.233	31	0.156	0.153	6	10.588	70
80	326, 603	0.259	0.248	-16	9.976	58	0.287	0.278	-38	5.042	22	0.158	0.155	-8	8.014	52
90	326, 390	0.254	0.243	-20	8.462	47	0.392	0.379	-51	4.451	1	0.220	0.215	-17	5.676	36
100	326, 225	0.270	0.258	-21	8.884	49	0.393	0.379	-51	4.454	5	0.219	0.215	-12	6.732	44
110	326, 152	0.272	0.260	-20	8.558	47	0.375	0.363	-48	4.441	4	0.208	0.204	-10	6.545	42
120	326, 094	0.267	0.255	-19	8.418	47	0.380	0.367	-49	4.414	3	0.209	0.205	-12	6.194	40
130	326, 058	0.266	0.254	-19	8.638	48	0.379	0.367	-49	4.329	4	0.203	0.199	-11	6.362	41
140	325, 982	0.258	0.247	-17	8.353	45	0.363	0.351	-46	4.380	2	0.197	0.193	-10	6.059	38
150	325, 952	0.258	0.247	-16	8.468	45	0.353	0.341	-44	4.282	3	0.192	0.188	-8	6.088	39
Gaussian with log link																
0	437, 251	4.557	4.357	-238	100.000	38	3.231	3.121	0	100.000	261	4.027	3.942	106	100.000	367
10	342, 325	0.879	0.840	26	25.171	132	0.422	0.408	-17	15.628	74	0.530	0.519	52	22.034	143
20	334, 417	0.661	0.632	-5	22.474	125	0.532	0.514	-64	10.764	51	0.330	0.323	-3	17.317	112
30	330, 901	0.560	0.536	-3	21.780	126	0.474	0.458	-55	11.199	59	0.266	0.261	3	17.802	117
40	328, 444	0.411	0.393	-10	13.639	78	0.315	0.304	-29	8.610	44	0.264	0.258	19	14.162	92
50	327, 574	0.341	0.326	-16	12.936	75	0.334	0.323	-35	8.294	42	0.262	0.257	12	13.642	89
60	327, 029	0.315	0.302	-17	11.991	69	0.312	0.301	-36	7.024	36	0.192	0.188	10	12.465	82
70	326, 637	0.279	0.267	-16	10.620	61	0.266	0.257	-31	6.142	31	0.162	0.158	9	10.797	71
80	326, 449	0.266	0.254	-21	10.069	59	0.304	0.294	-40	5.195	25	0.153	0.149	-4	9.234	61
90	326, 287	0.273	0.261	-22	9.742	57	0.300	0.290	-40	5.082	25	0.141	0.138	-5	8.990	59
100	326, 082	0.269	0.257	-23	8.052	45	0.370	0.358	-48	4.094	6	0.210	0.205	-13	6.314	41
110	326, 021	0.258	0.247	-19	8.043	44	0.343	0.331	-43	4.102	5	0.198	0.193	-7	6.381	41
120	325, 950	0.252	0.241	-17	7.891	42	0.329	0.318	-41	4.086	3	0.191	0.187	-7	5.883	37
130	325, 881	0.251	0.240	-18	8.049	45	0.359	0.347	-46	4.238	2	0.194	0.190	-10	5.924	38
140	325, 849	0.245	0.234	-17	7.978	44	0.340	0.328	-43	4.045	4	0.183	0.179	-7	6.131	40
150	325, 823	0.240	0.229	-15	7.980	44	0.316	0.305	-38	4.014	6	0.170	0.167	-2	6.434	42

Table 8: AIC scores and out-of-sample validation figures of the gaussian GLMs of BEL with identity, inverse and log link functions under 150-443 after each tenth iteration.

<i>k</i>	AIC	v.mae	v.mae ^a	v.res	v.mae ⁰	v.res ⁰	ns.mae	ns.mae ^a	ns.res	ns.mae ⁰	ns.res ⁰	cr.mae	cr.mae ^a	cr.res	cr.mae ⁰	cr.res ⁰
Gamma with identity link																
0	437,243	4.557	4.357	-238	100.000	38	3.231	3.121	0	100.000	261	4.027	3.942	106	100.000	367
10	345,605	0.872	0.834	-1	23.485	114	0.315	0.304	6	19.861	105	0.530	0.519	68	25.266	167
20	333,911	0.553	0.529	-12	16.265	79	0.599	0.579	-76	8.268	0	0.464	0.454	-43	9.895	34
30	330,707	0.503	0.481	0	17.404	99	0.425	0.411	-49	7.754	35	0.267	0.262	-2	12.959	82
40	328,589	0.376	0.359	-13	13.317	76	0.341	0.330	-39	7.187	35	0.238	0.233	6	12.341	80
50	327,668	0.348	0.333	-15	13.173	77	0.356	0.344	-44	6.656	34	0.227	0.222	-4	11.348	74
60	327,135	0.305	0.292	-16	11.190	65	0.304	0.294	-37	6.059	30	0.175	0.172	3	10.843	71
70	326,686	0.273	0.261	-15	9.730	55	0.257	0.249	-30	5.364	26	0.165	0.161	9	9.928	65
80	326,461	0.268	0.257	-21	9.471	54	0.287	0.277	-36	5.151	25	0.149	0.146	2	9.549	63
90	326,328	0.259	0.248	-23	8.889	52	0.304	0.293	-40	4.373	20	0.148	0.145	-6	8.255	55
100	326,246	0.238	0.227	-20	8.321	48	0.262	0.253	-34	4.279	19	0.137	0.134	-1	7.845	52
110	326,184	0.233	0.223	-18	8.045	45	0.255	0.246	-33	3.907	16	0.130	0.127	-1	7.182	47
120	326,135	0.228	0.218	-16	8.191	46	0.253	0.245	-33	3.696	15	0.129	0.126	-2	6.870	45
130	326,093	0.244	0.233	-17	9.530	55	0.272	0.263	-35	4.628	22	0.124	0.122	0	8.596	57
140	326,068	0.238	0.228	-17	9.416	54	0.271	0.261	-35	4.523	22	0.125	0.123	-1	8.371	55
150	326,041	0.236	0.226	-14	9.329	53	0.260	0.251	-33	4.321	20	0.121	0.118	1	8.206	54
Gamma with inverse link																
0	437,243	4.557	4.357	-238	100.000	38	3.231	3.121	0	100.000	261	4.027	3.942	106	100.000	367
10	343,969	1.037	0.991	0	33.818	193	0.661	0.639	-64	21.601	115	0.397	0.389	44	33.752	223
20	335,495	0.679	0.649	-7	20.888	115	0.530	0.512	-65	9.637	43	0.335	0.328	-9	15.410	99
30	332,646	0.627	0.600	-9	26.098	152	0.621	0.600	-82	12.361	64	0.346	0.339	-24	18.470	122
40	329,192	0.409	0.391	-10	14.061	81	0.317	0.306	-27	9.719	50	0.289	0.283	23	15.405	101
50	328,114	0.339	0.324	-12	12.599	73	0.313	0.302	-30	8.084	40	0.271	0.265	15	13.146	85
60	327,513	0.328	0.313	-16	12.247	71	0.294	0.284	-29	8.341	43	0.240	0.235	18	13.902	91
70	327,115	0.285	0.272	-12	11.127	64	0.251	0.243	-28	6.463	33	0.166	0.162	11	10.915	72
80	326,795	0.252	0.241	-17	8.376	45	0.315	0.305	-39	4.069	9	0.196	0.192	-8	6.416	40
90	326,615	0.250	0.239	-20	8.113	45	0.384	0.371	-51	4.414	0	0.218	0.213	-16	5.478	34
100	326,445	0.263	0.252	-20	8.724	48	0.382	0.369	-49	4.410	5	0.211	0.206	-11	6.595	43
110	326,370	0.266	0.255	-19	8.251	45	0.369	0.357	-47	4.494	2	0.205	0.201	-9	6.288	40
120	326,310	0.258	0.247	-17	8.003	44	0.357	0.345	-45	4.435	2	0.196	0.192	-8	6.087	39
130	326,277	0.259	0.248	-17	8.331	47	0.357	0.344	-45	4.356	4	0.187	0.183	-7	6.509	42
140	326,246	0.262	0.250	-17	8.583	48	0.357	0.345	-45	4.304	5	0.183	0.179	-7	6.620	43
150	326,222	0.254	0.243	-15	8.410	46	0.327	0.316	-40	4.111	7	0.171	0.167	-3	6.722	44
Gamma with log link																
0	437,243	4.557	4.357	-238	100.000	38	3.231	3.121	0	100.000	261	4.027	3.942	106	100.000	367
1	388,234	2.365	2.261	-4	67.494	277	0.773	0.747	22	54.214	287	1.193	1.168	170	65.932	435
10	342,942	0.870	0.832	21	24.998	131	0.440	0.425	-24	15.145	71	0.505	0.494	43	21.396	138
20	334,881	0.649	0.621	-5	19.899	110	0.519	0.501	-65	8.283	36	0.312	0.306	-11	14.105	90
30	331,227	0.544	0.520	-4	21.752	126	0.479	0.463	-57	11.010	58	0.262	0.257	0	17.458	115
40	328,727	0.374	0.357	-10	14.009	81	0.329	0.318	-33	8.553	43	0.268	0.263	15	13.990	91
50	327,806	0.328	0.313	-16	12.750	74	0.327	0.316	-33	8.325	42	0.272	0.266	14	13.779	90
60	327,270	0.302	0.289	-15	11.825	68	0.297	0.287	-33	7.147	37	0.197	0.193	14	12.637	83
70	326,866	0.264	0.253	-15	10.159	58	0.249	0.241	-28	6.071	31	0.165	0.162	12	10.693	70
80	326,669	0.255	0.244	-19	9.819	57	0.288	0.279	-37	5.085	24	0.146	0.143	-2	9.090	60
90	326,433	0.266	0.254	-23	8.891	51	0.327	0.316	-45	4.079	15	0.171	0.167	-12	7.353	48
100	326,302	0.265	0.253	-23	7.839	44	0.361	0.349	-47	4.030	5	0.205	0.201	-12	6.246	40
110	326,224	0.256	0.244	-18	8.139	45	0.335	0.324	-41	4.211	8	0.191	0.187	-3	7.043	46
120	326,147	0.250	0.239	-18	7.817	43	0.340	0.328	-43	4.122	4	0.188	0.184	-6	6.247	41
130	326,111	0.247	0.236	-17	7.750	43	0.341	0.329	-43	4.115	3	0.186	0.183	-7	6.060	39
140	326,050	0.247	0.236	-17	7.730	43	0.336	0.324	-42	4.073	4	0.179	0.176	-6	6.117	40
150	326,022	0.243	0.232	-15	7.820	43	0.323	0.312	-40	4.040	3	0.174	0.170	-4	6.010	39

Table 9: AIC scores and out-of-sample validation figures of the gamma GLMs of BEL with identity, inverse and log link functions under 150-443 after each tenth iteration.

k	AIC	v.mae	v.mae ^a	v.res	v.mae ⁰	v.res ⁰	ns.mae	ns.mae ^a	ns.res	ns.mae ⁰	ns.res ⁰	cr.mae	cr.mae ^a	cr.res	cr.mae ⁰	cr.res ⁰
inverse gaussian with identity link																
0	437, 338	4.557	4.357	-238	100.000	38	3.231	3.121	0	100.000	261	4.027	3.942	106	100.000	367
10	346, 132	0.871	0.833	-1	23.559	115	0.314	0.304	7	20.269	107	0.534	0.523	70	25.673	169
20	334, 430	0.549	0.524	-13	15.996	77	0.599	0.579	-77	8.273	-1	0.468	0.458	-44	9.809	32
30	331, 453	0.488	0.467	-4	15.939	89	0.517	0.499	-67	6.532	11	0.413	0.405	-40	9.280	38
40	328, 985	0.370	0.354	-13	13.279	76	0.338	0.327	-39	7.193	35	0.238	0.233	6	12.301	80
50	328, 064	0.332	0.317	-15	12.727	74	0.338	0.327	-40	6.871	35	0.232	0.227	1	11.664	76
60	327, 533	0.298	0.285	-17	10.994	64	0.304	0.294	-37	5.868	29	0.172	0.168	3	10.646	69
70	327, 082	0.274	0.262	-15	9.387	53	0.243	0.235	-27	5.535	27	0.171	0.167	13	10.253	67
80	326, 849	0.267	0.255	-20	9.426	54	0.278	0.268	-34	5.271	25	0.152	0.148	5	9.783	65
90	326, 715	0.247	0.236	-21	8.546	49	0.275	0.266	-35	4.399	20	0.140	0.137	-1	8.302	55
100	326, 630	0.236	0.225	-20	7.879	45	0.262	0.253	-34	3.979	16	0.140	0.137	-2	7.249	48
110	326, 564	0.225	0.215	-17	7.728	43	0.243	0.235	-31	3.850	15	0.129	0.126	0	6.958	46
120	326, 507	0.237	0.226	-18	8.776	50	0.270	0.260	-35	4.120	19	0.130	0.127	-3	7.710	51
130	326, 475	0.240	0.230	-17	9.225	53	0.265	0.256	-34	4.516	21	0.123	0.120	0	8.400	55
140	326, 447	0.241	0.230	-16	9.415	54	0.270	0.261	-35	4.543	21	0.124	0.122	-1	8.426	56
150	326, 352	0.249	0.238	-17	9.375	54	0.337	0.326	-44	4.224	12	0.150	0.146	-4	7.930	52
Inverse gaussian with inverse link																
0	437, 338	4.557	4.357	-238	100.000	38	3.231	3.121	0	100.000	261	4.027	3.942	106	100.000	367
10	344, 458	1.129	1.079	-25	35.685	202	1.138	1.099	-150	14.423	63	0.639	0.626	-63	22.713	149
20	336, 004	0.682	0.652	-5	21.011	117	0.534	0.516	-67	8.866	41	0.321	0.314	-12	14.895	95
30	333, 060	0.626	0.598	-10	24.463	142	0.623	0.602	-83	10.859	55	0.376	0.369	-31	16.233	107
40	329, 632	0.412	0.394	-14	15.912	93	0.345	0.333	-29	12.096	64	0.318	0.311	28	18.446	121
50	328, 515	0.335	0.320	-12	12.387	71	0.305	0.295	-29	8.122	40	0.276	0.270	18	13.333	86
60	327, 916	0.321	0.307	-15	11.970	70	0.286	0.276	-27	8.385	44	0.247	0.241	20	13.973	91
70	327, 543	0.278	0.266	-12	10.488	60	0.246	0.238	-28	6.106	31	0.164	0.161	9	10.331	67
80	327, 196	0.249	0.238	-17	8.227	45	0.308	0.297	-38	4.037	9	0.193	0.189	-7	6.381	40
90	327, 012	0.247	0.236	-19	8.016	44	0.376	0.363	-49	4.390	-1	0.212	0.207	-15	5.407	33
100	326, 837	0.261	0.250	-20	8.469	46	0.375	0.363	-48	4.428	4	0.208	0.204	-10	6.569	43
110	326, 762	0.262	0.250	-18	8.090	44	0.365	0.353	-46	4.505	2	0.201	0.197	-8	6.242	40
120	326, 699	0.259	0.248	-18	8.106	45	0.367	0.355	-47	4.402	2	0.192	0.188	-9	6.082	39
130	326, 667	0.259	0.247	-17	7.987	44	0.352	0.340	-44	4.303	2	0.187	0.183	-8	5.958	38
140	326, 642	0.258	0.246	-16	8.243	46	0.340	0.328	-42	4.228	6	0.173	0.169	-5	6.602	43
150	326, 617	0.253	0.242	-15	8.152	44	0.324	0.313	-39	4.148	5	0.172	0.169	-3	6.476	42
Inverse gaussian with log link																
0	437, 338	4.557	4.357	-238	100.000	38	3.231	3.121	0	100.000	261	4.027	3.942	106	100.000	367
10	343, 530	0.866	0.828	-19	24.925	131	0.450	0.435	-28	14.940	69	0.494	0.484	39	21.122	136
20	335, 355	0.644	0.616	-5	19.653	109	0.526	0.509	-67	7.947	33	0.318	0.311	-14	13.490	85
30	331, 675	0.536	0.512	-4	21.697	125	0.482	0.465	-58	10.885	57	0.262	0.256	-2	17.245	113
40	329, 140	0.366	0.350	-10	13.913	80	0.325	0.314	-32	8.604	44	0.269	0.264	16	14.011	91
50	328, 190	0.324	0.310	-16	12.640	73	0.319	0.308	-32	8.482	43	0.274	0.268	16	13.966	91
60	327, 666	0.296	0.283	-15	11.626	67	0.290	0.280	-31	7.181	37	0.201	0.197	15	12.695	83
70	327, 263	0.261	0.250	-15	9.948	57	0.244	0.236	-27	6.042	30	0.172	0.168	12	10.531	69
80	327, 061	0.251	0.240	-18	9.746	56	0.284	0.275	-37	4.988	24	0.145	0.142	-1	8.964	59
90	326, 825	0.263	0.251	-23	8.769	51	0.321	0.310	-44	4.059	15	0.168	0.165	-11	7.316	48
100	326, 695	0.261	0.249	-22	7.727	43	0.352	0.340	-45	4.048	6	0.203	0.199	-10	6.341	41
110	326, 598	0.239	0.229	-17	7.408	40	0.343	0.332	-43	4.444	-1	0.185	0.181	-7	5.572	35
120	326, 530	0.249	0.238	-18	7.520	41	0.343	0.331	-43	4.247	1	0.191	0.187	-7	5.928	38
130	326, 494	0.246	0.235	-17	7.602	42	0.337	0.326	-43	4.108	2	0.183	0.179	-6	5.964	39
140	326, 471	0.246	0.235	-17	7.772	43	0.332	0.321	-42	4.068	4	0.177	0.173	-6	6.092	39
150	326, 413	0.247	0.237	-15	7.716	42	0.324	0.313	-40	4.095	2	0.172	0.168	-4	5.892	38
Inverse gaussian with $\frac{1}{\mu^2}$ link																
0	437, 338	4.557	4.357	-238	100.000	38	3.231	3.121	0	100.000	261	4.027	3.942	106	100.000	367
10	344, 467	0.985	0.941	-14	31.473	176	0.993	0.959	-130	12.573	46	0.561	0.549	-52	18.986	124
20	336, 815	0.668	0.639	-7	21.404	122	0.591	0.571	-75	9.506	38	0.372	0.364	-22	14.521	91
30	331, 792	0.478	0.457	-5	15.821	90	0.367	0.354	-28	10.573	53	0.373	0.365	33	17.496	114
40	329, 080	0.421	0.403	-1	15.183	89	0.295	0.285	-19	10.660	56	0.316	0.309	34	16.657	109
50	329, 020	0.376	0.359	-10	14.443	85	0.300	0.290	-21	11.439	60	0.320	0.313	34	17.553	115
60	328, 452	0.330	0.316	-12	12.905	75	0.290	0.280	-24	9.196	48	0.273	0.267	25	14.952	98
70	327, 925	0.316	0.302	-16	11.733	69	0.301	0.291	-35	7.090	35	0.200	0.195	6	11.701	76
80	327, 639	0.262	0.250	-18	8.128	43	0.298	0.288	-35	4.425	11	0.208	0.203	-1	7.205	45
90	327, 265	0.278	0.266	-22	8.311	46	0.355	0.343	-44	4.383	9	0.202	0.197	-7	7.090	46
100	327, 148	0.288	0.275	-22	8.166	44	0.357	0.345	-44	4.408	8	0.207	0.203	-6	7.039	46
110	327, 078	0.274	0.262	-20	7.943	43	0.354	0.342	-44	4.451	4	0.196	0.192	-7	6.434	41
120	326, 920	0.269	0.257	-18	8.350	46	0.374	0.361	-47	4.579	3	0.198	0.193	-9	6.419	41
130	326, 887	0.270	0.258	-18	8.437	47	0.360	0.348	-44	4.544	6	0.196	0.192	-4	7.151	46
140	326, 807	0.267	0.255	-18	8.193	45	0.345	0.333	-43	4.318	5	0.188	0.184	-5	6.661	43
150	326, 778	0.262	0.250	-16</												

k	AIC	v.mae	v.mae ^a	v.res	v.mae ⁰	v.res ⁰	ns.mae	ns.mae ^a	ns.res	ns.mae ⁰	ns.res ⁰	cr.mae	cr.mae ^a	cr.res	cr.mae ⁰	cr.res ⁰
Gaussian with identity link																
0	437, 251	4.557	4.357	-238	100.000	38	3.231	3.121	0	100.000	261	4.027	3.942	106	100.000	367
10	345, 045	0.839	0.802	0	21.468	104	0.389	0.376	23	21.659	113	0.650	0.636	89	27.112	179
20	333, 447	0.565	0.540	-10	16.780	82	0.597	0.577	-75	8.274	2	0.454	0.445	-40	10.083	38
30	330, 361	0.518	0.496	1	17.501	100	0.418	0.404	-47	7.970	37	0.264	0.259	1	13.378	85
40	328, 832	0.475	0.454	-10	16.888	98	0.509	0.492	-66	6.234	27	0.291	0.285	-26	10.497	68
50	327, 432	0.368	0.352	-15	13.268	78	0.391	0.378	-50	6.060	29	0.221	0.217	-9	10.674	69
60	326, 787	0.306	0.293	-17	10.760	62	0.301	0.290	-36	5.863	29	0.183	0.179	5	10.651	69
70	326, 453	0.291	0.278	-18	10.451	60	0.281	0.272	-33	6.060	30	0.175	0.171	8	10.958	72
80	326, 245	0.263	0.251	-23	9.389	54	0.309	0.298	-41	4.837	22	0.157	0.154	-4	8.945	59
90	326, 116	0.267	0.256	-24	9.196	54	0.313	0.303	-42	4.689	22	0.158	0.155	-7	8.587	57
100	326, 038	0.250	0.239	-18	9.152	53	0.276	0.266	-35	4.637	22	0.136	0.133	0	8.606	57
110	325, 963	0.239	0.229	-18	9.132	52	0.269	0.260	-35	4.577	22	0.132	0.129	-1	8.358	55
120	325, 922	0.242	0.231	-16	9.519	54	0.273	0.263	-35	4.569	21	0.129	0.126	-1	8.380	55
130	325, 889	0.251	0.240	-18	10.506	61	0.287	0.277	-37	5.421	27	0.127	0.125	0	9.724	64
140	325, 865	0.246	0.235	-15	10.530	61	0.269	0.260	-34	5.329	27	0.123	0.120	2	9.526	63
150	325, 841	0.242	0.232	-14	10.556	61	0.274	0.265	-35	5.119	26	0.123	0.120	0	9.261	61
160	325, 821	0.243	0.232	-15	10.483	60	0.278	0.268	-36	5.018	25	0.127	0.124	0	9.144	60
170	325, 811	0.238	0.228	-13	10.140	58	0.265	0.256	-33	4.968	24	0.130	0.127	2	8.884	59
180	325, 766	0.241	0.230	-12	10.128	57	0.300	0.290	-37	4.552	18	0.149	0.146	2	8.716	58
190	325, 506	0.201	0.192	-13	6.458	32	0.275	0.266	-33	4.124	-2	0.173	0.169	-4	4.721	27
200	325, 488	0.186	0.178	-9	6.111	29	0.262	0.254	-29	4.460	-4	0.181	0.177	3	4.920	27
210	325, 482	0.184	0.176	-9	6.210	30	0.258	0.249	-28	4.337	-3	0.170	0.167	3	4.846	28
220	325, 468	0.185	0.177	-8	6.433	32	0.258	0.250	-28	4.286	-3	0.165	0.161	3	4.850	28
224	325, 459	0.194	0.186	-9	6.659	34	0.268	0.259	-30	4.200	-2	0.168	0.165	1	5.007	29
Gaussian with inverse link																
0	437, 251	4.557	4.357	-238	100.000	38	3.231	3.121	0	100.000	261	4.027	3.942	106	100.000	367
10	343, 426	1.036	0.990	1	33.705	192	0.650	0.628	-63	21.481	114	0.391	0.382	44	33.482	221
20	334, 985	0.689	0.659	-6	21.313	118	0.515	0.498	-62	10.319	49	0.324	0.317	-4	16.493	107
30	331, 426	0.512	0.490	-16	18.836	109	0.393	0.380	-45	12.277	65	0.248	0.243	15	18.960	125
40	328, 875	0.433	0.414	-5	14.354	82	0.317	0.306	-26	9.312	47	0.294	0.288	26	15.188	99
50	327, 877	0.383	0.366	-8	12.959	76	0.285	0.276	-24	8.961	46	0.271	0.265	25	14.592	95
60	327, 274	0.337	0.323	-16	12.572	73	0.328	0.316	-37	7.636	38	0.219	0.215	10	13.087	85
70	326, 875	0.290	0.277	-14	11.248	64	0.271	0.261	-32	6.233	31	0.156	0.153	6	10.588	70
80	326, 603	0.259	0.248	-16	9.976	58	0.287	0.278	-38	5.042	22	0.158	0.155	-8	8.014	52
90	326, 390	0.254	0.243	-20	8.462	47	0.392	0.379	-51	4.451	1	0.220	0.215	-17	5.676	36
100	326, 224	0.269	0.257	-21	9.365	53	0.403	0.389	-52	4.500	7	0.225	0.220	-12	7.174	47
110	326, 135	0.266	0.254	-19	8.894	49	0.377	0.364	-49	4.334	5	0.205	0.201	-12	6.497	42
120	326, 069	0.266	0.254	-19	8.564	48	0.381	0.368	-50	4.271	4	0.204	0.200	-14	6.102	39
130	326, 033	0.265	0.253	-19	8.498	47	0.386	0.373	-50	4.445	2	0.212	0.207	-14	5.917	38
140	325, 950	0.253	0.242	-17	8.151	44	0.358	0.346	-46	4.345	1	0.189	0.185	-11	5.598	35
150	325, 924	0.255	0.244	-17	8.485	46	0.364	0.352	-46	4.288	3	0.192	0.188	-11	5.894	38
160	325, 886	0.258	0.247	-15	8.842	48	0.349	0.337	-44	4.199	5	0.178	0.174	-8	6.359	41
170	325, 869	0.249	0.238	-14	8.503	46	0.331	0.320	-40	4.254	5	0.174	0.171	-5	6.182	40
180	325, 850	0.248	0.237	-12	8.505	45	0.312	0.302	-37	4.099	6	0.164	0.161	-3	6.095	40
190	325, 820	0.238	0.228	-12	8.240	43	0.313	0.303	-37	4.137	4	0.169	0.166	-3	5.825	38
200	325, 803	0.244	0.234	-13	8.458	45	0.320	0.309	-38	4.073	6	0.171	0.167	-4	6.132	40
210	325, 800	0.241	0.231	-13	8.376	45	0.313	0.302	-36	4.059	6	0.171	0.167	-2	6.248	41
213	325, 797	0.241	0.230	-12	8.325	44	0.310	0.299	-36	4.063	6	0.171	0.167	-1	6.284	41
Gaussian with log link																
0	437, 251	4.557	4.357	-238	100.000	38	3.231	3.121	0	100.000	261	4.027	3.942	106	100.000	367
10	342, 325	0.879	0.840	26	25.171	132	0.422	0.408	-17	15.628	74	0.530	0.519	52	22.034	143
20	334, 417	0.661	0.632	-5	22.474	125	0.532	0.514	-64	10.764	51	0.330	0.323	-3	17.317	112
30	330, 901	0.560	0.536	-3	21.780	126	0.474	0.458	-55	11.199	59	0.266	0.261	3	17.802	117
40	328, 444	0.411	0.393	-10	13.639	78	0.315	0.304	-29	8.610	44	0.264	0.258	19	14.162	92
50	327, 574	0.341	0.326	-16	12.936	75	0.334	0.323	-35	8.294	42	0.262	0.257	12	13.642	89
60	327, 029	0.315	0.302	-17	11.991	69	0.312	0.301	-36	7.024	36	0.192	0.188	10	12.465	82
70	326, 637	0.279	0.267	-16	10.620	61	0.266	0.257	-31	6.142	31	0.162	0.158	9	10.797	71
80	326, 349	0.266	0.254	-21	10.069	59	0.304	0.294	-40	5.195	25	0.153	0.149	-4	9.234	61
90	326, 287	0.273	0.261	-22	9.742	57	0.300	0.290	-40	5.082	25	0.141	0.138	-5	8.990	59
100	326, 082	0.269	0.257	-23	8.052	45	0.370	0.358	-48	4.094	6	0.210	0.205	-13	6.314	41
110	326, 021	0.258	0.247	-19	8.043	44	0.343	0.331	-43	4.102	5	0.198	0.193	-7	6.381	41
120	325, 950	0.252	0.241	-17	7.891	42	0.329	0.318	-41	4.086	3	0.191	0.187	-7	5.883	37
130	325, 743	0.208	0.199	-13	6.208	30	0.310	0.299	-38	4.994	-10	0.191	0.187	-8	4.273	21
140	325, 693	0.211	0.202	-13	6.620	34	0.302	0.292	-36	4.522	-3	0.186	0.182	-3	5.037	30
150	325, 665	0.210	0.200	-13	6.729	35	0.298	0.288	-36	4.385	-2	0.180	0.176	-3	5.168	31
160	325, 626	0.214	0.205	-14	6.549	33	0.302	0.292	-36	4.410	-3	0.183	0.179	-4	5.076	30
170	325, 610	0.214	0.204	-14	6.590	33	0.291	0.281	-35	4						

k	AIC	v.mae	v.mae^a	v.res	v.mae⁰	v.res⁰	ns.mae	ns.mae^a	ns.res	ns.mae⁰	ns.res⁰	cr.mae	cr.mae^a	cr.res	cr.mae⁰	cr.res⁰
Gamma with identity link																
0 437, 243 4.557 4.357	-238	100.000	38	3.231	3.121	0	100.000	261	4.027	3.942	106	100.000	367			
10 345, 605 0.872 0.834	-	1	23.485	114	0.315	0.304	-	6	19.861	105	0.530	0.519	68	25.266	167	
20 333, 911 0.553 0.529	-	12	16.265	79	0.599	0.579	-	76	8.268	0	0.464	0.454	-43	9.895	34	
30 330, 707 0.503 0.481	-	0	17.404	99	0.425	0.411	-	49	7.754	35	0.267	0.262	-2	12.959	82	
40 328, 589 0.376 0.359	-	13	13.317	76	0.341	0.330	-	39	7.187	35	0.238	0.233	6	12.341	80	
50 327, 668 0.348 0.333	-	15	13.173	77	0.356	0.344	-	44	6.656	34	0.227	0.222	-4	11.348	74	
60 327, 135 0.305 0.292	-	16	11.190	65	0.304	0.294	-	37	6.059	30	0.175	0.172	3	10.843	71	
70 326, 686 0.273 0.261	-	15	9.730	55	0.257	0.249	-	30	5.364	26	0.165	0.161	9	9.928	65	
80 326, 461 0.268 0.257	-	21	9.471	54	0.287	0.277	-	36	5.151	25	0.149	0.146	2	9.549	63	
90 326, 328 0.259 0.248	-	23	8.889	52	0.304	0.293	-	40	4.373	20	0.148	0.145	-6	8.255	55	
100 326, 244 0.240 0.229	-	20	9.273	54	0.282	0.273	-	37	4.759	22	0.144	0.141	-2	8.662	57	
110 326, 178 0.236 0.225	-	18	8.837	51	0.262	0.254	-	34	4.454	20	0.135	0.132	0	8.139	54	
120 326, 117 0.237 0.226	-	18	9.668	56	0.275	0.266	-	36	4.845	24	0.129	0.126	-1	8.799	58	
130 326, 084 0.245 0.235	-	17	10.148	59	0.270	0.260	-	35	5.236	26	0.122	0.120	1	9.375	62	
140 326, 058 0.243 0.232	-	17	10.153	58	0.273	0.264	-	35	5.092	25	0.125	0.122	-1	9.122	60	
150 326, 031 0.239 0.229	-	14	10.130	58	0.263	0.254	-	33	4.914	24	0.121	0.118	2	9.014	60	
160 325, 871 0.232 0.222	-	15	7.898	44	0.317	0.307	-	39	3.918	5	0.174	0.170	-4	6.237	40	
170 325, 729 0.199 0.190	-	13	6.235	30	0.280	0.271	-	34	4.288	-5	0.176	0.172	-2	4.684	27	
180 325, 718 0.201 0.192	-	13	6.171	30	0.279	0.270	-	34	4.253	-5	0.172	0.169	-2	4.623	27	
190 325, 703 0.197 0.189	-	12	6.158	30	0.278	0.268	-	33	4.269	-5	0.171	0.168	-3	4.521	26	
200 325, 697 0.194 0.185	-	11	5.943	28	0.264	0.255	-	30	4.416	-5	0.169	0.165	0	4.470	25	
210 325, 689 0.190 0.181	-	10	5.992	28	0.261	0.252	-	29	4.381	-5	0.169	0.165	1	4.534	25	
212 325, 689 0.189 0.180	-	11	5.975	28	0.261	0.252	-	29	4.384	-5	0.169	0.165	1	4.545	25	
Gamma with inverse link																
0 437, 243 4.557 4.357	-238	100.000	38	3.231	3.121	0	100.000	261	4.027	3.942	106	100.000	367			
10 343, 969 1.037 0.991	-	0	33.818	193	0.661	0.639	-	64	21.601	115	0.397	0.389	44	33.752	223	
20 335, 495 0.679 0.649	-	7	20.888	115	0.530	0.512	-	65	9.637	43	0.335	0.328	-9	15.410	99	
30 332, 646 0.627 0.600	-	9	26.098	152	0.621	0.600	-	82	12.361	64	0.346	0.339	-24	18.470	122	
40 329, 192 0.409 0.391	-	10	14.061	81	0.317	0.306	-	27	9.719	50	0.289	0.283	23	15.405	101	
50 328, 114 0.339 0.324	-	12	12.599	73	0.313	0.302	-	30	8.084	40	0.271	0.265	15	13.146	85	
60 327, 513 0.328 0.313	-	16	12.247	71	0.294	0.284	-	29	8.341	43	0.240	0.235	18	13.902	91	
70 327, 115 0.285 0.272	-	12	11.127	64	0.251	0.243	-	28	6.463	33	0.166	0.162	11	10.915	72	
80 326, 795 0.252 0.241	-	17	8.376	45	0.315	0.305	-	39	4.069	9	0.196	0.192	-8	6.416	40	
90 326, 615 0.250 0.239	-	20	8.113	45	0.384	0.371	-	51	4.414	0	0.218	0.213	-16	5.478	34	
100 326, 445 0.263 0.252	-	20	9.213	52	0.387	0.374	-	50	4.469	8	0.219	0.214	-10	7.316	48	
110 326, 355 0.272 0.260	-	21	8.812	49	0.384	0.371	-	50	4.313	5	0.209	0.205	-14	6.489	42	
120 326, 297 0.267 0.255	-	20	8.378	46	0.377	0.365	-	48	4.470	2	0.206	0.202	-11	6.140	39	
130 326, 248 0.259 0.248	-	17	8.210	45	0.365	0.352	-	46	4.437	1	0.200	0.196	-10	5.933	38	
140 326, 214 0.258 0.247	-	17	8.212	45	0.355	0.343	-	45	4.404	3	0.192	0.188	-9	6.077	39	
150 326, 190 0.260 0.248	-	17	8.701	49	0.349	0.337	-	44	4.217	7	0.180	0.176	-7	6.781	44	
160 326, 147 0.247 0.236	-	15	8.556	47	0.329	0.317	-	40	4.091	7	0.174	0.170	-4	6.643	43	
170 326, 070 0.247 0.236	-	15	8.355	46	0.332	0.321	-	41	4.077	5	0.173	0.169	-6	6.182	40	
180 326, 045 0.243 0.233	-	14	8.143	43	0.307	0.297	-	37	4.001	6	0.164	0.160	-3	6.107	40	
190 326, 026 0.236 0.225	-	13	7.996	42	0.305	0.295	-	36	4.039	5	0.165	0.161	-2	5.973	39	
200 325, 979 0.239 0.229	-	12	8.320	45	0.284	0.274	-	31	4.162	11	0.154	0.151	5	7.110	47	
208 325, 969 0.234 0.223	-	11	8.162	44	0.288	0.278	-	31	4.185	9	0.158	0.154	5	6.832	45	
Gamma with log link																
0 437, 243 4.557 4.357	-238	100.000	38	3.231	3.121	0	100.000	261	4.027	3.942	106	100.000	367			
10 342, 942 0.870 0.832	-	21	24.998	131	0.440	0.425	-	24	15.145	71	0.505	0.494	43	21.396	138	
20 334, 881 0.649 0.621	-	5	19.899	110	0.519	0.501	-	65	8.283	36	0.312	0.306	-11	14.105	90	
30 331, 227 0.544 0.520	-	4	21.752	126	0.479	0.463	-	57	11.010	58	0.262	0.257	0	17.458	115	
40 328, 727 0.374 0.357	-	10	14.009	81	0.329	0.318	-	33	8.553	43	0.268	0.263	15	13.990	91	
50 327, 806 0.328 0.313	-	16	12.750	74	0.327	0.316	-	33	8.325	42	0.272	0.266	14	13.779	90	
60 327, 270 0.302 0.289	-	15	11.825	68	0.297	0.287	-	33	7.147	37	0.197	0.193	14	12.637	83	
70 326, 866 0.264 0.253	-	15	10.159	58	0.249	0.241	-	28	6.071	31	0.165	0.162	12	10.693	70	
80 326, 669 0.255 0.244	-	19	9.819	57	0.288	0.279	-	37	5.085	24	0.146	0.143	-2	9.090	60	
90 326, 433 0.266 0.254	-	23	8.891	51	0.327	0.316	-	45	4.079	15	0.171	0.167	-12	7.353	48	
100 326, 302 0.265 0.253	-	23	7.839	44	0.361	0.349	-	47	4.030	5	0.205	0.201	-12	6.246	40	
110 326, 224 0.256 0.244	-	18	8.139	45	0.335	0.324	-	41	4.211	8	0.191	0.187	-3	7.043	46	
120 326, 015 0.220 0.210	-	17	6.898	36	0.317	0.306	-	40	4.411	-1	0.194	0.190	-7	5.364	33	
130 325, 973 0.216 0.207	-	15	6.654	33	0.307	0.296	-	37	4.544	-4	0.196	0.192	-4	5.114	30	
140 325, 919 0.212 0.203	-	15	6.334	31	0.302	0.292	-	37	4.556	-5	0.191	0.187	-4	4.883	28	
150 325, 878 0.215 0.205	-	14	6.486	33	0.297	0.287	-	36	4.375	-3	0.181	0.177	-3	4.968	29	
160 325, 858 0.216 0.206	-	14	6.619	34	0.299	0.289	-	35	4.442	-2	0.181	0.177	-1	5.275	32	
170 325, 826 0																

<i>k</i>	AIC	v.mae	v.mae ^a	v.res	v.mae ⁰	v.res ⁰	ns.mae	ns.mae ^a	ns.res	ns.mae ⁰	ns.res ⁰	cr.mae	cr.mae ^a	cr.res	cr.mae ⁰	cr.res ⁰
Inverse gaussian with identity link																
0	437, 338	4.557	4.357	-238	100.000	38	3.231	3.121	0	100.000	261	4.027	3.942	106	100.000	367
10	346, 132	0.871	0.833	-13	23.559	115	0.314	0.304	7	20.269	107	0.534	0.523	70	25.673	169
20	334, 430	0.549	0.524	-13	15.996	77	0.599	0.579	-77	8.273	-1	0.468	0.458	-44	9.809	32
30	331, 453	0.488	0.467	-4	15.939	89	0.517	0.499	-67	6.532	11	0.413	0.405	-40	9.280	38
40	328, 985	0.370	0.354	-13	13.279	76	0.338	0.327	-39	7.193	35	0.238	0.233	6	12.301	80
50	328, 064	0.332	0.317	-15	12.727	74	0.338	0.327	-40	6.871	35	0.232	0.227	1	11.664	76
60	327, 533	0.298	0.285	-17	10.994	64	0.304	0.294	-37	5.868	29	0.172	0.168	3	10.646	69
70	327, 082	0.274	0.262	-15	9.387	53	0.243	0.235	-27	5.535	27	0.171	0.167	13	10.253	67
80	326, 849	0.267	0.255	-20	9.426	54	0.278	0.268	-34	5.271	25	0.152	0.148	5	9.783	65
90	326, 715	0.247	0.236	-21	8.546	49	0.275	0.266	-35	4.399	20	0.140	0.137	-1	8.302	55
100	326, 627	0.234	0.224	-20	8.454	49	0.266	0.257	-34	4.414	20	0.144	0.141	-1	8.023	53
110	326, 557	0.225	0.215	-17	8.350	47	0.246	0.238	-31	4.337	19	0.132	0.129	2	7.841	52
120	326, 505	0.233	0.223	-17	8.897	51	0.256	0.247	-33	4.428	21	0.125	0.123	0	8.106	54
130	326, 465	0.243	0.232	-16	9.965	58	0.265	0.256	-34	5.126	26	0.122	0.120	1	9.216	61
140	326, 442	0.244	0.233	-16	10.175	59	0.273	0.264	-35	5.079	25	0.125	0.122	0	9.098	60
150	326, 357	0.252	0.241	-16	10.133	58	0.352	0.340	-45	4.601	15	0.169	0.166	-1	8.831	58
160	326, 130	0.206	0.197	-15	6.294	31	0.293	0.283	-36	4.360	-5	0.187	0.183	-4	4.711	26
170	326, 112	0.204	0.195	-15	6.173	30	0.289	0.279	-35	4.284	-5	0.179	0.175	-4	4.688	27
180	326, 099	0.203	0.194	-14	6.130	30	0.283	0.273	-34	4.277	-5	0.177	0.173	-3	4.654	26
190	326, 088	0.204	0.195	-14	6.143	30	0.282	0.272	-34	4.280	-5	0.178	0.174	-3	4.699	27
200	326, 076	0.204	0.195	-14	6.172	30	0.286	0.276	-34	4.347	-4	0.184	0.180	-3	4.823	27
210	326, 071	0.199	0.190	-12	6.140	30	0.273	0.264	-32	4.277	-4	0.183	0.179	0	4.868	28
217	326, 069	0.191	0.183	-11	5.967	28	0.261	0.252	-29	4.364	-5	0.178	0.175	2	4.779	27
Inverse gaussian with inverse link																
0	437, 338	4.557	4.357	-238	100.000	38	3.231	3.121	0	100.000	261	4.027	3.942	106	100.000	367
10	344, 458	1.129	1.079	-25	35.685	202	1.138	1.099	-150	14.423	63	0.639	0.626	-63	22.713	149
20	336, 004	0.682	0.652	-5	21.011	117	0.534	0.516	-67	8.866	41	0.321	0.314	-12	14.895	95
30	333, 060	0.626	0.598	-10	24.463	142	0.623	0.602	-83	10.859	55	0.376	0.369	-31	16.233	107
40	329, 632	0.412	0.394	-14	15.912	93	0.345	0.333	-29	12.096	64	0.318	0.311	28	18.446	121
50	328, 515	0.335	0.320	-12	12.387	71	0.305	0.295	-29	8.122	40	0.276	0.270	18	13.333	86
60	327, 916	0.321	0.307	-15	11.970	70	0.286	0.276	-27	8.385	44	0.247	0.241	20	13.973	91
70	327, 543	0.278	0.266	-12	10.488	60	0.246	0.238	-28	6.106	31	0.164	0.161	9	10.331	67
80	327, 196	0.249	0.238	-17	8.227	45	0.308	0.297	-38	4.037	9	0.193	0.189	-7	6.381	40
90	327, 012	0.247	0.236	-19	8.016	44	0.376	0.363	-49	4.390	-1	0.212	0.207	-15	5.407	33
100	326, 836	0.261	0.250	-20	9.073	51	0.382	0.369	-49	4.438	8	0.215	0.211	-9	7.237	47
110	326, 750	0.268	0.257	-21	8.679	47	0.386	0.373	-50	4.510	4	0.217	0.212	-12	6.490	42
120	326, 674	0.263	0.251	-19	8.191	45	0.378	0.365	-49	4.499	1	0.207	0.203	-12	6.011	38
130	326, 636	0.261	0.250	-18	8.380	46	0.373	0.360	-48	4.402	2	0.198	0.193	-12	5.985	38
140	326, 607	0.258	0.247	-17	8.253	46	0.349	0.337	-44	4.289	4	0.185	0.181	-8	6.277	40
150	326, 581	0.258	0.246	-17	8.437	47	0.350	0.338	-44	4.228	6	0.183	0.179	-7	6.505	42
160	326, 538	0.246	0.235	-15	8.445	47	0.326	0.315	-40	4.077	7	0.173	0.169	-4	6.572	43
170	326, 522	0.249	0.238	-15	8.148	45	0.322	0.311	-39	4.119	6	0.175	0.172	-2	6.603	43
180	326, 468	0.245	0.234	-14	8.583	47	0.298	0.288	-34	4.303	13	0.162	0.159	4	7.724	51
190	326, 455	0.243	0.233	-14	8.506	47	0.299	0.289	-34	4.290	13	0.163	0.160	4	7.641	50
200	326, 399	0.231	0.221	-12	7.918	42	0.286	0.277	-31	4.208	9	0.158	0.155	6	6.856	45
210	326, 365	0.233	0.223	-12	7.983	43	0.288	0.279	-31	4.208	9	0.159	0.155	5	6.765	45
219	326, 363	0.233	0.223	-11	8.040	43	0.283	0.274	-31	4.130	9	0.153	0.150	5	6.786	45

Table 13: AIC scores and out-of-sample validation figures of the inverse gaussian GLMs of BEL with identity, inverse, log and $\frac{1}{\mu^2}$ link functions under 300-886 after each tenth and the final iteration.

k	AIC	v.mae	v.mae ^a	v.res	v.mae ⁰	v.res ⁰	ns.mae	ns.mae ^a	ns.res	ns.mae ⁰	ns.res ⁰	cr.mae	cr.mae ^a	cr.res	cr.mae ⁰	cr.res ⁰
Inverse gaussian with log link																
0	437, 338	4.557	4.357	-238	100.000	38	3.231	3.121	0	100.000	261	4.027	3.942	106	100.000	367
10	343, 530	0.866	0.828	19	24.925	131	0.450	0.435	-28	14.940	69	0.494	0.484	39	21.122	136
20	335, 355	0.644	0.616	-5	19.653	109	0.526	0.509	-67	7.947	33	0.318	0.311	-14	13.490	85
30	331, 675	0.536	0.512	-4	21.697	125	0.482	0.465	-58	10.885	57	0.262	0.256	-2	17.245	113
40	329, 140	0.366	0.350	-10	13.913	80	0.325	0.314	-32	8.604	44	0.269	0.264	16	14.011	91
50	328, 190	0.324	0.310	-16	12.640	73	0.319	0.308	-32	8.482	43	0.274	0.268	16	13.966	91
60	327, 666	0.296	0.283	-15	11.626	67	0.290	0.280	-31	7.181	37	0.201	0.197	15	12.695	83
70	327, 263	0.261	0.250	-15	9.948	57	0.244	0.236	-27	6.042	30	0.172	0.168	12	10.531	69
80	327, 061	0.251	0.240	-18	9.746	56	0.284	0.275	-37	4.988	24	0.145	0.142	-1	8.964	59
90	326, 825	0.263	0.251	-23	8.769	51	0.321	0.310	-44	4.059	15	0.168	0.165	-11	7.316	48
100	326, 695	0.261	0.249	-22	7.727	43	0.352	0.340	-45	4.048	6	0.203	0.199	-10	6.341	41
110	326, 589	0.240	0.230	-19	7.484	41	0.342	0.330	-44	4.124	1	0.192	0.188	-11	5.484	35
120	326, 409	0.216	0.207	-16	6.397	32	0.299	0.289	-37	4.534	-2	0.195	0.191	-4	5.170	30
130	326, 363	0.216	0.207	-15	6.314	31	0.308	0.298	-37	4.693	-6	0.201	0.196	-4	4.957	28
140	326, 331	0.218	0.208	-15	6.537	33	0.303	0.292	-36	4.505	-3	0.195	0.191	-1	5.362	32
150	326, 270	0.216	0.207	-14	6.457	32	0.302	0.291	-36	4.524	-4	0.189	0.185	-2	5.049	30
160	326, 249	0.217	0.208	-14	6.596	34	0.298	0.288	-36	4.418	-2	0.182	0.178	-1	5.291	32
170	326, 231	0.217	0.207	-15	6.492	32	0.296	0.286	-35	4.391	-3	0.179	0.175	-2	5.189	31
180	326, 206	0.214	0.205	-15	6.426	32	0.302	0.291	-36	4.466	-4	0.179	0.175	-3	4.950	29
190	326, 191	0.206	0.197	-13	6.472	33	0.288	0.279	-34	4.422	-3	0.173	0.170	0	5.149	31
200	326, 176	0.208	0.199	-13	6.545	33	0.286	0.276	-33	4.430	-2	0.179	0.175	0	5.288	31
210	326, 161	0.208	0.199	-13	6.501	33	0.286	0.276	-33	4.439	-2	0.184	0.180	1	5.318	32
220	326, 153	0.202	0.193	-10	6.280	30	0.260	0.251	-27	4.455	-2	0.178	0.174	5	5.190	31
222	326, 153	0.201	0.192	-10	6.291	30	0.261	0.252	-28	4.494	-3	0.180	0.177	5	5.176	30
Inverse gaussian with $\frac{1}{\mu^2}$ link																
0	437, 338	4.557	4.357	-238	100.000	38	3.231	3.121	0	100.000	261	4.027	3.942	106	100.000	367
10	344, 467	0.985	0.941	-14	31.473	176	0.993	0.959	-130	12.573	46	0.561	0.549	-52	18.986	124
20	336, 815	0.668	0.639	-7	21.404	122	0.591	0.571	-75	9.506	38	0.372	0.364	-22	14.521	91
30	331, 792	0.478	0.457	-5	15.821	90	0.367	0.354	-28	10.573	53	0.373	0.365	33	17.496	114
40	330, 089	0.421	0.403	-1	15.183	89	0.295	0.285	-19	10.660	56	0.316	0.309	34	16.657	109
50	329, 020	0.376	0.359	-10	14.443	85	0.300	0.290	-21	11.439	60	0.320	0.313	34	17.553	115
60	328, 452	0.330	0.316	-12	12.905	75	0.290	0.280	-24	9.196	48	0.273	0.267	25	14.952	98
70	327, 925	0.316	0.302	-16	11.733	69	0.301	0.291	-35	7.090	35	0.200	0.195	6	11.701	76
80	327, 639	0.262	0.250	-18	8.128	43	0.298	0.288	-35	4.425	11	0.208	0.203	-1	7.205	45
90	327, 265	0.278	0.266	-22	8.311	46	0.355	0.343	-44	4.383	9	0.202	0.197	-7	7.090	46
100	327, 148	0.288	0.275	-22	8.166	44	0.357	0.345	-44	4.408	8	0.207	0.203	-6	7.039	46
110	327, 077	0.275	0.262	-20	7.965	42	0.366	0.353	-45	4.676	2	0.207	0.202	-7	6.410	40
120	326, 916	0.274	0.262	-18	8.313	45	0.393	0.380	-47	5.133	1	0.228	0.223	-5	6.790	43
130	326, 876	0.269	0.257	-18	8.133	43	0.396	0.382	-47	5.217	0	0.234	0.229	-5	6.625	42
140	326, 789	0.259	0.248	-18	8.149	44	0.395	0.381	-47	5.074	1	0.249	0.244	-6	6.697	42
150	326, 576	0.227	0.217	-15	6.896	34	0.341	0.329	-39	5.291	-5	0.221	0.217	-3	5.510	31
160	326, 479	0.214	0.205	-16	6.274	29	0.291	0.281	-35	4.571	-6	0.206	0.202	-8	4.617	22
170	326, 451	0.210	0.201	-15	6.035	26	0.285	0.275	-34	4.611	-8	0.202	0.198	-8	4.441	19
180	326, 426	0.196	0.187	-13	5.753	25	0.250	0.242	-28	4.373	-6	0.187	0.183	-2	4.426	21
190	326, 408	0.195	0.187	-13	5.682	24	0.249	0.241	-28	4.360	-6	0.188	0.184	-2	4.464	21
200	326, 397	0.193	0.184	-13	5.686	24	0.245	0.237	-27	4.252	-5	0.186	0.182	-3	4.382	20
210	326, 305	0.187	0.179	-13	5.721	27	0.237	0.229	-26	3.811	0	0.162	0.159	2	4.510	27
220	326, 172	0.176	0.168	-14	5.110	26	0.197	0.191	-22	3.346	4	0.146	0.143	6	4.919	31
230	326, 160	0.175	0.168	-14	4.994	25	0.206	0.199	-21	3.583	3	0.159	0.155	8	5.114	32
240	326, 141	0.166	0.159	-11	5.012	24	0.197	0.190	-16	3.909	5	0.182	0.178	14	5.560	35
250	326, 124	0.174	0.166	-12	5.058	25	0.193	0.186	-15	3.833	9	0.188	0.184	17	6.266	41

Table 13: Cont.

<i>k</i>	AIC	v.mae	v.mae ^a	v.res	v.mae ⁰	v.res ⁰	ns.mae	ns.mae ^a	ns.res	ns.mae ⁰	ns.res ⁰	cr.mae	cr.mae ^a	cr.res	cr.mae ⁰	cr.res ⁰
Gaussian with identity link under 150-443																
150 325, 850	0.247	0.237	-14	9.924	57	0.271	0.262	-35	4.612	22	0.122	0.120	-1	8.537	56	
Gaussian with inverse link under 150-443																
150 325, 952	0.258	0.247	-16	8.468	45	0.353	0.341	-44	4.282	3	0.192	0.188	-8	6.088	39	
Gaussian with log link under 150-443																
150 325, 823	0.240	0.229	-15	7.980	44	0.316	0.305	-38	4.014	6	0.170	0.167	-2	6.434	42	
Gamma with identity link under 150-443																
150 326, 041	0.236	0.226	-14	9.329	53	0.260	0.251	-33	4.321	20	0.121	0.118	1	8.206	54	
Gamma with inverse link under 150-443																
150 326, 222	0.254	0.243	-15	8.410	46	0.327	0.316	-40	4.111	7	0.171	0.167	-3	6.722	44	
Gamma with log link under 150-443																
150 326, 022	0.243	0.232	-15	7.820	43	0.323	0.312	-40	4.040	3	0.174	0.170	-4	6.010	39	
Inverse gaussian with identity link under 150-443																
150 326, 352	0.249	0.238	-17	9.375	54	0.337	0.326	-44	4.224	12	0.150	0.146	-4	7.930	52	
Inverse gaussian with inverse link under 150-443																
150 326, 617	0.253	0.242	-15	8.152	44	0.324	0.313	-39	4.148	5	0.172	0.169	-3	6.476	42	
Inverse gaussian with log link under 150-443																
150 326, 413	0.247	0.237	-15	7.716	42	0.324	0.313	-40	4.095	2	0.172	0.168	-4	5.892	38	
Inverse gaussian with $\frac{1}{\mu^2}$ link under 150-443																
150 326, 778	0.262	0.250	-16	8.258	44	0.332	0.321	-41	4.238	5	0.177	0.174	-3	6.518	42	
Gaussian with identity link under 300-886																
224 325, 459	0.194	0.186	-9	6.659	34	0.268	0.259	-30	4.200	-2	0.168	0.165	1	5.007	29	
Gaussian with inverse link under 300-886																
213 325, 797	0.241	0.230	-12	8.325	44	0.310	0.299	-36	4.063	6	0.171	0.167	-1	6.284	41	
Gaussian with log link under 300-886																
214 325, 552	0.206	0.197	-10	6.640	32	0.267	0.258	-29	4.402	-2	0.177	0.173	3	5.180	30	
Gamma with identity link under 300-886																
212 325, 689	0.189	0.180	-11	5.975	28	0.261	0.252	-29	4.384	-5	0.169	0.165	1	4.545	25	
Gamma with inverse link under 300-886																
208 325, 969	0.234	0.223	-11	8.162	44	0.288	0.278	-31	4.185	9	0.158	0.154	5	6.832	45	
Gamma with log link under 300-886																
226 325, 767	0.198	0.189	-8	6.256	29	0.249	0.241	-24	4.532	-1	0.184	0.180	8	5.417	32	
Inverse gaussian with identity link under 300-886																
217 326, 069	0.191	0.183	-11	5.967	28	0.261	0.252	-29	4.364	-5	0.178	0.175	2	4.779	27	
Inverse gaussian with inverse link under 300-886																
219 326, 363	0.233	0.223	-11	8.040	43	0.283	0.274	-31	4.130	9	0.153	0.150	5	6.786	45	
Inverse gaussian with log link under 300-886																
222 326, 153	0.201	0.192	-10	6.291	30	0.261	0.252	-28	4.494	-3	0.180	0.177	5	5.176	30	
Inverse gaussian with $\frac{1}{\mu^2}$ link under 300-886																
250 326, 124	0.174	0.166	-12	5.058	25	0.193	0.186	-15	3.833	9	0.188	0.184	17	6.266	41	

Table 14: AIC scores and out-of-sample validation figures of the gaussian, gamma and inverse gaussian GLMs of BEL with identity, inverse, log and $\frac{1}{\mu^2}$ link functions under 150-443 and 300-886 after the final iteration. Highlighted in green and red respectively the best and worst AIC scores and validation figures.

k	K_{\max}	v.mae	v.mae ^a	v.res	v.mae ⁰	v.res ⁰	ns.mae	ns.mae ^a	ns.res	ns.mae ⁰	ns.res ⁰	cr.mae	cr.mae ^a	cr.res	cr.mae ⁰	cr.res ⁰
4 Thin plate regression splines under gaussian with identity link in stagewise selection of length 5																
0	150	4.557	4.357	-238	100.000	38	3.231	3.121	0	100.000	261	4.027	3.942	106	100.000	367
10	150	0.632	0.604	28	22.019	116	0.345	0.334	-8	13.247	65	0.479	0.469	66	21.072	139
20	150	0.406	0.388	0	11.330	44	0.375	0.362	-42	7.254	-12	0.341	0.334	-6	7.709	24
30	150	0.399	0.382	-11	12.268	59	0.465	0.449	-61	5.744	-6	0.314	0.307	-26	6.116	29
40	150	0.371	0.355	-8	11.415	53	0.480	0.463	-64	6.380	-16	0.340	0.332	-34	5.283	13
50	150	0.392	0.375	-13	12.079	59	0.520	0.503	-70	5.961	-12	0.365	0.358	-39	5.368	19
60	150	0.306	0.292	-15	9.833	48	0.405	0.391	-51	5.283	-2	0.273	0.267	-10	6.484	39
70	150	0.272	0.260	-15	9.896	56	0.321	0.310	-35	5.227	22	0.232	0.228	12	10.460	69
80	150	0.249	0.238	-17	8.627	49	0.308	0.297	-36	4.588	16	0.205	0.201	9	9.100	60
90	150	0.261	0.250	-17	9.262	54	0.325	0.314	-39	4.639	18	0.195	0.191	5	9.340	62
100	150	0.254	0.243	-18	9.593	55	0.340	0.328	-42	4.626	17	0.196	0.192	3	9.312	62
110	150	0.255	0.244	-18	9.407	54	0.336	0.324	-40	4.640	18	0.207	0.203	4	9.325	62
120	150	0.243	0.233	-16	8.474	48	0.307	0.296	-38	4.023	13	0.186	0.182	1	7.819	51
130	150	0.241	0.230	-16	8.481	49	0.308	0.298	-37	4.108	13	0.183	0.179	2	8.075	53
140	150	0.235	0.225	-15	8.018	45	0.295	0.285	-35	3.865	10	0.173	0.169	2	7.182	47
150	150	0.240	0.229	-15	8.192	46	0.291	0.281	-35	3.907	13	0.176	0.172	3	7.641	50
5 Thin plate regression splines under gaussian with identity link																
0	100	4.557	4.357	-238	100.000	38	3.231	3.121	0	100.000	261	4.027	3.942	106	100.000	367
10	100	0.643	0.615	27	23.278	125	0.344	0.332	-6	15.238	78	0.493	0.483	69	23.151	153
20	100	0.387	0.370	1	10.371	35	0.364	0.352	-40	7.855	-20	0.335	0.328	-6	7.454	14
30	100	0.382	0.366	-10	11.235	50	0.454	0.439	-60	6.247	-14	0.317	0.310	-28	5.603	18
40	100	0.368	0.352	-11	10.931	48	0.463	0.447	-61	6.266	-16	0.337	0.329	-33	5.343	12
50	100	0.355	0.339	-11	10.086	40	0.481	0.465	-64	7.752	-28	0.351	0.344	-37	5.481	0
60	100	0.344	0.329	-9	10.015	40	0.490	0.474	-66	8.152	-30	0.364	0.356	-38	5.593	-3
70	100	0.339	0.324	-6	10.035	45	0.476	0.460	-64	7.578	-27	0.345	0.337	-37	5.078	0
80	100	0.295	0.282	-11	9.397	49	0.404	0.390	-51	5.513	-6	0.241	0.236	-11	5.820	34
90	100	0.296	0.283	-12	9.694	52	0.393	0.380	-49	5.155	0	0.206	0.202	-7	6.605	41
100	100	0.287	0.274	-11	9.431	48	0.397	0.383	-50	5.402	-5	0.202	0.198	-9	5.945	36
8 Thin plate regression splines under gaussian with identity link																
0	150	4.557	4.357	-238	100.000	38	3.231	3.121	0	100.000	261	4.027	3.942	106	100.000	367
10	150	0.639	0.611	27	23.176	125	0.340	0.329	-3	15.517	80	0.516	0.505	73	23.627	156
20	150	0.375	0.359	3	9.604	26	0.334	0.322	-33	8.378	-24	0.341	0.333	1	7.711	10
30	150	0.361	0.345	-7	10.444	41	0.415	0.401	-52	6.961	-19	0.304	0.297	-21	5.871	13
40	150	0.356	0.340	-5	10.098	36	0.425	0.410	-54	7.920	-28	0.311	0.304	-27	5.647	-1
50	150	0.339	0.324	-7	9.712	33	0.418	0.404	-53	7.746	-27	0.311	0.304	-26	5.596	0
60	150	0.325	0.311	-6	9.037	26	0.411	0.397	-52	8.706	-34	0.310	0.304	-26	5.850	-8
70	150	0.325	0.311	-4	9.180	31	0.429	0.414	-55	8.773	-34	0.326	0.319	-30	5.912	-9
80	150	0.309	0.296	-5	8.618	29	0.430	0.415	-55	8.984	-35	0.336	0.329	-29	6.382	-9
90	150	0.313	0.299	-5	8.981	32	0.384	0.371	-48	7.390	-26	0.300	0.293	-26	5.430	-4
100	150	0.328	0.313	-6	9.910	47	0.400	0.387	-51	5.572	-12	0.291	0.285	-25	5.064	13
110	150	0.256	0.245	-10	7.985	38	0.326	0.315	-40	4.655	-6	0.201	0.197	-6	5.002	28
120	150	0.253	0.242	-9	7.340	30	0.321	0.310	-39	5.542	-14	0.209	0.204	-5	4.541	20
130	150	0.252	0.241	-9	7.767	34	0.326	0.315	-40	5.197	-11	0.205	0.201	-5	4.770	24
140	150	0.245	0.234	-8	7.592	33	0.322	0.311	-41	5.315	-15	0.197	0.193	-7	4.317	20
150	150	0.217	0.208	-11	6.477	32	0.239	0.231	-26	3.652	2	0.179	0.175	6	5.578	34
10 Thin plate regression splines under gaussian with identity link																
0	150	4.557	4.357	-238	100.000	38	3.231	3.121	0	100.000	261	4.027	3.942	106	100.000	367
10	150	0.642	0.614	27	23.354	126	0.344	0.332	-5	15.463	80	0.509	0.499	71	23.654	156
20	150	0.382	0.365	2	10.101	33	0.341	0.329	-34	7.780	-18	0.338	0.331	1	7.728	18
30	150	0.370	0.354	-7	10.922	45	0.416	0.402	-52	6.497	-14	0.305	0.299	-20	6.103	18
40	150	0.354	0.338	-7	10.412	39	0.404	0.391	-51	6.747	-20	0.308	0.301	-24	5.600	8
50	150	0.347	0.331	-7	10.119	38	0.426	0.412	-54	7.258	-24	0.310	0.304	-27	5.467	4
60	150	0.342	0.327	-4	9.766	34	0.400	0.387	-50	7.600	-26	0.298	0.292	-23	5.615	0
70	150	0.334	0.319	-4	9.601	35	0.428	0.414	-55	8.158	-30	0.318	0.311	-29	5.618	-5
80	150	0.315	0.301	-5	9.093	35	0.432	0.418	-55	8.113	-29	0.334	0.327	-29	6.087	-3
90	150	0.323	0.309	-5	9.436	38	0.388	0.375	-49	6.558	-20	0.297	0.291	-26	5.194	2
100	150	0.309	0.296	-6	8.722	27	0.409	0.395	-54	8.780	-36	0.261	0.255	-27	4.994	-9
110	150	0.309	0.295	-6	8.542	26	0.411	0.397	-54	8.711	-37	0.284	0.278	-33	4.768	-15
120	150	0.206	0.197	-9	5.768	25	0.216	0.209	-23	3.806	-4	0.164	0.161	5	4.519	24
130	150	0.205	0.196	-10	5.759	24	0.226	0.218	-24	3.952	-5	0.175	0.172	4	4.579	24
140	150	0.214	0.205	-10	6.761	34	0.228	0.220	-25	3.363	5	0.167	0.163	6	5.762	36
150	150	0.212	0.203	-10	7.070	37	0.230	0.223	-24	3.575	8	0.173	0.170	8	6.337	40

Table 15: Out-of-sample validation figures of selected GAMs of BEL with varying spline function number per dimension and fixed spline function type under 150-443 after each tenth and the finally selected smooth function.

	$J = 4, k = 50$	$J = 4, k = 100$	$J = 4, k = 150$	$J = 10, k = 50$	$J = 10, k = 100$	$J = 10, k = 150$									
k	df	p-val	sign	df	p-val	sign	df	p-val	sign	df	p-val	sign	df	p-val	sign
76		1.000	4.4 ₋₁₃	***	2.334	3.8 ₋₁₄	***		2.469	1 ₋₁	*	2.077	1.8 ₋₁		
77		1.353	4 ₋₉	***	1.411	8.8 ₋₉	***		1.000	2.5 ₋₂	*	1.000	1.1 ₋₂	*	
78		1.000	1.5 ₋₅	***	1.000	6.5 ₋₆	***		1.000	2 ₋₁₆	***	1.000	1.6 ₋₄	***	
79		1.000	3 ₋₅	***	1.000	1.5 ₋₅	***		5.186	1.5 ₋₆	***	1.000	2 ₋₁₆	***	
80		1.000	1 ₋₇	***	1.000	7.8 ₋₈	***		1.892	2.2 ₋₂	*	1.795	1.9 ₋₂	*	
81		2.725	1.3 ₋₄	***	2.739	7.1 ₋₅	***		1.000	5.2 ₋₆	***	1.000	5.8 ₋₁		
82		1.000	7.6 ₋₅	***	2.175	1.4 ₋₅	***		1.000	1.8 ₋₃	**	1.000	5.1 ₋₁		
83		2.240	1.3 ₋₃	**	2.075	9 ₋₄	***		7.020	2 ₋₁₆	***	4.809	2.9 ₋₃	**	
84		1.000	6.8 ₋₅	***	2.902	1.5 ₋₅	***		4.003	1.5 ₋₁		4.722	9.8 ₋₃	**	
85		1.000	7.5 ₋₅	***	1.000	4 ₋₆	***		1.000	1 ₋₉	***	1.000	1.8 ₋₄	***	
86		1.000	3.7 ₋₄	***	1.000	7.7 ₋₄	***		3.115	1.2 ₋₁		2.748	1.2 ₋₁		
87		1.000	3.4 ₋₄	***	1.000	9.1 ₋₅	***		5.294	1.4 ₋₁		5.598	1.3 ₋₁		
88		1.000	1.9 ₋₄	***	1.000	9.6 ₋₅	***		2.263	1.5 ₋₁		1.788	2.5 ₋₁		
89		2.828	2.1 ₋₃	**	3.000	6 ₋₅	***		1.000	3.4 ₋₄	***	1.000	3.3 ₋₄	***	
90		1.000	7.8 ₋₄	***	1.000	5.6 ₋₄	***		1.000	3.7 ₋₂	*	1.000	3.8 ₋₂	*	
91		1.000	2.5 ₋₃	**	1.000	2.9 ₋₃	**		1.000	1.8 ₋₃	**	1.000	1.2 ₋₃	**	
92		1.000	3.8 ₋₃	**	1.000	3.5 ₋₃	**		1.000	1.7 ₋₂	*	1.000	1.2 ₋₂	*	
93		1.000	1.8 ₋₃	**	1.000	1.1 ₋₃	**		1.000	3.8 ₋₂	*	1.000	2.8 ₋₂	*	
94		2.776	3.6 ₋₅	***	1.000	1.8 ₋₇	***		5.921	4.2 ₋₃	**	3.962	2 ₋₁₆	***	
95		2.103	4.9 ₋₂	*	1.974	1.3 ₋₁			8.154	2 ₋₁₆	***	2.290	2 ₋₁₆	***	
96		2.023	1.2 ₋₄	***	1.000	4.6 ₋₁₀	***		1.000	2.8 ₋₁₂	***	1.000	1.6 ₋₅	***	
97		2.811	1.5 ₋₂	*	2.873	5.9 ₋₃	**		3.748	7.1 ₋₄	***	1.000	1.2 ₋₆	***	
98		1.000	7.1 ₋₃	**	1.000	1.1 ₋₂	*		1.000	3.9 ₋₆	***	7.349	2.8 ₋₁		
99		1.000	1.4 ₋₂	*	1.000	1.9 ₋₂	*		2.149	1.2 ₋₃	**	1.000	2.8 ₋₈	***	
100		2.764	2.9 ₋₂	*	2.321	9 ₋₂	.		1.000	3.1 ₋₃	**	1.000	2.1 ₋₁		
101					1.000	1.1 ₋₄	***					1.000	8.2 ₋₁₀	***	
102					1.000	7.7 ₋₂	.					1.000	1.6 ₋₂	*	
103					1.000	2.9 ₋₃	**					4.084	5.8 ₋₄	***	
104					1.000	6.8 ₋₅	***					1.000	3.2 ₋₂	*	
105					1.000	9.3 ₋₃	**					1.000	6.8 ₋₂	.	
106					1.000	2.1 ₋₉	***					1.000	5.2 ₋₃	**	
107					1.000	1.9 ₋₂	*					3.397	1 ₋₁		
108					2.187	9.6 ₋₂	.					1.248	3.4 ₋₁		
109					1.000	2.1 ₋₃	**					3.079	3.9 ₋₁		
110					1.000	4.6 ₋₂	*					1.000	3.9 ₋₄	***	
111					1.000	2 ₋₁₆	***					0.979	4.3 ₋₈	***	
112					1.000	2.9 ₋₂	*					8.555	2 ₋₁₆	***	
113					1.000	9.5 ₋₁						8.952	1.7 ₋₁₂	***	
114					1.644	9.6 ₋₂	.					1.000	2 ₋₁₆	***	
115					1.000	2 ₋₂	*					1.000	2 ₋₁₆	***	
116					1.000	1.8 ₋₂	*					1.000	1.7 ₋₁₃	***	
117					1.000	4.8 ₋₃	**					2.988	3.4 ₋₁₃	***	
118					1.000	2.4 ₋₂	*					8.401	1.2 ₋₁₀	***	
119					2.704	8.3 ₋₂	.					2.493	4.7 ₋₅	***	
120					1.000	1.8 ₋₂	*					1.000	4.1 ₋₇	***	
121					1.413	6.7 ₋₁						1.000	9 ₋₅	***	
122					1.886	6.2 ₋₁						2.745	1.2 ₋₃	**	
123					1.000	1.4 ₋₅	***					1.000	3.4 ₋₃	**	
124					2.499	1.8 ₋₁						1.000	1.5 ₋₂	*	
125					1.000	3.6 ₋₂	*					1.000	1.4 ₋₂	*	
126					2.416	1 ₋₁						1.000	5.8 ₋₃	**	
127					1.000	5.1 ₋₅	***					3.120	5.7 ₋₂	.	
128					1.000	3.8 ₋₂	*					1.000	9.2 ₋₄	***	
129					1.000	1.3 ₋₃	**					1.000	3.9 ₋₃	**	
130					1.000	5.7 ₋₂	.					3.778	1.7 ₋₁		
131					1.000	1.3 ₋₂	*					2.752	2.7 ₋₂	*	
132					1.000	1.2 ₋₂	*					1.000	6.9 ₋₃	**	
133					1.970	2.5 ₋₁						1.000	4.8 ₋₃	**	
134					1.000	3.5 ₋₂	*					1.000	5.5 ₋₂	.	
135					1.000	5.9 ₋₄	***					1.000	3.8 ₋₂	*	
136					1.176	7.1 ₋₃	**					5.289	1.4 ₋₁		
137					2.357	3.4 ₋₁						1.000	3.7 ₋₂	*	
138					1.000	6.7 ₋₂	.					1.000	2 ₋₄	***	
139					1.000	7.9 ₋₂	.					1.000	5.1 ₋₃	**	
140					1.000	6.9 ₋₂	.					1.000	1.6 ₋₁		
141					1.000	4.7 ₋₂	*					8.453	2.5 ₋₃	**	
142					1.000	1.3 ₋₃	**					1.000	4 ₋₂	*	
143					2.602	4.1 ₋₂	*					3.975	1.4 ₋₁		
144					1.631	4.6 ₋₁						1.000	4.2 ₋₄	***	
145					1.000	8.3 ₋₂	.					1.000	3.7 ₋₃	**	
146					1.000	1 ₋₂	*					2.147	1.9 ₋₁		
147					1.000	3.6 ₋₂	*					1.000	5 ₋₂	.	
148					1.251	1.6 ₋₁						1.000	4.1 ₋₂	*	
149					2.376	2.1 ₋₁						1.000	5.4 ₋₂	.	
150					1.482	2 ₋₁						1.000	6.3 ₋₂	.	

Table 16: Cont.

<i>k</i>	<i>K</i> _{max}	v.mae	v.mae ^a	v.res	v.mae ⁰	v.res ⁰	ns.mae	ns.mae ^a	ns.res	ns.mae ⁰	ns.res ⁰	cr.mae	cr.mae ^a	cr.res	cr.mae ⁰	cr.res ⁰
5 Thin plate regression splines under gaussian with identity link																
0	100	4.557	4.357	-238	100.000	38	3.231	3.121	0	100.000	261	4.027	3.942	106	100.000	367
10	100	0.643	0.615	27	23.278	125	0.344	0.332	-6	15.238	78	0.493	0.483	69	23.151	153
20	100	0.387	0.370	1	10.371	35	0.364	0.352	-40	7.855	-20	0.335	0.328	-6	7.454	14
30	100	0.382	0.366	-10	11.235	50	0.454	0.439	-60	6.247	-14	0.317	0.310	-28	5.603	18
40	100	0.368	0.352	-11	10.931	48	0.463	0.447	-61	6.266	-16	0.337	0.329	-33	5.343	12
50	100	0.355	0.339	-11	10.086	40	0.481	0.465	-64	7.752	-28	0.351	0.344	-37	5.481	0
60	100	0.344	0.329	-9	10.015	40	0.490	0.474	-66	8.152	-30	0.364	0.356	-38	5.593	-3
70	100	0.339	0.324	-6	10.035	45	0.476	0.460	-64	7.578	-27	0.345	0.337	-37	5.078	0
80	100	0.295	0.282	-11	9.397	49	0.404	0.390	-51	5.513	-6	0.241	0.236	-11	5.820	34
90	100	0.296	0.283	-12	9.694	52	0.393	0.380	-49	5.155	0	0.206	0.202	-7	6.605	41
100	100	0.287	0.274	-11	9.431	48	0.397	0.383	-50	5.402	-5	0.202	0.198	-9	5.945	36
5 Cubic regression splines under gaussian with identity link																
0	100	4.557	4.357	-238	100.000	38	3.231	3.121	0	100.000	261	4.027	3.942	106	100.000	367
10	100	0.637	0.609	28	22.739	122	0.337	0.326	-4	14.733	75	0.505	0.494	71	22.781	150
20	100	0.388	0.371	2	10.094	32	0.358	0.346	-40	8.256	-25	0.319	0.313	-5	7.161	10
30	100	0.389	0.372	-6	11.426	50	0.436	0.421	-55	6.652	-14	0.289	0.283	-19	5.849	22
40	100	0.359	0.343	-9	10.508	41	0.448	0.433	-59	7.171	-23	0.310	0.303	-29	5.175	6
50	100	0.345	0.330	-9	9.906	35	0.476	0.460	-63	8.736	-34	0.328	0.321	-34	5.373	-5
60	100	0.338	0.323	-7	9.817	34	0.475	0.459	-63	9.192	-37	0.330	0.324	-34	5.491	-8
70	100	0.307	0.294	-8	9.341	47	0.430	0.416	-58	6.081	-18	0.234	0.229	-26	3.871	15
80	100	0.289	0.277	-13	10.157	55	0.410	0.396	-53	5.106	0	0.237	0.232	-11	6.939	43
90	100	0.283	0.271	-13	10.307	56	0.407	0.394	-53	5.067	1	0.229	0.224	-10	7.035	44
100	100	0.268	0.256	-12	9.903	52	0.399	0.386	-51	5.182	-2	0.226	0.221	-9	6.533	40
5 Duchon splines under gaussian with identity link																
0	100	4.557	4.357	-238	100.000	38	3.231	3.121	0	100.000	261	4.027	3.942	106	100.000	367
10	100	0.753	0.720	-4	20.570	98	0.428	0.413	-39	11.806	49	0.408	0.399	6	15.241	93
20	100	0.704	0.673	-22	17.488	74	0.441	0.426	-51	8.606	31	0.380	0.372	-16	11.600	66
30	100	0.661	0.632	-32	19.699	95	0.376	0.363	-40	14.235	73	0.319	0.312	11	19.168	124
40	100	0.663	0.634	-21	18.426	84	0.292	0.282	-18	14.138	73	0.377	0.370	33	19.007	123
50	100	0.666	0.636	-17	18.534	86	0.287	0.277	-12	14.785	76	0.410	0.402	41	19.896	130
56	100	0.666	0.636	-18	18.532	86	0.288	0.279	-14	14.643	75	0.406	0.397	40	19.757	129
5 Eilers and Marx style P-splines under gaussian with identity link																
0	100	4.557	4.357	-238	100.000	38	3.231	3.121	0	100.000	261	4.027	3.942	106	100.000	367
10	100	0.643	0.615	29	22.836	123	0.344	0.332	-9	13.951	70	0.471	0.461	65	21.854	144
20	100	0.389	0.372	1	10.496	37	0.365	0.353	-41	7.778	-20	0.336	0.329	-8	7.402	13
30	100	0.384	0.367	-9	11.377	53	0.459	0.444	-60	6.138	-13	0.320	0.313	-30	5.512	17
40	100	0.371	0.354	-10	10.977	49	0.454	0.439	-60	6.095	-16	0.327	0.320	-34	5.092	11
50	100	0.357	0.341	-9	10.459	45	0.467	0.451	-62	6.909	-22	0.335	0.328	-34	5.059	6
60	100	0.339	0.324	-10	9.932	43	0.492	0.476	-66	7.640	-28	0.365	0.357	-40	5.155	-2
70	100	0.343	0.328	-10	10.523	52	0.546	0.527	-75	7.681	-27	0.366	0.358	-46	4.576	2
80	100	0.334	0.319	-7	9.920	45	0.520	0.503	-67	8.655	-29	0.346	0.339	-36	5.036	1
90	100	0.228	0.218	-10	6.973	35	0.279	0.269	-31	4.299	0	0.208	0.204	3	5.810	34
100	100	0.225	0.215	-11	6.897	34	0.256	0.248	-30	3.716	2	0.164	0.161	1	5.212	32

Table 17: Out-of-sample validation figures of selected GAMs of BEL with varying spline function type and fixed spline function number of 5 per dimension under 100-443 after each tenth and the finally selected smooth function.

k	K_{\max}	v.mae	v.mae ^a	v.res	v.mae ⁰	v.res ⁰	ns.mae	ns.mae ^a	ns.mae ⁰	ns.res	ns.res ⁰	cr.mae	cr.mae ^a	cr.res	cr.mae ⁰	cr.res ⁰
10 Thin plate regression splines under gaussian with identity link																
0 150 4.557 4.357 -238 100.000 38 3.231 3.121 0 100.000 261 4.027 3.942 106 100.000 367																
10 150 0.642 0.614 27 23.354 126 0.344 0.332 -5 15.463 80 0.509 0.499 71 23.654 156																
20 150 0.382 0.365 2 10.101 33 0.341 0.329 -34 7.780 -18 0.338 0.331 1 7.728 18																
30 150 0.370 0.354 -7 10.922 45 0.416 0.402 -52 6.497 -14 0.305 0.299 -20 6.103 18																
40 150 0.354 0.338 -7 10.412 39 0.404 0.391 -51 6.747 -20 0.308 0.301 -24 5.600 8																
50 150 0.347 0.331 -7 10.119 38 0.426 0.412 -54 7.258 -24 0.310 0.304 -27 5.467 4																
60 150 0.342 0.327 -4 9.766 34 0.400 0.387 -50 7.600 -26 0.298 0.292 -23 5.615 0																
70 150 0.334 0.319 -4 9.601 35 0.428 0.414 -55 8.158 -30 0.318 0.311 -29 5.618 -5																
80 150 0.315 0.301 -5 9.093 35 0.432 0.418 -55 8.113 -29 0.334 0.327 -29 6.087 -3																
90 150 0.323 0.309 -5 9.436 38 0.388 0.375 -49 6.558 -20 0.297 0.291 -26 5.194 2																
100 150 0.309 0.296 -6 8.722 27 0.409 0.395 -54 8.780 -36 0.261 0.255 -27 4.994 -9																
110 150 0.309 0.295 -6 8.542 26 0.411 0.397 -54 8.711 -37 0.284 0.278 -33 4.768 -15																
120 150 0.206 0.197 -9 5.768 25 0.216 0.209 -23 3.806 -4 0.164 0.161 5 4.519 24																
130 150 0.205 0.196 -10 5.759 24 0.226 0.218 -24 3.952 -5 0.175 0.172 4 4.579 24																
140 150 0.214 0.205 -10 6.761 34 0.228 0.220 -25 3.363 5 0.167 0.163 6 5.762 36																
150 150 0.212 0.203 -10 7.070 37 0.230 0.223 -24 3.575 8 0.173 0.170 8 6.337 40																
10 Cubic regression splines under gaussian with identity link																
0 125 4.557 4.357 -238 100.000 38 3.231 3.121 0 100.000 261 4.027 3.942 106 100.000 367																
10 125 0.638 0.610 27 23.397 127 0.341 0.329 -3 15.829 82 0.519 0.509 73 23.960 158																
20 125 0.380 0.364 2 10.038 34 0.339 0.328 -34 7.650 -16 0.345 0.338 0 7.865 18																
30 125 0.377 0.360 -6 11.458 53 0.411 0.397 -50 6.035 -5 0.309 0.302 -14 6.976 30																
40 125 0.364 0.348 -10 10.929 47 0.421 0.407 -53 5.791 -10 0.315 0.308 -25 5.824 18																
50 125 0.348 0.333 -11 10.437 44 0.436 0.421 -56 6.263 -15 0.319 0.312 -27 5.636 13																
60 125 0.342 0.327 -5 9.791 36 0.403 0.389 -50 7.282 -23 0.308 0.302 -23 5.789 4																
70 125 0.355 0.340 -3 10.502 48 0.442 0.427 -56 7.001 -20 0.327 0.320 -30 5.570 6																
80 125 0.349 0.334 -2 10.275 46 0.434 0.419 -55 7.159 -22 0.326 0.319 -29 5.592 4																
90 125 0.282 0.269 -5 7.978 37 0.275 0.266 -30 4.426 -3 0.215 0.210 -2 5.088 25																
100 125 0.263 0.251 -5 7.109 29 0.301 0.291 -37 5.637 -17 0.200 0.196 -8 3.969 12																
110 125 0.255 0.244 -7 6.999 30 0.303 0.292 -37 5.435 -15 0.202 0.198 -6 4.230 16																
120 125 0.257 0.246 -7 7.052 30 0.304 0.294 -37 5.371 -14 0.200 0.196 -6 4.232 17																
125 125 0.254 0.243 -7 7.139 31 0.299 0.289 -36 5.189 -13 0.197 0.192 -6 4.228 17																
10 Duchon splines under gaussian with identity link																
0 100 4.557 4.357 -238 100.000 38 3.231 3.121 0 100.000 261 4.027 3.942 106 100.000 367																
10 100 0.786 0.752 -5 22.143 110 0.445 0.430 -44 12.588 57 0.406 0.397 1 16.238 102																
20 100 0.783 0.749 -32 20.489 101 0.494 0.477 -62 11.319 58 0.357 0.350 -21 15.316 98																
30 100 0.782 0.748 -39 21.134 98 0.538 0.520 -59 12.715 64 0.422 0.413 -3 18.621 121																
40 100 0.816 0.780 -45 22.125 98 0.559 0.540 -63 13.071 65 0.450 0.440 -10 18.616 119																
50 100 0.823 0.787 -45 21.473 96 0.555 0.536 -63 12.672 63 0.451 0.441 -10 18.114 116																
53 100 0.821 0.785 -44 21.348 94 0.545 0.526 -61 12.593 62 0.446 0.437 -8 18.091 116																
10 Eilers and Marx style P-splines under gaussian with identity link in stagewise selection of length 5																
0 150 4.557 4.357 -238 100.000 38 3.231 3.121 0 100.000 261 4.027 3.942 106 100.000 367																
10 150 0.648 0.619 27 23.688 128 0.349 0.337 -7 15.566 80 0.506 0.495 71 23.889 158																
20 150 0.398 0.380 1 10.946 45 0.358 0.346 -37 7.063 -7 0.338 0.331 1 8.102 31																
30 150 0.393 0.376 -9 11.983 59 0.435 0.421 -55 5.575 -2 0.299 0.293 -17 6.928 36																
40 150 0.371 0.355 -8 11.374 55 0.449 0.434 -57 5.738 -9 0.314 0.308 -26 5.770 23																
50 150 0.363 0.347 -9 10.956 50 0.460 0.444 -60 6.249 -14 0.315 0.308 -28 5.492 17																
60 150 0.349 0.334 -8 10.479 46 0.443 0.428 -56 6.526 -17 0.305 0.298 -26 5.427 14																
70 150 0.349 0.333 -6 10.629 51 0.464 0.449 -60 6.687 -17 0.325 0.318 -29 5.501 13																
80 150 0.350 0.335 -7 10.465 48 0.468 0.452 -60 7.036 -19 0.335 0.328 -29 5.563 11																
90 150 0.350 0.335 -7 10.639 51 0.470 0.454 -60 6.683 -17 0.330 0.323 -29 5.453 14																
100 150 0.334 0.319 -8 9.960 46 0.468 0.452 -60 7.170 -20 0.339 0.332 -29 5.835 11																
110 150 0.337 0.323 -9 10.249 48 0.450 0.435 -58 6.171 -15 0.329 0.322 -31 5.267 12																
120 150 0.339 0.324 -7 10.283 45 0.433 0.419 -55 6.420 -17 0.320 0.313 -28 5.340 10																
130 150 0.269 0.257 -13 8.912 43 0.365 0.352 -46 4.891 -4 0.244 0.238 -12 5.503 30																
140 150 0.255 0.244 -12 8.157 36 0.356 0.344 -44 5.415 -10 0.246 0.241 -10 5.196 24																
150 150 0.261 0.250 -12 8.514 39 0.368 0.355 -46 5.267 -9 0.245 0.240 -12 5.162 25																

Table 18: Out-of-sample validation figures of selected GAMs of BEL with varying spline function type and fixed spline function number of 10 per dimension under between 100-443 and 150-443 after each tenth and the finally selected smooth function.

k	K_{\max}	v.mae	v.mae ^a	v.res	v.mae ⁰	v.res ⁰	ns.mae	ns.mae ^a	ns.res	ns.mae ⁰	ns.res ⁰	cr.mae	cr.mae ^a	cr.res	cr.mae ⁰	cr.res ⁰
8 Thin plate regression splines under gaussian with identity link																
0	150	4.557	4.357	-238	100.000	38	3.231	3.121	0	100.000	261	4.027	3.942	106	100.000	367
10	150	0.639	0.611	27	23.176	125	0.340	0.329	-3	15.517	80	0.516	0.505	73	23.627	156
20	150	0.375	0.359	3	9.604	26	0.334	0.322	-33	8.378	-24	0.341	0.333	1	7.711	10
30	150	0.361	0.345	-7	10.444	41	0.415	0.401	-52	6.961	-19	0.304	0.297	-21	5.871	13
40	150	0.356	0.340	-5	10.098	36	0.425	0.410	-54	7.920	-28	0.311	0.304	-27	5.647	-1
50	150	0.339	0.324	-7	9.712	33	0.418	0.404	-53	7.746	-27	0.311	0.304	-26	5.596	0
60	150	0.325	0.311	-6	9.037	26	0.411	0.397	-52	8.706	-34	0.310	0.304	-26	5.850	-8
70	150	0.325	0.311	-4	9.180	31	0.429	0.414	-55	8.773	-34	0.326	0.319	-30	5.912	-9
80	150	0.309	0.296	-5	8.618	29	0.430	0.415	-55	8.984	-35	0.336	0.329	-29	6.382	-9
90	150	0.313	0.299	-5	8.981	32	0.384	0.371	-48	7.390	-26	0.300	0.293	-26	5.430	-4
100	150	0.328	0.313	-6	9.910	47	0.400	0.387	-51	5.572	-12	0.291	0.285	-25	5.064	13
110	150	0.256	0.245	-10	7.985	38	0.326	0.315	-40	4.655	-6	0.201	0.197	-6	5.002	28
120	150	0.253	0.242	-9	7.340	30	0.321	0.310	-39	5.542	-14	0.209	0.204	-5	4.541	20
130	150	0.252	0.241	-9	7.767	34	0.326	0.315	-40	5.197	-11	0.205	0.201	-5	4.770	24
140	150	0.245	0.234	-8	7.592	33	0.322	0.311	-41	5.315	-15	0.197	0.193	-7	4.317	20
150	150	0.217	0.208	-11	6.477	32	0.239	0.231	-26	3.652	2	0.179	0.175	6	5.578	34
8 Thin plate regression splines under gaussian with log link in stagewise selection of length 5																
0	50	4.557	4.357	-238	100.000	38	3.231	3.121	0	100.000	261	4.027	3.942	106	100.000	367
10	50	0.757	0.724	10	21.570	101	0.444	0.429	39	22.141	116	0.755	0.739	106	27.693	182
20	50	0.401	0.383	1	10.278	23	0.359	0.347	-35	9.154	-28	0.362	0.354	-1	8.110	7
30	50	0.396	0.379	-5	11.249	43	0.438	0.424	-53	7.692	-20	0.339	0.332	-19	6.803	14
40	50	0.382	0.365	-5	11.036	45	0.470	0.454	-60	7.846	-25	0.351	0.344	-31	6.234	4
50	50	0.370	0.353	-8	10.487	39	0.464	0.448	-60	8.000	-28	0.340	0.333	-32	5.901	0
8 Thin plate regression splines under gamma with identity link in stagewise selection of length 5																
0	100	4.557	4.357	-238	100.000	38	3.231	3.121	0	100.000	261	4.027	3.942	106	100.000	367
10	100	0.637	0.609	29	22.743	123	0.334	0.323	-3	14.941	77	0.510	0.500	72	22.871	151
20	100	0.370	0.354	4	9.537	27	0.324	0.313	-31	8.076	-22	0.340	0.333	1	7.725	10
30	100	0.359	0.344	-8	10.558	44	0.414	0.400	-52	6.415	-15	0.305	0.298	-22	5.909	16
40	100	0.329	0.314	-9	9.643	37	0.402	0.388	-51	6.673	-21	0.321	0.314	-26	5.702	4
50	100	0.342	0.327	-7	9.631	33	0.409	0.395	-52	7.553	-27	0.326	0.320	-28	5.863	-3
60	100	0.324	0.310	-6	9.114	28	0.409	0.395	-52	8.421	-32	0.327	0.320	-28	6.067	-9
70	100	0.328	0.314	-6	9.617	41	0.451	0.435	-59	7.631	-26	0.349	0.342	-35	5.796	-2
80	100	0.270	0.258	-9	7.944	37	0.324	0.313	-38	5.068	-7	0.221	0.217	-2	5.461	29
90	100	0.279	0.267	-10	8.926	47	0.341	0.329	-40	4.595	2	0.224	0.219	-2	6.713	41
100	100	0.272	0.260	-11	8.654	44	0.335	0.324	-40	4.532	0	0.216	0.211	-2	6.397	38
8 Thin plate regression splines under gamma with log link in stagewise selection of length 5																
0	110	4.557	4.357	-238	100.000	38	3.231	3.121	0	100.000	261	4.027	3.942	106	100.000	367
10	110	0.762	0.729	13	21.360	95	0.458	0.443	45	21.527	112	0.773	0.756	108	26.743	176
20	110	0.442	0.422	2	12.416	49	0.396	0.382	-44	7.515	-12	0.349	0.342	-8	8.083	24
30	110	0.387	0.370	-3	11.147	45	0.414	0.400	-49	7.058	-16	0.338	0.331	-18	6.847	16
40	110	0.372	0.356	-6	10.826	43	0.458	0.442	-59	7.546	-24	0.360	0.352	-34	6.225	1
50	110	0.357	0.342	-9	10.240	36	0.458	0.443	-60	7.977	-29	0.357	0.349	-36	6.073	-5
60	110	0.351	0.336	-5	9.866	30	0.439	0.424	-56	9.066	-36	0.353	0.346	-35	6.537	-15
70	110	0.354	0.339	-5	10.130	37	0.458	0.442	-59	8.442	-31	0.364	0.356	-37	6.271	-9
80	110	0.359	0.344	-6	10.122	37	0.463	0.447	-60	8.529	-32	0.371	0.363	-37	6.412	-9
90	110	0.282	0.270	-10	9.017	47	0.364	0.352	-44	4.991	-2	0.249	0.244	-6	6.286	36
100	110	0.268	0.256	-11	7.807	37	0.320	0.309	-38	4.748	-5	0.209	0.204	-1	5.604	32
110	110	0.259	0.247	-11	7.373	34	0.312	0.302	-37	4.801	-7	0.201	0.197	0	5.354	31

Table 20: Out-of-sample validation figures of selected GAMs of BEL with varying random component link function combination and fixed spline function number of 8 per dimension under between 50-443 and 150-443 after each tenth and the finally selected smooth function.

<i>k</i>	<i>K</i> _{max}	v.mae	v.mae ^a	v.res	v.mae ⁰	v.res ⁰	ns.mae	ns.mae ^a	ns.res	ns.mae ⁰	ns.res ⁰	cr.mae	cr.mae ^a	cr.res	cr.mae ⁰	cr.res ⁰
8 Thin plate regression splines under gaussian with log link																
0 25 4.557 4.357 -238 100.000 38 3.231 3.121 0 100.000 261 4.027 3.942 106 100.000 367																
10 25 0.663 0.634 26 23.298 123 0.341 0.330 1 16.218 84 0.547 0.536 78 24.370 161																
20 25 0.398 0.381 2 10.221 23 0.361 0.349 -35 9.380 -28 0.375 0.367 -1 8.460 6																
25 25 0.411 0.393 2 11.892 47 0.410 0.397 -47 7.709 -17 0.324 0.317 -11 7.120 19																
8 Thin plate regression splines under gaussian with log link in stagewise selection of length 5																
0 50 4.557 4.357 -238 100.000 38 3.231 3.121 0 100.000 261 4.027 3.942 106 100.000 367																
10 50 0.757 0.724 10 21.570 101 0.444 0.429 39 22.141 116 0.755 0.739 106 27.693 182																
20 50 0.401 0.383 1 10.278 23 0.359 0.347 -35 9.154 -28 0.362 0.354 -1 8.110 7																
30 50 0.396 0.379 -5 11.249 43 0.438 0.424 -53 7.692 -20 0.339 0.332 -19 6.803 14																
40 50 0.382 0.365 -5 11.036 45 0.470 0.454 -60 7.846 -25 0.351 0.344 -31 6.234 4																
50 50 0.370 0.353 -8 10.487 39 0.464 0.448 -60 8.000 -28 0.340 0.333 -32 5.901 0																
8 Thin plate regression splines under gamma with identity link																
0 71 4.557 4.357 -238 100.000 38 3.231 3.121 0 100.000 261 4.027 3.942 106 100.000 367																
10 71 0.637 0.609 29 22.743 123 0.334 0.323 -3 14.941 77 0.510 0.500 72 22.871 151																
20 71 0.386 0.369 8 10.141 31 0.310 0.299 -26 7.904 -18 0.358 0.350 8 8.140 16																
30 71 0.359 0.344 -8 10.558 44 0.414 0.400 -52 6.415 -15 0.305 0.298 -22 5.909 16																
40 71 0.329 0.314 -9 9.643 37 0.402 0.388 -51 6.673 -21 0.321 0.314 -26 5.702 4																
50 71 0.338 0.324 -7 9.543 32 0.412 0.399 -53 7.748 -28 0.324 0.318 -29 5.805 -4																
60 71 0.324 0.310 -6 9.114 28 0.409 0.395 -52 8.421 -32 0.327 0.320 -28 6.067 -9																
70 71 0.327 0.313 -5 9.417 36 0.434 0.419 -56 8.017 -29 0.342 0.335 -32 5.967 -5																
71 71 0.291 0.278 -4 8.639 41 0.341 0.329 -43 5.205 -12 0.196 0.192 -17 3.898 14																
8 Thin plate regression splines under gamma with identity link in stagewise selection of length 5																
0 100 4.557 4.357 -238 100.000 38 3.231 3.121 0 100.000 261 4.027 3.942 106 100.000 367																
10 100 0.637 0.609 29 22.743 123 0.334 0.323 -3 14.941 77 0.510 0.500 72 22.871 151																
20 100 0.370 0.354 4 9.537 27 0.324 0.313 -31 8.076 -22 0.340 0.333 1 7.725 10																
30 100 0.359 0.344 -8 10.558 44 0.414 0.400 -52 6.415 -15 0.305 0.298 -22 5.909 16																
40 100 0.329 0.314 -9 9.643 37 0.402 0.388 -51 6.673 -21 0.321 0.314 -26 5.702 4																
50 100 0.342 0.327 -7 9.631 33 0.409 0.395 -52 7.553 -27 0.326 0.320 -28 5.863 -3																
60 100 0.324 0.310 -6 9.114 28 0.409 0.395 -52 8.421 -32 0.327 0.320 -28 6.067 -9																
70 100 0.328 0.314 -6 9.617 41 0.451 0.435 -59 7.631 -26 0.349 0.342 -35 5.796 -2																
80 100 0.270 0.258 -9 7.944 37 0.324 0.313 -38 5.068 -7 0.221 0.217 -2 5.461 29																
90 100 0.279 0.267 -10 8.926 47 0.341 0.329 -40 4.595 2 0.224 0.219 -2 6.713 41																
100 100 0.272 0.260 -11 8.654 44 0.335 0.324 -40 4.532 0 0.216 0.211 -2 6.397 38																

Table 21: Out-of-sample validation figures of selected GAMs of BEL in adaptive forward stepwise and stagewise selection of length 5 under between 25-443 and 100-443 after each tenth and the finally selected smooth function.

<i>k</i>	<i>K</i> _{max}	v.mae	v.mae ^α	v.res	v.mae ⁰	v.res ⁰	ns.mae	ns.mae ^α	ns.res	ns.mae ⁰	ns.res ⁰	cr.mae	cr.mae ^α	cr.res	cr.mae ⁰	cr.res ⁰
5 Eilers and Marx style P-splines under gaussian with identity link																
0 100 4.557 4.357 -238 100.000 38 3.231 3.121 0 100.000 261 4.027 3.942 106 100.000 367																
10 100 0.643 0.615 29 22.836 123 0.344 0.332 -9 13.951 70 0.471 0.461 65 21.854 144																
20 100 0.389 0.372 1 10.496 37 0.365 0.353 -41 7.778 -20 0.336 0.329 -8 7.402 13																
30 100 0.384 0.367 -9 11.377 53 0.459 0.444 -60 6.138 -13 0.320 0.313 -30 5.512 17																
40 100 0.371 0.354 -10 10.977 49 0.454 0.439 -60 6.095 -16 0.327 0.320 -34 5.092 11																
50 100 0.357 0.341 -9 10.459 45 0.467 0.451 -62 6.909 -22 0.335 0.328 -34 5.059 6																
60 100 0.339 0.324 -10 9.932 43 0.492 0.476 -66 7.640 -28 0.365 0.357 -40 5.155 -2																
70 100 0.343 0.328 -10 10.523 52 0.546 0.527 -75 7.681 -27 0.366 0.358 -46 4.576 2																
80 100 0.334 0.319 -7 9.920 45 0.520 0.503 -67 8.655 -29 0.346 0.339 -36 5.036 1																
90 100 0.228 0.218 -10 6.973 35 0.279 0.269 -31 4.299 0 0.208 0.204 3 5.810 34																
100 100 0.225 0.215 -11 6.897 34 0.256 0.248 -30 3.716 2 0.164 0.161 1 5.212 32																
8 Eilers and Marx style P-splines under inverse gaussian with $\frac{1}{\mu^2}$ link in dynamically stagewise selection of proportion 0.25																
0 91 4.557 4.357 -238 100.000 38 3.231 3.121 0 100.000 261 4.027 3.942 106 100.000 367																
5 91 1.574 1.505 -18 41.688 233 0.732 0.708 -75 30.201 161 0.384 0.376 42 42.135 278																
11 91 0.817 0.781 -3 22.381 113 0.396 0.383 -34 13.475 68 0.412 0.404 23 19.322 124																
21 91 0.679 0.650 -9 24.203 138 0.763 0.738 -102 8.222 31 0.424 0.415 -44 13.548 89																
37 91 0.525 0.502 1 15.485 79 0.521 0.504 -63 6.154 0 0.397 0.389 -30 7.461 33																
62 91 0.505 0.482 -1 14.208 64 0.507 0.490 -61 6.842 -10 0.418 0.410 -33 7.405 18																
91 91 0.309 0.296 -11 9.688 45 0.335 0.324 -36 5.239 6 0.279 0.273 2 7.420 43																
10 Eilers and Marx style P-splines under gaussian with identity link in stagewise selection of length 5																
0 150 4.557 4.357 -238 100.000 38 3.231 3.121 0 100.000 261 4.027 3.942 106 100.000 367																
10 150 0.648 0.619 27 23.688 128 0.349 0.337 -7 15.566 80 0.506 0.495 71 23.889 158																
20 150 0.398 0.380 1 10.946 45 0.358 0.346 -37 7.063 -7 0.338 0.331 1 8.102 31																
30 150 0.393 0.376 -9 11.983 59 0.435 0.421 -55 5.575 -2 0.299 0.293 -17 6.928 36																
40 150 0.371 0.355 -8 11.374 55 0.449 0.434 -57 5.738 -9 0.314 0.308 -26 5.770 23																
50 150 0.363 0.347 -9 10.956 50 0.460 0.444 -60 6.249 -14 0.315 0.308 -28 5.492 17																
60 150 0.349 0.334 -8 10.479 46 0.443 0.428 -56 6.526 -17 0.305 0.298 -26 5.427 14																
70 150 0.349 0.333 -6 10.629 51 0.464 0.449 -60 6.687 -17 0.325 0.318 -29 5.501 13																
80 150 0.350 0.335 -7 10.465 48 0.468 0.452 -60 7.036 -19 0.335 0.328 -29 5.563 11																
90 150 0.350 0.335 -7 10.639 51 0.470 0.454 -60 6.683 -17 0.330 0.323 -29 5.453 14																
100 150 0.334 0.319 -8 9.960 46 0.468 0.452 -60 7.170 -20 0.339 0.332 -29 5.835 11																
110 150 0.337 0.323 -9 10.249 48 0.450 0.435 -58 6.171 -15 0.329 0.322 -31 5.267 12																
120 150 0.339 0.324 -7 10.283 45 0.433 0.419 -55 6.420 -17 0.320 0.313 -28 5.340 10																
130 150 0.269 0.257 -13 8.912 43 0.365 0.352 -46 4.891 -4 0.244 0.238 -12 5.503 30																
140 150 0.255 0.244 -12 8.157 36 0.356 0.344 -44 5.415 -10 0.246 0.241 -10 5.196 24																
150 150 0.261 0.250 -12 8.514 39 0.368 0.355 -46 5.267 -9 0.245 0.240 -12 5.162 25																

Table 22: Out-of-sample validation figures of selected GAMs of BEL with varying spline function number per dimension and fixed spline function type under between 91-443 and 150-443 after each tenth and the finally selected smooth function or after each dynamically stagewise selected smooth function block. Thereby furthermore a variation in the random component link function combination.

k	K_{\max}	$v.\text{mae}$	$v.\text{mae}^0$	$v.\text{res}$	$v.\text{res}^0$	$ns.\text{mae}$	$ns.\text{mae}^0$	$ns.\text{res}$	$ns.\text{res}^0$	$cr.\text{mae}$	$cr.\text{mae}^0$	$cr.\text{res}$	$cr.\text{mae}^0$	$cr.\text{res}^0$		
4 Thin plate regression splines under gaussian with identity link																
150	150	0.240	0.229	-15	8.192	46	0.291	0.281	-35	3.907	13	0.176	0.172	3	7.641	50
5 Thin plate regression splines under gaussian with identity link																
100	100	0.287	0.274	-11	9.431	48	0.397	0.383	-50	5.402	-5	0.202	0.198	-9	5.945	36
8 Thin plate regression splines under gaussian with identity link																
150	150	0.217	0.208	-11	6.477	32	0.239	0.231	-26	3.652	2	0.179	0.175	6	5.578	34
10 Thin plate regression splines under gaussian with identity link																
150	150	0.212	0.203	-10	7.070	37	0.230	0.223	-24	3.575	8	0.173	0.170	8	6.337	40
5 Cubic regression splines under gaussian with identity link																
100	100	0.268	0.256	-12	9.903	52	0.399	0.386	-51	5.182	-2	0.226	0.221	-9	6.533	40
5 Duchon splines under gaussian with identity link																
56	100	0.666	0.636	-18	18.532	86	0.288	0.279	-14	14.643	75	0.406	0.397	40	19.757	129
5 Eilers and Marx style P-splines under gaussian with identity link																
100	100	0.225	0.215	-11	6.897	34	0.256	0.248	-30	3.716	2	0.164	0.161	1	5.212	32
10 Cubic regression splines under gaussian with identity link																
125	125	0.254	0.243	-7	7.139	31	0.299	0.289	-36	5.189	-13	0.197	0.192	-6	4.228	17
10 Duchon splines under gaussian with identity link																
53	100	0.821	0.785	-44	21.348	94	0.545	0.526	-61	12.593	62	0.446	0.437	-8	18.091	116
10 Eilers and Marx style P-splines under gaussian with identity link in stagewise selection of length 5																
150	150	0.261	0.250	-12	8.514	-39	0.368	0.355	-46	5.267	9	0.245	0.240	-12	5.162	-25
8 Thin plate regression splines under gaussian with log link																
25	25	0.411	0.393	2	11.892	47	0.410	0.397	-47	7.709	-17	0.324	0.317	-11	7.120	19
8 Thin plate regression splines under gaussian with log link in stagewise selection of length 5																
50	50	0.370	0.353	-8	10.487	39	0.464	0.448	-60	8.000	-28	0.340	0.333	-32	5.901	0
8 Thin plate regression splines under gamma with identity link																
71	71	0.291	0.278	-4	8.639	41	0.341	0.329	-43	5.205	-12	0.196	0.192	-17	3.898	14
8 Thin plate regression splines under gamma with identity link in stagewise selection of length 5																
100	100	0.272	0.260	-11	8.654	44	0.335	0.324	-40	4.532	0	0.216	0.211	-2	6.397	38
4 Thin plate regression splines under gaussian with identity link in stagewise selection of length 5																
150	150	0.240	0.229	-15	8.192	46	0.291	0.281	-35	3.907	13	0.176	0.172	3	7.641	50
4 Thin plate regression splines under gaussian with log link in stagewise selection of length 5																
40	40	0.438	0.419	-7	13.382	66	0.524	0.506	-69	6.189	-10	0.373	0.365	-39	5.913	20
4 Thin plate regression splines under gamma with identity link in stagewise selection of length 5																
70	70	0.270	0.259	-16	9.999	57	0.325	0.314	-36	5.280	23	0.245	0.240	10	10.416	69
4 Thin plate regression splines under gaussian with log link in stagewise selection of length 5																
120	120	0.252	0.241	-16	8.368	47	0.263	0.254	-29	4.585	20	0.171	0.167	9	8.830	58
4 Thin plate regression splines under inverse gaussian with identity link in stagewise selection of length 5																
85	85	0.250	0.239	-17	8.739	50	0.325	0.314	-38	4.585	14	0.218	0.213	6	8.871	58
4 Thin plate regression splines under inverse gaussian with log link in stagewise selection of length 5																
75	75	0.258	0.246	-14	9.181	52	0.300	0.290	-33	5.049	19	0.223	0.219	13	9.837	65
4 Thin plate regression splines under inverse gaussian with $\frac{1}{\mu^2}$ link in stagewise selection of length 5																
55	55	0.328	0.314	-9	10.595	56	0.328	0.317	-35	5.325	15	0.241	0.236	16	10.249	67
8 Thin plate regression splines under gamma with log link in stagewise selection of length 5																
110	110	0.259	0.247	-11	7.373	34	0.312	0.302	-37	4.801	-7	0.201	0.197	0	5.354	31
8 Eilers and Marx style P-splines under inverse gaussian with $\frac{1}{\mu^2}$ link in dynamic stagewise selection of proportion 0.25																
91	91	0.309	0.296	-11	9.688	45	0.335	0.324	-36	5.239	6	0.279	0.273	2	7.420	43

Table 23: Maximum allowed numbers of smooth functions and out-of-sample validation figures of all derived GAMs of BEL under between 25-443 and 150-443 after the final iteration. Highlighted in green and red respectively the best and worst validation figures.

m	r_m^1	r_m^2	r_m^3	r_m^4	r_m^5	r_m^6	r_m^7	r_m^8	r_m^9	r_m^{10}	r_m^{11}	r_m^{12}	r_m^{13}	r_m^{14}	r_m^{15}	BP.p-val	AIC	v.mae	ns.mae	cr.mae
0	0	0	0	0	0	0	0	0	0	0	0	0	0	0	0	1_{-20}	325, 850	0.238	0.252	0.154
1	1	0	0	0	0	0	0	0	0	0	0	0	0	0	0	1_{-20}	322, 452	0.238	0.246	0.122
2	0	0	0	0	0	0	1	0	0	0	0	0	0	0	0	1_{-20}	315, 980	0.239	0.255	0.153
3	0	0	0	0	1	0	0	0	0	0	0	0	0	0	0	1_{-20}	314, 077	0.237	0.226	0.165
4	0	0	0	0	0	0	0	0	0	0	0	0	0	0	1	1_{-20}	312, 280	0.231	0.206	0.184
5	0	0	0	0	0	0	0	0	1	0	0	0	0	0	0	1_{-20}	312, 114	0.231	0.205	0.185
6	0	0	0	0	1	0	0	0	0	0	0	0	0	0	0	1_{-20}	311, 949	0.231	0.203	0.186
7	0	1	0	0	0	0	0	0	0	0	0	0	0	0	0	1_{-20}	311, 794	0.232	0.202	0.187
8	0	0	0	0	0	0	0	0	0	0	1	0	0	0	0	1_{-20}	311, 700	0.235	0.200	0.190
9	1	0	0	0	0	0	0	1	0	0	0	0	0	0	0	1_{-20}	311, 610	0.233	0.198	0.190
10	0	0	0	0	0	0	0	2	0	0	0	0	0	0	0	1_{-20}	311, 363	0.227	0.194	0.195
11	0	0	0	0	0	1	0	0	0	0	0	0	0	0	0	1_{-20}	311, 293	0.229	0.194	0.197
12	0	0	0	0	2	0	0	0	0	0	0	0	0	0	0	1_{-20}	311, 237	0.228	0.193	0.198
13	0	0	0	0	0	1	0	0	0	0	0	0	0	0	0	1_{-20}	311, 196	0.230	0.193	0.198
14	0	0	0	0	0	0	1	0	0	0	0	0	0	0	0	1.5_{-20}	311, 161	0.231	0.193	0.200
15	1	0	0	0	0	0	0	0	0	0	0	0	0	0	1	7.1_{-19}	311, 136	0.231	0.191	0.202
16	0	0	0	0	0	0	0	1	0	0	0	0	0	0	1	5_{-15}	311, 091	0.228	0.189	0.201
17	0	0	1	0	0	0	0	0	0	0	0	0	0	0	0	5.8_{-13}	311, 067	0.228	0.188	0.203
18	0	0	0	0	0	2	0	0	0	0	0	0	0	0	0	8.3_{-13}	311, 048	0.228	0.187	0.204
19	0	0	0	0	1	0	0	1	0	0	0	0	0	0	0	3.2_{-12}	311, 030	0.228	0.188	0.204
20	1	0	0	0	1	0	0	0	0	0	0	0	0	0	0	2.7_{-12}	311, 003	0.230	0.188	0.205
21	0	0	0	0	0	1	1	0	0	0	0	0	0	0	0	1.3_{-11}	310, 988	0.230	0.188	0.206
22	0	0	0	1	0	0	0	1	0	0	0	0	0	0	0	9.4_{-11}	310, 974	0.230	0.187	0.207

Table 24: FGLS variance models of BEL corresponding to $M_{\max} \in \{2, 6, 10, 14, 18, 22\}$ derived by adaptive selection from the set of basis functions of the 150-443 OLS proxy function given in Table 1 with exponents summing up to at max two. Furthermore, p-values of Breusch-Pagan test, AIC scores and out-of-sample MAEs in % after each iteration.

m	r_m^1	r_m^2	r_m^3	r_m^4	r_m^5	r_m^6	r_m^7	r_m^8	r_m^9	r_m^{10}	r_m^{11}	r_m^{12}	r_m^{13}	r_m^{14}	r_m^{15}	BP.p-val	AIC	v.mae	ns.mae	cr.mae
0	0	0	0	0	0	0	0	0	0	0	0	0	0	0	0	1_{-20}	325, 459	0.195	0.275	0.175
1	1	0	0	0	0	0	0	0	0	0	0	0	0	0	0	1_{-20}	322, 077	0.199	0.273	0.166
2	0	0	0	0	0	0	0	1	0	0	0	0	0	0	0	1_{-20}	315, 615	0.196	0.275	0.175
3	0	0	0	0	1	0	0	0	0	0	0	0	0	0	0	1_{-20}	313, 659	0.195	0.255	0.175
4	0	0	0	0	0	0	0	0	0	0	0	0	0	0	1	1_{-20}	311, 864	0.198	0.239	0.182
5	0	0	0	0	0	0	0	0	1	0	0	0	0	0	0	1_{-20}	311, 704	0.198	0.236	0.182
6	0	1	0	0	0	0	0	0	0	0	0	0	0	0	0	1_{-20}	311, 554	0.200	0.240	0.183
7	2	0	0	0	0	0	0	0	0	0	0	0	0	0	0	1_{-20}	311, 454	0.199	0.241	0.183
8	0	0	0	0	0	0	0	0	0	0	1	0	0	0	0	1_{-20}	311, 360	0.199	0.238	0.186
9	0	0	0	0	0	1	0	0	0	0	0	0	0	0	0	1_{-20}	311, 318	0.201	0.236	0.188
10	0	0	0	0	0	1	0	0	0	0	0	0	0	0	0	1_{-20}	311, 287	0.203	0.234	0.189
11	0	0	0	0	0	1	0	1	0	0	0	0	0	0	0	1_{-20}	311, 260	0.203	0.233	0.189
12	0	0	0	0	0	0	0	2	0	0	0	0	0	0	0	1_{-20}	311, 237	0.203	0.232	0.189
13	1	0	0	0	0	0	0	1	0	0	0	0	0	0	0	3.7_{-17}	311, 001	0.200	0.223	0.192
14	1	0	0	0	0	0	0	0	0	0	0	0	0	0	1	1.7_{-16}	310, 980	0.200	0.222	0.194
15	0	0	0	0	0	0	0	1	0	0	0	0	0	0	1	7.6_{-13}	310, 934	0.200	0.220	0.196
16	0	0	1	0	0	0	0	0	0	0	0	0	0	0	0	4.2_{-11}	310, 912	0.200	0.218	0.197
17	0	0	0	0	0	0	2	0	0	0	0	0	0	0	0	1.3_{-10}	310, 895	0.200	0.219	0.198
18	0	0	0	0	1	1	0	0	0	0	0	0	0	0	0	2.3_{-10}	310, 881	0.200	0.217	0.198
19	0	0	0	0	0	0	0	0	0	0	0	0	0	2	0	7.6_{-10}	310, 867	0.200	0.218	0.197
20	0	0	0	0	0	0	0	1	0	0	1	0	0	0	0	3.4_{-9}	310, 854	0.200	0.218	0.196
21	0	0	0	0	0	0	0	0	0	0	0	0	1	0	0	9.9_{-9}	310, 843	0.200	0.218	0.196
22	1	0	0	0	0	0	0	0	0	0	1	0	0	0	0	3.1_{-8}	310, 832	0.200	0.217	0.196

Table 25: FGLS variance models of BEL corresponding to $M_{\max} \in \{2, 6, 10, 14, 18, 22\}$ derived by adaptive selection from the set of basis functions of the 300-886 OLS proxy function given in Table 3 with exponents summing up to at max two. Furthermore, p-values of Breusch-Pagan test, AIC scores and out-of-sample MAEs in % after each iteration.

<i>m</i>	v.mae	v.mae ^a	v.res	v.mae ⁰	v.res ⁰	ns.mae	ns.mae ^a	ns.res	ns.mae ⁰	ns.res ⁰	cr.mae	cr.mae ^a	cr.res	cr.mae ⁰	cr.res ⁰
0	0.238	0.228	-15	8.103	45	0.252	0.243	-30	3.984	16	0.154	0.151	3	7.379	49
1	0.238	0.228	-15	8.668	49	0.246	0.238	-30	4.120	19	0.122	0.120	3	7.873	52
2	0.239	0.229	-16	8.147	46	0.255	0.246	-30	4.032	17	0.153	0.149	2	7.489	49
3	0.237	0.226	-15	7.789	43	0.226	0.218	-24	4.423	20	0.165	0.162	10	8.117	54
4	0.231	0.221	-13	7.684	42	0.206	0.199	-18	4.817	22	0.184	0.180	17	8.756	58
5	0.231	0.221	-13	7.666	42	0.205	0.198	-18	4.803	22	0.185	0.181	17	8.740	58
6	0.231	0.221	-13	7.577	41	0.203	0.196	-18	4.762	22	0.186	0.183	17	8.637	57
7	0.232	0.222	-12	7.661	42	0.202	0.195	-17	4.787	22	0.187	0.183	18	8.691	57
8	0.235	0.225	-12	7.774	42	0.200	0.193	-17	4.914	23	0.190	0.186	19	8.912	59
9	0.233	0.223	-11	7.692	42	0.198	0.191	-16	4.838	23	0.190	0.186	19	8.763	58
10	0.227	0.217	-10	7.460	40	0.194	0.188	-15	4.708	21	0.195	0.191	20	8.537	56
11	0.229	0.219	-10	7.447	40	0.194	0.187	-15	4.686	21	0.197	0.193	20	8.455	56
12	0.228	0.218	-10	7.426	40	0.193	0.186	-14	4.687	21	0.198	0.194	20	8.444	56
13	0.230	0.220	-9	7.513	41	0.193	0.187	-14	4.696	21	0.198	0.194	21	8.491	56
14	0.231	0.221	-9	7.527	41	0.193	0.186	-14	4.701	21	0.200	0.195	21	8.497	56
15	0.231	0.221	-9	7.523	41	0.191	0.185	-13	4.742	21	0.202	0.197	22	8.569	57
16	0.228	0.218	-9	7.437	40	0.189	0.182	-13	4.730	21	0.201	0.197	22	8.557	56
17	0.228	0.218	-9	7.421	40	0.188	0.182	-13	4.747	21	0.203	0.199	22	8.568	56
18	0.228	0.218	-9	7.433	40	0.187	0.181	-13	4.780	22	0.204	0.200	22	8.621	57
19	0.228	0.218	-9	7.435	40	0.188	0.182	-13	4.786	22	0.204	0.200	22	8.628	57
20	0.230	0.219	-9	7.442	40	0.188	0.182	-13	4.796	22	0.205	0.201	22	8.650	57
21	0.230	0.220	-9	7.466	40	0.188	0.181	-13	4.800	22	0.206	0.201	23	8.648	57
22	0.230	0.220	-8	7.436	40	0.187	0.180	-12	4.802	22	0.207	0.203	23	8.639	57

Table 26: Iteration-wise out-of-sample validation figures in adaptive variance model selection of BEL corresponding to $M_{\max} \in \{2, 6, 10, 14, 18, 22\}$ based on the 150-443 OLS proxy function given in Table 1 with exponents summing up to at max two. Simultaneously type I FGGLS regression results.

<i>m</i>	v.mae	v.mae ^a	v.res	v.mae ⁰	v.res ⁰	ns.mae	ns.mae ^a	ns.res	ns.mae ⁰	ns.res ⁰	cr.mae	cr.mae ^a	cr.res	cr.mae ⁰	cr.res ⁰
0	0.195	0.186	-9	6.468	33	0.275	0.266	-30	4.601	-3	0.175	0.171	5	5.315	32
1	0.199	0.190	-9	6.648	34	0.273	0.263	-31	4.272	-3	0.166	0.162	1	5.005	30
2	0.196	0.187	-9	6.527	33	0.275	0.266	-30	4.564	-3	0.175	0.171	5	5.401	32
3	0.195	0.186	-9	6.487	33	0.255	0.247	-27	4.350	1	0.175	0.171	9	5.916	37
4	0.198	0.189	-9	6.305	32	0.239	0.231	-23	4.262	4	0.182	0.178	13	6.303	40
5	0.198	0.190	-9	6.298	32	0.236	0.228	-22	4.252	4	0.182	0.178	14	6.336	40
6	0.200	0.191	-9	6.399	33	0.240	0.232	-23	4.292	4	0.183	0.179	13	6.389	40
7	0.199	0.190	-9	6.364	32	0.241	0.233	-23	4.304	4	0.183	0.179	13	6.324	40
8	0.199	0.190	-8	6.381	32	0.238	0.230	-22	4.313	4	0.186	0.182	14	6.407	40
9	0.201	0.193	-8	6.432	33	0.236	0.228	-22	4.313	5	0.188	0.184	15	6.521	41
10	0.203	0.194	-8	6.473	33	0.234	0.226	-21	4.310	5	0.189	0.185	16	6.621	42
11	0.203	0.195	-8	6.492	33	0.233	0.225	-21	4.303	5	0.189	0.185	16	6.628	42
12	0.203	0.194	-8	6.476	33	0.232	0.224	-21	4.294	5	0.189	0.186	16	6.641	42
13	0.200	0.191	-7	6.254	32	0.223	0.216	-19	4.252	5	0.192	0.188	17	6.615	42
14	0.200	0.191	-7	6.246	31	0.222	0.214	-19	4.257	6	0.194	0.190	18	6.697	42
15	0.200	0.191	-7	6.216	31	0.220	0.213	-18	4.243	6	0.196	0.192	19	6.773	43
16	0.200	0.191	-7	6.180	31	0.218	0.211	-18	4.239	6	0.197	0.193	19	6.753	43
17	0.200	0.192	-7	6.197	31	0.219	0.211	-18	4.249	6	0.198	0.194	19	6.804	43
18	0.200	0.191	-7	6.194	31	0.217	0.210	-18	4.250	6	0.198	0.194	19	6.801	43
19	0.200	0.191	-7	6.207	31	0.218	0.210	-18	4.238	6	0.197	0.193	19	6.787	43
20	0.200	0.191	-7	6.229	32	0.218	0.211	-18	4.226	6	0.196	0.192	19	6.793	43
21	0.200	0.192	-7	6.240	32	0.218	0.211	-18	4.224	7	0.196	0.192	19	6.814	43
22	0.200	0.192	-7	6.256	32	0.217	0.210	-18	4.223	7	0.196	0.192	19	6.844	44

Table 27: Iteration-wise out-of-sample validation figures in adaptive variance model selection of BEL corresponding to $M_{\max} \in \{2, 6, 10, 14, 18, 22\}$ based on the 300-886 OLS proxy function given in Table 3 with exponents summing up to at max two. Simultaneously type I FGGLS regression results.

<i>k</i>	AIC	v.mae	v.mae ^a	v.res	v.mae ⁰	v.res ⁰	ns.mae	ns.mae ^a	ns.res	ns.mae ⁰	ns.res ⁰	cr.mae	cr.mae ^a	cr.res	cr.mae ⁰	cr.res ⁰
<i>M</i> _{max} = 2 in variance model selection																
0 437, 251	4.557	4.357	-238	100.000	38	3.231	3.121	0	100.000	261	4.027	3.942	106	100.000	367	
10 336, 390	1.786	1.708	184	44.082	198	1.402	1.354	209	39.152	209	2.290	2.242	344	52.033	344	
20 323, 883	0.826	0.790	25	22.007	111	0.424	0.409	-28	10.764	44	0.437	0.428	28	16.424	99	
30 319, 958	0.465	0.445	3	12.876	55	0.288	0.278	2	9.650	40	0.467	0.457	57	15.234	96	
40 318, 945	0.401	0.384	-16	11.036	51	0.357	0.345	-37	7.158	16	0.330	0.323	3	10.127	55	
50 318, 206	0.355	0.339	-24	9.270	35	0.336	0.324	-36	6.611	8	0.339	0.332	-8	8.602	36	
60 317, 485	0.323	0.309	-25	8.407	36	0.309	0.298	-36	5.548	11	0.279	0.273	-11	7.244	36	
70 317, 197	0.306	0.293	-28	7.631	28	0.345	0.334	-43	5.405	-1	0.272	0.266	-17	5.899	25	
80 316, 263	0.272	0.260	-24	6.946	32	0.320	0.310	-42	4.051	0	0.227	0.222	-17	4.898	25	
90 316, 021	0.260	0.249	-23	7.143	39	0.298	0.288	-37	3.854	10	0.173	0.169	-5	6.461	42	
100 315, 871	0.256	0.245	-23	7.424	41	0.294	0.284	-35	4.078	14	0.186	0.182	0	7.443	49	
110 315, 784	0.256	0.245	-22	7.396	41	0.302	0.292	-37	3.962	12	0.189	0.185	-3	7.013	46	
120 315, 719	0.257	0.245	-23	6.923	38	0.296	0.286	-36	3.870	11	0.181	0.177	-2	6.872	45	
130 315, 675	0.258	0.247	-25	6.506	35	0.295	0.285	-36	3.760	9	0.188	0.184	-3	6.461	42	
140 315, 649	0.252	0.241	-23	6.424	34	0.283	0.274	-34	3.749	9	0.184	0.180	-1	6.399	42	
150 315, 629	0.239	0.229	-21	6.467	34	0.261	0.252	-30	3.796	10	0.177	0.173	3	6.654	44	
<i>M</i> _{max} = 6 in variance model selection																
0 437, 251	4.557	4.357	-238	100.000	38	3.231	3.121	0	100.000	261	4.027	3.942	106	100.000	367	
10 332, 479	2.014	1.926	259	49.098	213	2.000	1.933	298	44.745	238	2.964	2.901	445	58.341	385	
20 320, 873	0.881	0.842	51	22.821	115	0.341	0.329	16	13.428	66	0.622	0.609	84	20.790	134	
30 316, 187	0.429	0.410	19	10.875	32	0.308	0.297	29	8.537	28	0.561	0.549	73	12.633	72	
40 315, 132	0.366	0.350	6	10.243	45	0.254	0.246	1	7.853	25	0.401	0.393	36	11.221	61	
50 314, 473	0.303	0.289	3	9.346	46	0.229	0.222	0	7.543	28	0.361	0.353	34	10.776	62	
60 313, 643	0.307	0.293	-18	7.567	28	0.251	0.242	-21	5.808	11	0.266	0.261	9	7.676	41	
70 313, 301	0.280	0.268	-17	7.768	30	0.222	0.214	-12	6.229	21	0.268	0.262	23	9.315	56	
80 313, 060	0.270	0.258	-20	7.092	28	0.230	0.222	-13	6.273	22	0.280	0.274	25	9.554	59	
90 312, 883	0.262	0.251	-22	6.754	29	0.239	0.231	-17	5.977	20	0.253	0.248	19	9.077	56	
100 312, 100	0.246	0.235	-19	6.177	29	0.202	0.195	-14	4.814	18	0.221	0.216	21	8.305	54	
110 311, 656	0.231	0.221	-16	6.446	33	0.189	0.182	-12	4.827	22	0.211	0.206	25	8.964	59	
120 311, 574	0.236	0.225	-16	6.545	34	0.209	0.202	-16	4.594	19	0.207	0.202	22	8.637	57	
130 311, 511	0.238	0.227	-17	6.551	35	0.207	0.200	-16	4.797	21	0.204	0.200	23	9.104	60	
140 311, 461	0.231	0.221	-16	6.026	31	0.189	0.183	-12	4.726	21	0.216	0.212	25	8.853	58	
150 311, 426	0.224	0.215	-14	5.904	31	0.177	0.171	-9	4.756	22	0.226	0.221	29	9.005	59	
<i>M</i> _{max} = 10 in variance model selection																
0 437, 251	4.557	4.357	-238	100.000	38	3.231	3.121	0	100.000	261	4.027	3.942	106	100.000	367	
10 328, 519	2.120	2.027	288	50.524	221	2.206	2.132	329	46.563	248	3.194	3.127	480	60.396	399	
20 319, 481	0.971	0.928	95	24.185	105	0.439	0.424	53	11.839	49	0.821	0.803	117	18.086	112	
30 316, 529	0.655	0.627	56	16.560	74	0.420	0.406	57	12.301	61	0.780	0.764	113	18.285	117	
40 314, 460	0.379	0.362	19	10.089	42	0.268	0.259	19	8.120	28	0.473	0.463	54	11.608	63	
50 313, 842	0.324	0.310	2	8.422	33	0.229	0.221	-4	6.420	12	0.339	0.331	20	8.600	36	
60 313, 022	0.297	0.284	-13	7.619	31	0.223	0.215	-13	6.123	17	0.277	0.271	14	8.292	43	
70 312, 692	0.282	0.269	-17	7.494	26	0.221	0.213	-5	6.762	24	0.326	0.319	35	10.467	64	
80 312, 443	0.271	0.259	-19	7.171	27	0.218	0.211	-7	6.625	25	0.303	0.297	33	10.306	65	
90 312, 264	0.261	0.249	-21	6.610	27	0.222	0.215	-11	6.300	23	0.278	0.272	28	9.806	62	
100 312, 187	0.262	0.250	-21	6.568	26	0.216	0.208	-10	6.265	23	0.272	0.266	28	9.707	61	
110 312, 108	0.256	0.244	-21	6.031	23	0.203	0.196	-5	6.324	25	0.288	0.282	31	9.754	61	
120 312, 043	0.261	0.250	-23	5.989	20	0.200	0.194	-4	6.287	25	0.293	0.287	33	9.857	62	
130 311, 078	0.226	0.216	-18	5.466	25	0.160	0.155	-4	5.115	24	0.244	0.239	32	9.192	60	
140 310, 918	0.220	0.210	-16	5.451	25	0.153	0.148	-4	4.820	23	0.233	0.228	31	8.859	58	
150 310, 868	0.212	0.203	-14	5.375	25	0.148	0.143	0	5.098	25	0.256	0.250	36	9.296	61	

Table 28: AIC scores and out-of-sample validation figures of type II FGLS proxy functions of BEL under 150-443 with variance models of varying complexity *M*_{max} after each tenth iteration.

<i>k</i>	AIC	v.mae	v.mae ^a	v.res	v.mae ⁰	v.res ⁰	ns.mae	ns.mae ^a	ns.res	ns.mae ⁰	ns.res ⁰	cr.mae	cr.mae ^a	cr.res	cr.mae ⁰	cr.res ⁰
<i>M</i>_{max} = 14 in variance model selection																
0 437, 251	4.557	4.357	-238	100.000	38	3.231	3.121	0	100.000	261	4.027	3.942	106	100.000	367	
10 326, 308	2.120	2.027	290	50.306	220	2.215	2.141	331	46.129	246	3.197	3.130	480	59.909	396	
20 319, 199	1.024	0.979	100	26.049	137	0.527	0.509	75	18.639	98	1.044	1.022	155	27.142	178	
30 316, 093	0.702	0.671	67	17.574	79	0.503	0.486	73	13.745	70	0.901	0.882	133	20.208	131	
40 314, 155	0.393	0.376	24	10.363	44	0.282	0.273	25	8.426	31	0.505	0.494	62	12.131	68	
50 313, 562	0.327	0.313	6	8.561	34	0.225	0.217	1	6.535	15	0.352	0.345	27	8.936	41	
60 312, 811	0.298	0.285	-10	7.608	29	0.203	0.196	4	7.086	29	0.336	0.329	37	10.283	62	
70 312, 455	0.289	0.276	-15	7.409	26	0.219	0.211	-2	6.863	25	0.343	0.335	38	10.612	65	
80 312, 235	0.273	0.261	-17	7.222	28	0.215	0.208	-4	6.738	26	0.322	0.316	37	10.662	67	
90 312, 057	0.264	0.253	-22	6.680	27	0.222	0.214	-10	6.406	24	0.283	0.277	28	9.981	63	
100 311, 953	0.255	0.244	-21	6.117	24	0.201	0.194	-5	6.381	25	0.290	0.284	31	9.780	61	
110 311, 898	0.252	0.241	-20	5.929	22	0.200	0.193	-4	6.236	24	0.293	0.287	32	9.583	60	
120 311, 832	0.263	0.251	-23	5.962	19	0.198	0.192	-3	6.300	25	0.303	0.296	34	9.878	62	
130 310, 916	0.223	0.213	-17	5.363	23	0.154	0.149	-1	5.233	25	0.263	0.257	36	9.305	61	
140 310, 757	0.215	0.206	-15	5.339	24	0.147	0.142	0	4.954	24	0.251	0.246	35	8.972	59	
150 310, 714	0.214	0.205	-14	5.368	25	0.146	0.141	-1	4.857	23	0.244	0.239	34	8.906	59	
<i>M</i>_{max} = 18 in variance model selection																
0 437, 251	4.557	4.357	-238	100.000	38	3.231	3.121	0	100.000	261	4.027	3.942	106	100.000	367	
10 326, 125	2.127	2.034	292	50.425	220	2.226	2.151	332	46.222	246	3.209	3.142	482	60.019	396	
20 318, 762	1.036	0.991	111	25.668	113	0.538	0.520	75	13.429	64	0.983	0.962	144	20.708	133	
30 315, 995	0.710	0.679	69	17.741	80	0.523	0.505	76	13.963	72	0.925	0.906	137	20.465	133	
40 314, 060	0.401	0.383	27	10.529	45	0.292	0.282	28	8.560	33	0.521	0.510	66	12.341	70	
50 313, 483	0.329	0.315	9	8.687	35	0.225	0.217	4	6.620	16	0.362	0.354	31	9.120	43	
60 312, 938	0.316	0.302	-5	7.840	30	0.209	0.202	5	6.855	26	0.347	0.340	41	10.297	62	
70 312, 363	0.270	0.258	-10	6.960	21	0.215	0.207	11	7.089	28	0.389	0.381	48	10.795	65	
80 312, 166	0.259	0.248	-12	6.558	22	0.204	0.198	9	7.008	29	0.369	0.361	47	10.718	67	
90 311, 963	0.234	0.223	-15	6.141	24	0.196	0.189	1	6.432	26	0.313	0.306	37	9.844	61	
100 311, 883	0.241	0.231	-18	6.031	24	0.194	0.187	-1	6.449	26	0.299	0.293	34	9.777	61	
110 311, 830	0.239	0.229	-18	5.836	22	0.193	0.187	0	6.298	25	0.303	0.296	35	9.610	60	
120 311, 766	0.244	0.234	-19	5.713	18	0.191	0.184	3	6.340	26	0.321	0.314	39	9.866	62	
130 311, 045	0.225	0.215	-15	5.396	23	0.148	0.143	0	5.061	24	0.259	0.254	35	8.950	59	
140 310, 694	0.213	0.204	-13	5.314	24	0.139	0.134	1	4.855	24	0.245	0.240	34	8.672	57	
150 310, 644	0.211	0.202	-14	5.131	23	0.139	0.135	1	4.816	23	0.250	0.245	35	8.618	57	
<i>M</i>_{max} = 22 in variance model selection																
0 437, 251	4.557	4.357	-238	100.000	38	3.231	3.121	0	100.000	261	4.027	3.942	106	100.000	367	
10 325, 988	2.127	2.034	292	50.414	220	2.226	2.151	332	46.259	246	3.210	3.143	482	60.061	397	
20 318, 926	1.034	0.988	105	26.160	137	0.569	0.550	83	19.043	101	1.098	1.075	163	27.621	181	
30 315, 805	0.712	0.681	71	17.763	79	0.537	0.519	78	14.063	72	0.943	0.923	140	20.603	134	
40 313, 973	0.409	0.391	29	10.730	46	0.301	0.291	31	8.709	34	0.539	0.527	70	12.589	72	
50 313, 411	0.349	0.334	7	8.950	34	0.223	0.216	3	6.618	16	0.357	0.349	30	9.081	42	
60 312, 873	0.308	0.295	-2	8.205	37	0.203	0.196	8	7.490	33	0.350	0.343	43	10.853	67	
70 312, 286	0.271	0.260	-9	6.950	21	0.217	0.210	12	7.124	28	0.398	0.389	50	10.856	66	
80 312, 091	0.261	0.249	-11	6.557	22	0.207	0.200	10	7.051	29	0.377	0.369	48	10.793	68	
90 311, 893	0.235	0.225	-15	6.043	23	0.196	0.189	1	6.367	25	0.314	0.307	36	9.683	60	
100 311, 815	0.238	0.228	-17	5.970	23	0.194	0.187	1	6.462	26	0.311	0.304	37	9.829	61	
110 311, 761	0.237	0.227	-17	5.780	21	0.194	0.188	2	6.364	25	0.313	0.307	37	9.694	60	
120 311, 697	0.243	0.232	-19	5.818	18	0.191	0.185	2	6.325	25	0.320	0.313	39	9.885	62	
130 311, 655	0.232	0.222	-17	5.688	18	0.195	0.188	8	6.714	29	0.353	0.346	46	10.509	67	
140 310, 748	0.215	0.206	-14	5.206	23	0.148	0.143	5	5.578	27	0.293	0.287	42	9.788	64	
150 310, 590	0.208	0.199	-13	5.209	23	0.139	0.134	5	5.193	26	0.275	0.270	40	9.256	61	

Table 28: Cont.

<i>k</i>	AIC	v.mae	v.mae ^a	v.res	v.mae ⁰	v.res ⁰	ns.mae	ns.mae ^a	ns.res	ns.mae ⁰	ns.res ⁰	cr.mae	cr.mae ^a	cr.res	cr.mae ⁰	cr.res ⁰
<i>M</i>_{max} = 2 in variance model selection																
0 437, 251	4.557	4.357	-238	100.000	38	3.231	3.121	0	100.000	261	4.027	3.942	106	100.000	367	
10 336, 390	1.786	1.708	184	44.082	198	1.402	1.354	209	39.152	209	2.290	2.242	344	52.033	344	
20 323, 883	0.826	0.790	25	22.007	111	0.424	0.409	-28	10.764	44	0.437	0.428	28	16.424	99	
30 319, 958	0.465	0.445	3	12.876	55	0.288	0.278	2	9.650	40	0.467	0.457	57	15.234	96	
40 318, 945	0.401	0.384	-16	11.036	51	0.357	0.345	-37	7.158	16	0.330	0.323	3	10.127	55	
50 318, 206	0.355	0.339	-24	9.270	35	0.336	0.324	-36	6.611	8	0.339	0.332	-8	8.602	36	
60 317, 485	0.323	0.309	-25	8.407	36	0.309	0.298	-36	5.548	11	0.279	0.273	-11	7.244	36	
70 317, 197	0.306	0.293	-28	7.631	28	0.345	0.334	-43	5.405	-1	0.272	0.266	-17	5.899	25	
80 316, 263	0.272	0.260	-24	6.946	32	0.320	0.310	-42	4.051	0	0.227	0.222	-17	4.898	25	
90 316, 021	0.260	0.249	-23	7.143	39	0.298	0.288	-37	3.854	10	0.173	0.169	-5	6.461	42	
100 315, 871	0.256	0.245	-23	7.424	41	0.294	0.284	-35	4.078	14	0.186	0.182	0	7.443	49	
110 315, 784	0.256	0.245	-22	7.396	41	0.302	0.292	-37	3.962	12	0.189	0.185	-3	7.013	46	
120 315, 719	0.257	0.245	-23	6.923	38	0.296	0.286	-36	3.870	11	0.181	0.177	-2	6.872	45	
130 315, 675	0.258	0.247	-25	6.506	35	0.295	0.285	-36	3.760	9	0.188	0.184	-3	6.461	42	
140 315, 641	0.250	0.239	-23	6.441	34	0.284	0.275	-34	3.741	9	0.182	0.178	-2	6.338	41	
150 315, 622	0.238	0.228	-20	6.433	34	0.258	0.250	-29	3.821	11	0.177	0.174	4	6.740	44	
160 315, 599	0.233	0.223	-20	6.578	35	0.256	0.247	-28	3.920	12	0.183	0.179	6	6.988	46	
170 315, 573	0.232	0.222	-19	6.616	35	0.254	0.246	-28	3.880	12	0.181	0.178	5	6.927	45	
180 315, 535	0.225	0.215	-19	6.502	35	0.252	0.243	-28	3.773	11	0.172	0.169	5	6.797	44	
190 315, 523	0.229	0.219	-19	6.809	37	0.244	0.236	-26	4.020	15	0.164	0.161	9	7.607	50	
200 315, 507	0.215	0.206	-18	6.738	36	0.243	0.235	-26	3.969	14	0.164	0.161	9	7.387	49	
210 315, 500	0.214	0.205	-18	6.704	35	0.234	0.226	-24	3.989	14	0.162	0.159	10	7.323	48	
220 315, 492	0.217	0.207	-18	6.769	35	0.239	0.231	-26	3.930	14	0.159	0.155	9	7.277	48	
224 315, 491	0.209	0.199	-17	6.584	34	0.226	0.219	-22	3.999	14	0.165	0.161	12	7.290	48	
<i>M</i>_{max} = 6 in variance model selection																
0 437, 251	4.557	4.357	-238	100.000	38	3.231	3.121	0	100.000	261	4.027	3.942	106	100.000	367	
10 332, 479	2.014	1.926	259	49.098	213	2.000	1.933	298	44.745	238	2.964	2.901	445	58.341	385	
20 320, 873	0.881	0.842	51	22.821	115	0.341	0.329	16	13.428	66	0.622	0.609	84	20.790	134	
30 316, 187	0.429	0.410	19	10.875	32	0.308	0.297	29	8.537	28	0.561	0.549	73	12.633	72	
40 315, 132	0.366	0.350	6	10.243	45	0.254	0.246	1	7.853	25	0.401	0.393	36	11.221	61	
50 314, 473	0.303	0.289	3	9.346	46	0.229	0.222	0	7.543	28	0.361	0.353	34	10.776	62	
60 313, 643	0.307	0.293	-18	7.567	28	0.251	0.242	-21	5.808	11	0.266	0.261	9	7.676	41	
70 313, 301	0.280	0.268	-17	7.768	30	0.222	0.214	-12	6.229	21	0.268	0.262	23	9.315	56	
80 313, 060	0.270	0.258	-20	7.092	28	0.230	0.222	-13	6.273	22	0.280	0.274	25	9.554	59	
90 312, 883	0.262	0.251	-22	6.754	29	0.239	0.231	-17	5.977	20	0.253	0.248	19	9.077	56	
100 312, 100	0.246	0.235	-19	6.177	29	0.202	0.195	-14	4.814	18	0.221	0.216	21	8.305	54	
110 311, 656	0.231	0.221	-16	6.446	33	0.189	0.182	-12	4.827	22	0.211	0.206	25	8.964	59	
120 311, 574	0.236	0.225	-16	6.545	34	0.209	0.202	-16	4.594	19	0.207	0.202	22	8.637	57	
130 311, 507	0.234	0.223	-16	6.706	36	0.206	0.199	-16	4.801	21	0.204	0.200	23	9.094	60	
140 311, 456	0.226	0.216	-16	6.102	32	0.189	0.182	-12	4.717	21	0.215	0.211	25	8.827	58	
150 311, 419	0.224	0.214	-15	5.899	31	0.178	0.172	-10	4.712	22	0.213	0.209	27	8.971	59	
160 311, 355	0.217	0.207	-15	5.536	29	0.160	0.154	-4	5.013	25	0.246	0.241	33	9.420	62	
170 311, 308	0.198	0.189	-13	5.090	23	0.141	0.137	-4	4.144	19	0.221	0.216	27	7.491	49	
180 311, 266	0.202	0.193	-14	5.112	24	0.132	0.127	-3	4.433	22	0.218	0.213	27	7.868	52	
190 311, 248	0.208	0.198	-16	5.287	23	0.143	0.138	-5	4.163	19	0.213	0.208	25	7.630	50	
200 311, 228	0.202	0.193	-14	5.269	24	0.137	0.133	-4	4.148	20	0.213	0.209	27	7.639	50	
210 311, 196	0.192	0.184	-14	5.032	20	0.125	0.121	4	4.655	23	0.253	0.248	32	7.919	52	
220 311, 164	0.195	0.187	-15	5.079	21	0.122	0.118	1	4.620	23	0.237	0.232	31	8.070	53	
230 311, 148	0.194	0.185	-15	5.146	22	0.122	0.118	1	4.571	23	0.236	0.231	29	7.949	52	
237 311, 144	0.196	0.188	-15	5.342	23	0.125	0.121	0	4.765	24	0.235	0.230	30	8.243	54	
<i>M</i>_{max} = 10 in variance model selection																
0 437, 251	4.557	4.357	-238	100.000	38	3.231	3.121	0	100.000	261	4.027	3.942	106	100.000	367	
10 331, 056	2.073	1.982	273	50.085	216	2.113	2.041	315	45.714	244	3.090	3.025	464	59.451	393	
20 320, 199	0.924	0.884	76	23.133	101	0.375	0.362	25	10.921	35	0.655	0.641	82	15.999	92	
30 316, 044	0.543	0.519	31	14.068	56	0.372	0.359	45	11.729	56	0.742	0.727	107	18.450	118	
40 314, 821	0.385	0.368	11	10.626	47	0.256	0.248	6	8.118	28	0.424	0.415	43	11.685	65	
50 314, 201	0.327	0.313	2	9.206	41	0.240	0.232	-8	6.713	17	0.336	0.329	21	9.103	45	
60 313, 386	0.269	0.257	-5	7.831	34	0.220	0.213	6	7.506	31	0.365	0.357	46	11.223	71	
70 312, 980	0.290	0.278	-17	7.316	26	0.210	0.203	-4	6.646	25	0.310	0.304	33	9.955	61	
80 312, 722	0.280	0.268	-18	7.425	31	0.223	0.215	-8	6.792	27	0.300	0.293	33	10.652	68	
90 312, 545	0.270	0.259	-22	7.110	32	0.233	0.225	-13	6.634	26	0.273	0.267	27	10.450	67	
100 312, 469	0.265	0.253	-21	6.800	29	0.224	0.217	-11	6.420	25	0.274	0.268	29	10.128	64	
110 312, 397	0.254	0.243	-19	6.136	25	0.202	0.195	-4	6.360	25	0.290	0.284	33	9.940	63	
120 312, 346	0.247	0.236	-19	5.940	22	0.193	0.187	1	6.468	27	0.307	0.301	38	10.078	64	
130 312, 299	0.240	0.230	-17	5.784	21	0.192	0.185	4	6.563	28	0.329	0.322	43	10.369	66	
140 312, 274	0.247	0.236	-18	5.811	22	0.193	0.186	5	6.870	31	0.338	0.331	45	10.944	71	
150 312, 243	0.249	0.238	-19	5.950	24	0.193	0.186	3	6.872	31	0.324	0.317	43	10.984	71	
160 312, 222	0.255	0.244	-19	6.162	25	0.198	0.191	1	6.859	30	0.324	0.318				

<i>k</i>	AIC	v.mae	v.mae ^a	v.res	v.mae ⁰	v.res ⁰	ns.mae	ns.mae ^a	ns.res	ns.mae ⁰	ns.res ⁰	cr.mae	cr.mae ^a	cr.res	cr.mae ⁰	cr.res ⁰
<i>M</i>_{max} = 14 in variance model selection																
0 437, 251	4.557	4.357	-238	100.000	38	3.231	3.121	0	100.000	261	4.027	3.942	106	100.000	367	
10 327, 049	2.133	2.039	292	50.561	222	2.233	2.157	333	46.686	249	3.222	3.154	484	60.524	400	
20 318, 965	1.020	0.976	108	25.288	111	0.507	0.490	69	12.759	57	0.931	0.912	136	19.634	124	
30 316, 262	0.694	0.663	65	17.386	78	0.484	0.468	69	13.341	68	0.872	0.853	128	19.643	127	
40 314, 272	0.392	0.375	23	10.373	44	0.277	0.268	23	8.322	30	0.493	0.483	59	11.941	66	
50 313, 691	0.349	0.333	1	8.772	32	0.228	0.220	-5	6.440	12	0.335	0.328	19	8.633	36	
60 312, 860	0.289	0.276	-10	7.475	30	0.204	0.197	-2	6.583	24	0.302	0.295	28	9.218	53	
70 312, 542	0.286	0.273	-16	7.501	26	0.219	0.211	-3	6.802	24	0.334	0.327	37	10.548	64	
80 312, 337	0.281	0.269	-18	7.254	27	0.215	0.207	-4	6.834	27	0.323	0.316	37	10.655	67	
90 312, 126	0.261	0.250	-21	6.672	27	0.221	0.213	-10	6.384	23	0.286	0.280	29	9.942	62	
100 312, 046	0.268	0.256	-22	6.695	27	0.222	0.215	-12	6.317	24	0.270	0.265	26	9.779	61	
110 311, 961	0.257	0.245	-22	5.979	23	0.200	0.193	-5	6.316	25	0.284	0.278	31	9.695	61	
120 311, 903	0.252	0.241	-21	5.892	19	0.193	0.186	1	6.411	26	0.311	0.304	37	9.977	63	
130 311, 860	0.244	0.233	-19	5.886	20	0.190	0.184	3	6.562	28	0.322	0.315	41	10.344	66	
140 311, 824	0.243	0.232	-20	5.880	19	0.190	0.183	5	6.758	30	0.335	0.328	44	10.696	69	
150 311, 800	0.247	0.236	-21	6.011	20	0.185	0.179	2	6.452	28	0.309	0.303	40	10.365	66	
160 310, 806	0.218	0.208	-16	5.451	25	0.140	0.135	0	5.234	27	0.255	0.249	37	9.596	63	
170 310, 710	0.210	0.201	-15	5.473	25	0.137	0.132	0	5.077	26	0.249	0.244	36	9.359	62	
180 310, 682	0.206	0.197	-14	5.303	24	0.136	0.131	2	5.064	26	0.266	0.260	39	9.492	63	
190 310, 661	0.200	0.191	-13	5.285	23	0.144	0.139	5	5.163	26	0.298	0.292	44	9.843	65	
200 310, 639	0.201	0.192	-13	5.413	22	0.143	0.138	4	5.088	25	0.293	0.287	44	9.726	64	
210 310, 606	0.203	0.194	-13	5.599	23	0.145	0.141	6	5.459	27	0.314	0.307	47	10.294	68	
220 310, 525	0.183	0.174	-13	4.672	12	0.148	0.143	-3	3.744	7	0.221	0.217	30	6.238	40	
230 310, 513	0.179	0.171	-14	4.668	13	0.153	0.148	-6	3.729	7	0.206	0.202	27	6.113	40	
240 310, 475	0.172	0.164	-14	4.347	10	0.130	0.126	-1	3.523	9	0.219	0.214	30	6.154	39	
250 310, 462	0.171	0.163	-14	4.307	10	0.134	0.130	-2	3.480	8	0.211	0.206	28	5.958	38	
258 310, 443	0.172	0.165	-14	4.371	10	0.134	0.129	-2	3.504	8	0.214	0.210	28	6.063	39	
<i>M</i>_{max} = 18 in variance model selection																
0 437, 251	4.557	4.357	-238	100.000	38	3.231	3.121	0	100.000	261	4.027	3.942	106	100.000	367	
10 325, 846	2.112	2.020	290	50.142	221	2.201	2.127	328	46.153	246	3.183	3.116	478	59.925	396	
20 318, 985	1.027	0.982	104	25.991	136	0.566	0.547	82	18.748	99	1.089	1.066	162	27.261	179	
30 315, 896	0.705	0.674	69	17.595	79	0.526	0.508	76	13.871	71	0.928	0.908	137	20.356	132	
40 314, 044	0.404	0.386	28	10.602	45	0.296	0.286	30	8.630	34	0.531	0.519	68	12.462	71	
50 313, 483	0.330	0.316	9	8.715	35	0.225	0.217	5	6.643	17	0.365	0.358	32	9.177	44	
60 312, 939	0.316	0.302	-5	7.833	31	0.210	0.203	5	6.895	26	0.352	0.345	42	10.382	63	
70 312, 359	0.270	0.258	-10	6.927	21	0.216	0.208	11	7.084	27	0.393	0.385	49	10.781	65	
80 312, 165	0.260	0.248	-12	6.555	22	0.206	0.199	10	7.018	29	0.373	0.365	48	10.721	67	
90 311, 964	0.233	0.223	-15	6.130	24	0.196	0.189	1	6.433	26	0.313	0.307	37	9.838	61	
100 311, 882	0.237	0.227	-17	5.756	20	0.190	0.183	2	6.218	24	0.305	0.298	36	9.431	58	
110 311, 827	0.239	0.229	-18	5.733	21	0.190	0.184	1	6.305	25	0.303	0.296	36	9.588	60	
120 311, 769	0.245	0.234	-20	5.762	18	0.189	0.183	3	6.425	27	0.319	0.313	39	9.924	62	
130 311, 716	0.224	0.214	-16	5.502	15	0.190	0.183	10	6.403	27	0.350	0.342	46	9.993	63	
140 311, 005	0.216	0.206	-13	5.222	21	0.142	0.137	6	5.361	26	0.291	0.285	42	9.416	62	
150 310, 660	0.203	0.194	-12	5.094	21	0.133	0.129	7	5.158	26	0.284	0.278	42	9.129	60	
160 310, 611	0.201	0.192	-12	5.033	21	0.137	0.133	8	5.360	27	0.303	0.297	45	9.568	63	
170 310, 586	0.196	0.187	-11	4.994	21	0.136	0.132	10	5.548	28	0.316	0.310	47	9.821	65	
180 310, 550	0.193	0.184	-12	4.987	21	0.135	0.130	1	4.264	20	0.241	0.236	35	8.200	54	
190 310, 535	0.196	0.187	-14	5.087	21	0.139	0.135	-3	4.049	18	0.217	0.212	31	7.884	52	
200 310, 511	0.182	0.174	-11	4.965	21	0.131	0.127	0	3.992	18	0.231	0.226	34	7.810	52	
210 310, 467	0.185	0.177	-12	5.011	20	0.131	0.127	0	3.967	17	0.231	0.226	34	7.741	51	
220 310, 463	0.181	0.173	-12	5.059	20	0.130	0.125	2	4.181	19	0.246	0.241	36	8.110	54	
230 310, 454	0.181	0.173	-11	5.409	23	0.138	0.133	1	4.405	20	0.246	0.241	36	8.436	56	
240 310, 440	0.182	0.174	-11	5.398	23	0.138	0.133	1	4.457	21	0.250	0.245	37	8.559	57	
250 310, 431	0.181	0.173	-11	5.509	23	0.138	0.133	1	4.525	21	0.251	0.246	37	8.638	57	
252 310, 425	0.185	0.176	-11	5.515	23	0.138	0.133	1	4.548	22	0.253	0.248	37	8.700	57	
<i>M</i>_{max} = 22 in variance model selection																
0 437, 251	4.557	4.357	-238	100.000	38	3.231	3.121	0	100.000	261	4.027	3.942	106	100.000	367	
10 325, 796	2.115	2.023	290	50.203	222	2.206	2.131	329	46.238	246	3.189	3.121	479	60.021	396	
20 318, 940	1.026	0.981	112	25.965	135	0.666	0.644	98	20.243	107	1.199	1.174	179	28.606	188	
30 315, 849	0.708	0.677	70	17.681	79	0.532	0.514	77	14.005	72	0.936	0.917	139	20.526	133	
40 314, 001	0.407	0.389	28	10.712	46	0.299	0.289	31	8.710	34	0.536	0.524	69	12.589	73	
50 313, 413	0.348	0.332	10	9.025	36	0.223	0.216	5	6.616	17	0.364	0.356	32	9.225	44	
60 312, 897	0.316	0.302	-4	7.866	31	0.211	0.203	6	6.983	27	0.358	0.351	44	10.549	65	
70 312, 317	0.271	0.259	-9	6.969	22	0.217	0.210	12	7.185	28	0.399	0.391	50	10.961	67	
80 312, 120	0.260	0.249	-11	6.565	23	0.207	0.200	10	7.119	30	0.379	0.371	49	10.896	69	
90 311, 920	0.235	0.224	-15	6.091	24	0.196	0.189	1	6.427	26	0.313	0.306	37	9.791	61	
100 311, 842	0.238	0.228	-16	6.034	23	0.194	0.187	1	6.531	27	0.311	0.304	37	9.949	63	
110 311, 784	0.241	0.230	-18	5.900	24	0.192	0.185	1	6.554	28	0.30					

<i>k</i>	M_{\max}	AIC	v.mae	v.mae $^\alpha$	v.res	v.mae 0	v.res 0	ns.mae	ns.mae $^\alpha$	ns.res	ns.mae 0	ns.res 0	cr.mae	cr.mae $^\alpha$	cr.res	cr.mae 0	cr.res 0
Type I algorithm under 150-443																	
150 2 315, 980 0.239 0.229 -16 8.147 46 0.255 0.246 -30 4.032 17 0.153 0.149 2 7.489 49																	
150	6 311, 949	0.231	0.221	-13	7.577	41	0.203	0.196	-18	4.762	22	0.186	0.183	17	8.637	57	
150	10 311, 363	0.227	0.217	-10	7.460	40	0.194	0.188	-15	4.708	21	0.195	0.191	20	8.537	56	
150	14 311, 161	0.231	0.221	-9	7.527	41	0.193	0.186	-14	4.701	21	0.200	0.195	21	8.497	56	
150	18 311, 048	0.228	0.218	-9	7.433	40	0.187	0.181	-13	4.780	22	0.204	0.200	22	8.621	57	
150	22 310, 974	0.230	0.220	-8	7.436	40	0.187	0.180	-12	4.802	22	0.207	0.203	23	8.639	57	
Type I algorithm under 300-886																	
224	2 315, 615	0.196	0.187	-9	6.527	33	0.275	0.266	-30	4.564	-3	0.175	0.171	5	5.401	32	
224	6 311, 554	0.200	0.191	-9	6.399	33	0.240	0.232	-23	4.292	4	0.183	0.179	13	6.389	40	
224	10 311, 287	0.203	0.194	-8	6.473	33	0.234	0.226	-21	4.310	5	0.189	0.185	16	6.621	42	
224	14 310, 980	0.200	0.191	-7	6.246	31	0.222	0.214	-19	4.257	6	0.194	0.190	18	6.697	42	
224	18 310, 881	0.200	0.191	-7	6.194	31	0.217	0.210	-18	4.250	6	0.198	0.194	19	6.801	43	
224	22 310, 832	0.200	0.192	-7	6.256	32	0.217	0.210	-18	4.223	7	0.196	0.192	19	6.844	44	
Type II algorithm under 150-443																	
150	2 315, 629	0.239	0.229	-21	6.467	34	0.261	0.252	-30	3.796	10	0.177	0.173	3	6.654	44	
150	6 311, 426	0.224	0.215	-14	5.904	31	0.177	0.171	-9	4.756	22	0.226	0.221	29	9.005	59	
150	10 310, 868	0.212	0.203	-14	5.375	25	0.148	0.143	0	5.098	25	0.256	0.250	36	9.296	61	
150	14 310, 714	0.214	0.205	-14	5.368	25	0.146	0.141	-1	4.857	23	0.244	0.239	34	8.906	59	
150	18 310, 644	0.211	0.202	-14	5.131	23	0.139	0.135	1	4.816	23	0.250	0.245	35	8.618	57	
150	22 310, 590	0.208	0.199	-13	5.209	23	0.139	0.134	5	5.193	26	0.275	0.270	40	9.256	61	
Type II algorithm under 300-886																	
224	2 315, 491	0.209	0.199	-17	6.584	34	0.226	0.219	-22	3.999	14	0.165	0.161	12	7.290	48	
237	6 311, 144	0.196	0.188	-15	5.342	23	0.125	0.121	0	4.765	24	0.235	0.230	30	8.243	54	
244	10 310, 905	0.208	0.199	-11	6.577	35	0.153	0.147	-2	5.617	29	0.252	0.247	37	10.259	68	
258	14 310, 443	0.172	0.165	-14	4.371	10	0.134	0.129	-2	3.504	8	0.214	0.210	28	6.063	39	
252	18 310, 425	0.185	0.176	-11	5.515	23	0.138	0.133	1	4.548	22	0.253	0.248	37	8.700	57	
224	22 310, 404	0.184	0.176	-12	5.112	20	0.132	0.128	1	4.076	18	0.239	0.234	35	7.934	52	

Table 30: AIC scores and out-of-sample validation figures of all derived FGLS proxy functions of BEL under 150-443 and 300-886 after the final iteration. Highlighted in green and red respectively the best and worst AIC scores and validation figures.

<i>k</i>	<i>K</i> _{max}	<i>t</i> _{min}	<i>o</i>	<i>p</i>	glm	v.mae	v.mae ^a	v.res	v.mae ⁰	v.res ⁰	ns.mae	ns.mae ^a	ns.res	ns.mae ⁰	ns.res ⁰	cr.mae	cr.mae ^a	cr.res	cr.mae ⁰	cr.res ⁰	
Sobol set²																					
148	206	0	6	s	inv.g, id	0.265	0.253	-24	10.317	55	0.575	0.555	-40	16.234	-56	0.822	0.805	80	17.657	64	
49	50	0	3	n	inv.g, log	0.370	0.354	0	9.168	19	0.705	0.681	-12	29.477	-102	0.525	0.514	25	16.891	-65	
60	66	0	4	s	inv.g, id	0.324	0.310	-11	8.517	16	1.712	1.654	151	44.504	132	0.917	0.897	102	19.877	83	
45	50	0	4	b	inv.g, id	0.347	0.332	-2	8.686	11	0.447	0.431	-36	22.702	-125	0.511	0.500	35	15.785	-54	
Sobol set and nested simulations set																					
45	50	0	4	b	inv.g, id	0.347	0.332	-2	8.686	11	0.447	0.431	-36	22.702	-125	0.511	0.500	35	15.785	-54	
17	19	0	4	b	inv.g, id	0.834	0.797	25	24.673	124	0.480	0.464	-4	41.356	-243	0.763	0.747	108	21.398	-132	
70	81	0	4	b	inv.g, id	0.335	0.320	-22	10.872	52	0.554	0.535	-35	14.073	-38	0.875	0.857	102	18.250	99	
33	34	0	3	n	inv.g, id	0.426	0.407	-10	10.871	21	1.565	1.512	108	52.384	1	0.662	0.648	32	20.997	-75	
Sobol set and capital region set																					
45	50	0	3	b	pois, log	0.379	0.362	0	9.556	28	0.480	0.464	-43	24.878	-139	0.510	0.500	28	16.938	-69	
31	34	0	3	b	pois, log	0.476	0.455	-13	12.752	46	0.593	0.573	-54	31.148	-175	0.661	0.647	18	23.088	-103	
45	50	0	4	b	inv.g, id	0.347	0.332	-2	8.686	11	0.447	0.431	-36	22.702	-125	0.511	0.500	35	15.785	-54	
59	66	0	3	b	pois, log	0.428	0.439	40	16.674	98	0.760	0.734	-12	22.511	-41	0.809	0.792	68	18.403	39	
Nested simulations set and Sobol set																					
134	144	1.6	-5	5	n	gaus, log	0.273	0.261	-22	10.255	54	1.025	0.990	-1	28.192	-23	1.515	1.484	179	32.616	157
45	50	0	4	s	inv.g, id	0.347	0.332	-2	8.686	11	0.447	0.431	-36	22.702	-125	0.511	0.500	35	15.785	-54	
60	66	0	4	s	inv.g, id	0.324	0.310	-11	8.517	16	1.712	1.654	151	44.504	132	0.917	0.897	102	19.877	83	
45	50	0	4	b	inv.g, id	0.347	0.332	-2	8.686	11	0.447	0.431	-36	22.702	-125	0.511	0.500	35	15.785	-54	
Nested simulations set²																					
45	50	0	4	b	inv.g, id	0.347	0.332	-2	8.686	11	0.447	0.431	-36	22.702	-125	0.511	0.500	35	15.785	-54	
146	159	9.4	-6	5	n	gaus, log	0.279	0.267	-24	10.008	53	1.025	0.990	0	26.779	-11	1.498	1.467	174	31.702	163
76	97	3.8	-5	4	b	inv.g, log	0.344	0.329	-17	10.676	52	0.538	0.520	-37	11.874	-24	0.804	0.787	88	16.584	100
107	113	0	4	n	gaus, log	0.321	0.307	-20	11.976	63	0.997	0.963	8	25.694	0	1.529	1.496	191	32.148	182	
Nested simulations set and capital region set																					
45	50	0	4	s	pois, id	0.353	0.338	-3	8.891	18	0.449	0.434	-36	23.634	-131	0.504	0.493	36	16.079	-58	
31	34	0	4	s	pois, id	0.437	0.418	-11	11.254	32	0.548	0.530	-45	28.444	-157	0.648	0.634	29	21.374	-84	
72	82	3.1	-5	4	b	inv.g, inv	0.365	0.349	-16	11.181	53	0.579	0.560	-49	14.528	-51	0.700	0.685	65	14.619	64
45	50	0	4	b	inv.g, id	0.347	0.332	-2	8.686	11	0.447	0.431	-36	22.702	-125	0.511	0.500	35	15.785	-54	
Capital region set and Sobol set																					
125	144	0	5	f	inv.g, inv	0.283	0.271	-20	10.336	54	0.630	0.608	-63	17.245	-76	0.675	0.660	45	14.737	32	
45	50	0	4	s	gaus, log	0.382	0.365	-1	9.916	32	0.469	0.453	-41	25.487	-144	0.495	0.485	32	16.868	-71	
114	144	1.9	-5	5	s	inv.g, 1/ μ^2	0.313	0.299	-12	9.414	40	0.708	0.684	-77	20.115	-97	0.626	0.612	36	14.095	17
45	50	0	4	b	gaus, log	0.382	0.365	-1	9.916	32	0.469	0.453	-41	25.487	-144	0.495	0.485	32	16.868	-71	
Capital region set and nested simulations set																					
45	50	0	4	f	gaus, log	0.386	0.369	-1	10.095	34	0.468	0.452	-41	25.709	-145	0.496	0.486	32	17.077	-73	
64	66	0	4	n	inv.g, 1/ μ^2	0.420	0.401	-3	11.506	39	0.840	0.811	3	25.969	-38	1.298	1.271	146	29.110	105	
148	175	0	6	s	inv.g, 1/ μ^2	0.311	0.297	-16	10.447	52	0.576	0.556	-55	14.565	-57	0.611	0.598	30	12.844	27	
77	81	0	4	n	inv.g, 1/ μ^2	0.387	0.370	-11	11.519	52	1.029	0.994	-28	25.831	-32	1.279	1.252	148	26.700	145	
Capital region set²																					
45	50	0	4	s	gaus, log	0.382	0.365	-1	9.916	32	0.469	0.453	-41	25.487	-144	0.495	0.485	32	16.868	-71	
33	34	0	3	n	inv.g, 1/ μ^2	0.564	0.539	-14	15.693	64	0.827	0.800	-54	38.645	-185	0.745	0.729	-2	26.338	-134	
148	175	0	6	s	inv.g, 1/ μ^2	0.311	0.297	-16	10.447	52	0.576	0.556	-55	14.565	-57	0.611	0.598	30	12.844	27	
148	175	4.7	-6	5	f	inv.g, inv	0.296	0.283	-20	10.416	53	0.549	0.530	-54	18.260	-87	0.664	0.650	32	16.307	-1

Table 31: Settings and out-of-sample validation figures of best performing MARS models derived in a two-step approach sorted by first and second step validation sets. Highlighted in green and red respectively the best and worst validation figures.

k	$h_k(\mathbf{X})$	$\hat{\beta}_{\text{MARS},k}$
0	1	15, 397.13
1	$h(X_8 - 0.104892)$	7, 901.89
2	$h(0.104892 - X_8)$	-8, 165.64
3	$h(0.205577 - X_1) \cdot h(0.104892 - X_8)$	688.83
4	$h(X_6 - 1.17224)$	265.08
5	$h(1.17224 - X_6)$	-280.94
6	$h(X_{15} - 53.8706)$	-2.11
7	$h(53.8706 - X_{15})$	1.16
8	$h(X_7 - -0.147599)$	-60.90
9	$h(-0.147599 - X_7)$	-334.77
10	$h(X_8 - -0.0456197)$	3, 183.07
11	$h(0.205577 - X_1) \cdot h(0.104892 - X_8) \cdot h(X_{15} - 64.6262)$	-9.48
12	$h(0.205577 - X_1) \cdot h(0.104892 - X_8) \cdot h(64.6262 - X_{15})$	29.85
13	$h(X_1 - 0.945371)$	-64.88
14	$h(0.945371 - X_1)$	124.45
15	$h(X_6 - 1.56058) \cdot h(0.104892 - X_8)$	-815.20
16	$h(1.56058 - X_6) \cdot h(0.104892 - X_8)$	1, 085.80
17	$h(1.44218 - X_2)$	-60.23
18	$h(X_1 - -1.61447) \cdot h(1.56058 - X_6) \cdot h(0.104892 - X_8)$	-233.14
19	$h(-1.61447 - X_1) \cdot h(1.56058 - X_6) \cdot h(0.104892 - X_8)$	415.92
20	$h(X_8 - 0.0159508) \cdot h(53.8706 - X_{15})$	8.94
21	$h(0.0159508 - X_8) \cdot h(53.8706 - X_{15})$	47.99
22	$h(X_9 - 0.247192)$	47.72
23	$h(0.247192 - X_9)$	-82.58
24	$h(0.993896 - X_{12})$	-63.61
25	$h(X_1 - 0.0195594) \cdot h(0.0159508 - X_8) \cdot h(53.8706 - X_{15})$	-12.58
26	$h(0.0195594 - X_1) \cdot h(0.0159508 - X_8) \cdot h(53.8706 - X_{15})$	-42.25
27	$h(X_7 - -0.147599) \cdot h(X_8 - -0.191689)$	2, 124.93
28	$h(X_7 - -0.147599) \cdot h(-0.191689 - X_8)$	1, 510.41
29	$h(X_3 - 0.323352) \cdot h(0.104892 - X_8)$	948.86
30	$h(0.323352 - X_3) \cdot h(0.104892 - X_8)$	-577.61
31	$h(X_1 - -1.26627) \cdot h(X_7 - -0.147599)$	101.15
32	$h(-1.26627 - X_1) \cdot h(X_7 - -0.147599)$	-10.00
33	$h(X_{14} - 0.684998)$	109.76
34	$h(0.684998 - X_{14})$	-37.89
35	$h(1.17224 - X_6) \cdot h(X_8 - -0.12538)$	216.62
36	$h(1.17224 - X_6) \cdot h(-0.12538 - X_8)$	2, 076.18
37	$h(0.945371 - X_1) \cdot h(X_8 - 0.0019988)$	-156.79
38	$h(0.945371 - X_1) \cdot h(0.0019988 - X_8)$	1, 262.56
39	$h(X_1 - -1.58818) \cdot h(X_6 - 1.56058) \cdot h(0.104892 - X_8)$	137.60
40	$h(1.56058 - X_6) \cdot h(0.104892 - X_8) \cdot h(X_{15} - 76.9327)$	-4.87
41	$h(1.56058 - X_6) \cdot h(0.104892 - X_8) \cdot h(76.9327 - X_{15})$	2.11
42	$h(0.205577 - X_1) \cdot h(X_2 - 1.43028) \cdot h(0.104892 - X_8)$	24, 003.07
43	$h(0.205577 - X_1) \cdot h(1.43028 - X_2) \cdot h(0.104892 - X_8)$	-161.88
44	$h(X_1 - 0.945371) \cdot h(X_8 - -0.0165546)$	-224.18
45	$h(X_1 - 0.945371) \cdot h(-0.0165546 - X_8)$	-987.47

Table 32: Best MARS model of BEL derived in a two-step approach with the final coefficients.

k	r_k^1	r_k^2	r_k^3	r_k^4	r_k^5	r_k^6	r_k^7	r_k^8	r_k^9	r_k^{10}	r_k^{11}	r_k^{12}	r_k^{13}	r_k^{14}	r_k^{15}
$K_{\max} = 16$ in adaptive basis function selection															
0	0	0	0	0	0	0	0	0	0	0	0	0	0	0	0
1	0	0	0	0	0	0	0	1	0	0	0	0	0	0	0
2	1	0	0	0	0	0	0	0	0	0	0	0	0	0	0
3	0	0	0	0	0	1	0	0	0	0	0	0	0	0	0
4	0	0	0	0	0	0	0	0	0	0	0	0	0	0	1
5	0	0	0	0	0	0	0	1	0	0	0	0	0	0	0
6	1	0	0	0	0	0	0	1	0	0	0	0	0	0	0
7	0	0	0	0	0	0	0	2	0	0	0	0	0	0	0
8	2	0	0	0	0	0	0	0	0	0	0	0	0	0	0
9	0	0	0	0	0	1	0	1	0	0	0	0	0	0	0
10	0	0	0	0	0	0	0	1	0	0	0	0	0	0	1
11	1	0	0	0	0	0	0	0	0	0	0	0	0	0	1
12	0	1	0	0	0	0	0	0	0	0	0	0	0	0	0
13	1	0	0	0	0	1	0	0	0	0	0	0	0	0	0
14	0	0	0	0	0	0	0	0	1	0	0	0	0	0	0
15	0	0	0	0	0	0	0	0	0	0	0	1	0	0	0
16	0	0	0	0	0	0	1	1	0	0	0	0	0	0	0
$K_{\max} = 27$ in adaptive basis function selection															
17	1	0	0	0	0	0	0	1	0	0	0	0	0	0	0
18	1	0	0	0	0	0	0	0	1	0	0	0	0	0	1
19	0	0	0	0	0	0	0	0	2	0	0	0	0	0	1
20	0	0	0	0	0	0	0	0	0	0	0	0	0	1	0
21	1	0	0	0	0	0	0	0	2	0	0	0	0	0	0
22	0	0	0	0	0	0	0	0	0	0	0	0	0	0	2
23	2	0	0	0	0	0	0	0	0	0	0	0	0	0	1
24	0	0	0	0	0	0	0	0	0	0	0	0	1	0	0
25	0	0	1	0	0	0	0	0	0	0	0	0	0	0	0
26	0	0	1	0	0	0	0	1	0	0	0	0	0	0	0
27	1	0	1	0	0	0	0	0	0	0	0	0	0	0	0

Table 33: Basis function sets of LC and LL proxy functions of BEL corresponding to $K_{\max} \in \{16, 27\}$ derived by adaptive OLS selection.

k	r_k^1	r_k^2	r_k^3	r_k^4	r_k^5	r_k^6	r_k^7	r_k^8	r_k^9	r_k^{10}	r_k^{11}	r_k^{12}	r_k^{13}	r_k^{14}	r_k^{15}
$K_{\max} = 15$ in risk factor wise basis function selection															
0	0	0	0	0	0	0	0	0	0	0	0	0	0	0	0
1	1	0	0	0	0	0	0	0	0	0	0	0	0	0	0
2	0	1	0	0	0	0	0	0	0	0	0	0	0	0	0
3	0	0	1	0	0	0	0	0	0	0	0	0	0	0	0
4	0	0	0	1	0	0	0	0	0	0	0	0	0	0	0
5	0	0	0	0	1	0	0	0	0	0	0	0	0	0	0
6	0	0	0	0	0	1	0	0	0	0	0	0	0	0	0
7	0	0	0	0	0	0	1	0	0	0	0	0	0	0	0
8	0	0	0	0	0	0	0	1	0	0	0	0	0	0	0
9	0	0	0	0	0	0	0	0	1	0	0	0	0	0	0
10	0	0	0	0	0	0	0	0	0	1	0	0	0	0	0
11	0	0	0	0	0	0	0	0	0	0	1	0	0	0	0
12	0	0	0	0	0	0	0	0	0	0	0	1	0	0	0
13	0	0	0	0	0	0	0	0	0	0	0	0	1	0	0
14	0	0	0	0	0	0	0	0	0	0	0	0	0	1	0
15	0	0	0	0	0	0	0	0	0	0	0	0	0	0	1
$K_{\max} = 22$ in combined risk factor wise and adaptive basis function selection															
16	1	0	0	0	0	0	0	1	0	0	0	0	0	0	0
17	0	0	0	0	0	1	0	1	0	0	0	0	0	0	0
18	0	0	0	0	0	0	1	0	0	0	0	0	0	0	1
19	1	0	0	0	0	0	0	0	0	0	0	0	0	0	1
20	1	0	0	0	0	1	0	0	0	0	0	0	0	0	0
21	0	0	0	0	0	0	1	1	0	0	0	0	0	0	0
22	1	0	0	0	0	0	1	0	0	0	0	0	0	0	0

Table 34: Basis function sets of LC and LL proxy functions of BEL corresponding to $K_{\max} \in \{15, 22\}$ derived by risk factor wise or combined risk factor wise and adaptive OLS selection.

<i>k</i>	<i>bw</i>	<i>o</i>	v.mae	v.mae ^a	v.res	v.mae ⁰	v.res ⁰	ns.mae	ns.mae ^a	ns.res	ns.mae ⁰	ns.res ⁰	cr.maecr.mae ^a	cr.res	cr.mae ⁰	cr.res ⁰			
LC regression with gaussian kernel and LOO-CV																			
16	0.1	2	0.55	0.52	-44	13	50	0.70	0.68	-86	12	-7	0.55	0.54	-35	12	45		
16	0.2	2	0.40	0.38	-26	11	47	0.52	0.50	-51	11	7	0.44	0.43	5	13	63		
16	0.3	2	0.37	0.35	-25	11	45	0.45	0.44	-37	11	19	0.44	0.43	5	12	60		
27	0.2	2	0.39	0.38	-26	11	43	0.51	0.49	-51	11	3	0.43	0.43	4	12	58		
16	0.1	4	2.80	2.68	-155	84	-407	8.05	7.78	-558	247	-825	5.04	4.94	-96	128	-363		
LL regression with gaussian kernel and LOO-CV																			
16	0.1	2	0.38	0.36	-11	12	57	0.57	0.55	-68	10	-15	0.41	0.40	-22	9	31		
16	0.2	2	0.34	0.33	-6	11	59	0.45	0.43	-49	8	2	0.37	0.36	5	10	55		
27	0.1	2	210.30	201.06-30.	682	5,	209-30,	589	131.04	126.61	-18,	981	3,	670-18,	902	4.09	4.00	-82	
27	0.2	22	726.472,	606.74	400,	254	67,	487	400,	3063,	502.24	3,	383.85	422,	443	98,	081	422,	481
LC regression with gaussian kernel and AIC																			
16	0.1	2	0.57	0.55	-43	14	55	0.65	0.62	-72	12	12	0.50	0.49	-12	14	72		
16	0.2	2	1.63	1.55	-38	41	73	1.94	1.88	266	57	286	2.57	2.51	384	61	404		
27	0.1	2	0.56	0.54	-42	14	56	0.64	0.62	-72	12	12	0.50	0.49	-12	14	72		
LC regression with Epanechnikov kernel and LOO-CV																			
15	0.1	2	0.53	0.50	-36	13	41	1.05	1.02	-38	22	24	0.51	0.50	-29	11	33		
15	0.2	2	0.41	0.39	-31	10	33	1.14	1.10	3	26	53	1.18	1.16	97	27	146		
15	0.3	2	0.40	0.38	-30	9	23	0.96	0.93	16	23	54	0.46	0.45	-6	11	33		
15	0.4	2	0.35	0.33	-22	9	18	1.11	1.08	12	28	39	0.47	0.46	-2	11	25		
15	0.5	2	0.34	0.33	-18	9	37	1.24	1.20	6	30	46	0.51	0.50	-22	11	18		
15	0.6	2	0.33	0.32	-17	10	50	1.16	1.12	21	27	74	0.46	0.45	-2	11	50		
15	0.7	2	0.33	0.32	-16	10	41	1.17	1.13	18	28	61	0.44	0.43	-14	9	28		
15	0.8	2	0.33	0.31	-16	10	45	1.21	1.17	29	29	76	1.16	1.13	101	26	148		
15	0.9	2	0.32	0.30	-20	12	61	1.14	1.10	40	27	107	1.14	1.11	111	29	178		
15	1.0	2	0.32	0.31	-22	10	49	1.19	1.15	52	29	109	1.13	1.11	106	27	163		
16	0.1	2	0.53	0.50	-40	13	43	1.20	1.16	2	28	71	0.51	0.50	-20	12	49		
16	0.2	2	0.41	0.39	-26	11	50	1.16	1.12	27	28	88	0.44	0.43	2	12	64		
16	0.3	2	0.36	0.34	-27	9	29	1.07	1.03	41	27	83	0.44	0.43	1	11	43		
16	0.4	2	0.33	0.32	-19	8	22	1.16	1.12	27	30	53	0.45	0.44	4	10	30		
16	0.5	2	0.32	0.31	-16	9	36	1.34	1.30	30	33	67	1.22	1.19	101	27	138		
16	0.1	4	0.45	0.43	-26	13	34	0.74	0.71	-68	16	-23	0.59	0.57	5	15	51		
16	0.2	4	3.29	3.15	-104	160	891	7.50	7.24	-14	329	966	8.06	7.89	176	295	1, 157		
16	0.1	6	3.31	3.16	-32	84	68	5.74	5.55	-96	158	-10	6.62	6.48	-53	148	32		
16	0.2	6	3.32	3.18	-71	85	-217	9.37	9.06	73	268	-87	13.18	12.90	246	304	86		
16	0.1	8	3.94	3.77	146	105	-119	10.71	10.35	-191	308	-470	8.84	8.65	-312	205	-591		
16	0.2	8	8.53	8.16	397	286	-639	7.79	7.52	70	347	-980	12.37	12.11	1, 365	390	315		
22	0.1	2	0.50	0.48	-37	12	44	1.07	1.03	-41	22	25	0.52	0.50	-30	11	37		
22	0.2	2	0.42	0.40	-28	10	39	1.07	1.03	-3	25	50	1.20	1.17	106	29	159		
22	0.3	2	0.39	0.37	-29	9	23	0.89	0.86	6	22	43	0.45	0.44	-3	11	34		
22	0.4	2	0.35	0.33	-21	8	16	1.05	1.02	3	27	26	0.49	0.48	-4	11	19		
22	0.5	2	0.33	0.31	-14	9	32	1.17	1.13	-2	28	29	0.47	0.46	-15	10	16		
22	0.6	2	0.33	0.32	-17	10	46	1.09	1.06	11	25	60	0.45	0.44	-1	11	48		
22	0.7	2	0.32	0.31	-15	9	39	1.23	1.18	26	29	66	1.17	1.14	99	26	139		
22	0.8	2	0.32	0.30	-15	10	46	1.19	1.15	32	28	78	1.12	1.10	106	26	152		
22	0.9	2	0.31	0.30	-19	11	58	1.15	1.11	39	27	102	1.12	1.10	111	28	174		
22	1.0	2	0.31	0.30	-21	10	48	1.13	1.09	41	27	96	1.12	1.10	107	27	162		
27	0.2	2	0.40	0.38	-26	11	45	1.15	1.12	26	28	83	0.44	0.43	1	12	58		
27	0.3	2	0.38	0.36	-28	9	24	0.90	0.87	7	22	45	0.46	0.45	-2	11	36		
27	0.4	2	0.35	0.33	-21	9	17	1.05	1.02	2	27	26	0.48	0.47	-4	11	20		
LL regression with Epanechnikov kernel and LOO-CV																			
15	0.1	2	0.45	0.43	-49	10	40	1.22	1.18	-100	22	-26	0.78	0.77	-104	11	-30		
15	0.2	2	0.36	0.34	-34	8	13	1.59	1.53	-145	40	-112	0.60	0.58	-54	11	-21		
15	0.3	2	0.32	0.31	-36	7	17	1.91	1.85	134	48	173	0.60	0.58	-36	11	3		
15	0.4	2	0.34	0.33	-40	8	33	1.83	1.76	-164	42	-106	0.43	0.42	-49	6	9		
15	0.5	2	0.33	0.31	-40	8	34	2.20	2.12	-219	53	-160	0.41	0.41	-45	6	15		
15	0.6	2	0.30	0.29	-33	7	29	0.94	0.91	8	19	56	0.33	0.32	-28	5	21		
15	0.7	2	0.31	0.30	-40	7	23	0.94	0.91	-13	19	36	0.36	0.35	-40	5	8		
15	0.8	2	0.29	0.28	-38	5	8	0.86	0.83	4	19	36	0.32	0.32	-29	5	3		
22	0.1	2	731.51	699.39	2,738	85,172	479,6121	21,564.87	1,511.98	-111,628	127,410	365,231	492.49	482.11	-19,404	76,575	457,455		
22	0.2	2	0.34	0.33	-34	8	0	0.83	0.80	-15	21	4	0.42	0.41	-25	8	-5		
22	0.3	2	98.03	93.73	14,396	148	-250	101.69	98.25	15,174	147	513	100.00	97.89	15,028	100	367		
22	0.4	2	98.05	93.75	14,397	147	-248	113.99	110.14	13,158	495	-1,503	100.00	97.89	15,028	100	367		
22	0.5	2	100.00	95.61	14,685	100	38	118.95	114.93	14,984	651	323	100.00	97.89	15,028	100	367		
22	0.6	2	99.72	95.34	14,644	106	-3	100.59	97.19	15,004	120	343	100.00	97.89	15,028	100	367		
22	0.7	2	100.00	95.61	14,685	100	38	100.00	96.62	14,922	100	261	100.00	97.89	15,028	100	367		
22	0.8	2	0.29	0.28	-39	5	9	152.43	147.27	22,622	4,264	22,655	0.31	0.30	-35	5	-2		
LC regression with uniform kernel and LOO-CV																			
16	0.1	2	0.75	0.71	-56	18	46	1.53	1.48	-52	32	36	0.73	0.72	-59	15	29		
16	0.5	2	1.22	1.17	-78	29	16	2.60	2.51	301	82	381	10.45	10.23	1,419	242	1,498		
27	0.1	2	0.64	0.61	-38	16	31	1.30	1.26	13	32	68	0.59	0.58	-2	15	53		
27	0.5	2	0.35	0.34	-16	12	53	1.34	1.30	25									